

**Development and Evaluation of a Physiologically
Based Pharmacokinetic (PBPK) Population Model
for Elderly Individuals**

Dissertation

zur Erlangung des Doktorgrades (Dr. rer. nat.)

der Mathematisch-Naturwissenschaftlichen Fakultät
der Rheinischen Friedrich-Wilhelms-Universität Bonn

vorgelegt von

Jan-Frederik Schlender

aus Hille

Bonn 2019

Angefertigt mit Genehmigung der Mathematisch-Naturwissenschaftlichen Fakultät der
Rheinischen Friedrich-Wilhelms-Universität Bonn.

1. Gutachter: Prof. Dr. Ulrich Jaehde

2. Gutachter: Prof. Dr. Thorsten Lehr

Tag der Promotion: 23. April 2019

Diese Dissertation ist auf dem Hochschulschriftenserver der ULB Bonn
http://hss.ulb.uni-bonn.de/diss_online elektronisch publiziert.

Erscheinungsjahr: 2019

Acknowledgement

This work was carried out at the Pharmaceutical Institute of the Rheinische Friedrich-Wilhelms-University of Bonn under the direction of Prof. Dr. Jaehde in affiliation with Bayer Technology Services.

As with every doctoral candidature, my work too did not develop and does not stand in isolation. I greatly appreciate the support of many contributors along the way. A couple of these I would like to mention here.

First of all, I want to thank my supervisor Prof. Dr. Jaehde. Due to the constellation of an almost external position during my candidature, I am very grateful to him that he often provided comprehensive feedback or valuable suggestions especially at short notice.

Likewise, I thank Prof. Dr. Lehr for taking over the role of the second evaluator as well as Prof. Dr. Wagner and Prof. Dr. Hofmann-Apitius for their willingness to participate in the examination board.

Special thanks also go to my supervisors at Bayer, Kirstin Thelen, Michaela Meyer and Stefan Willmann who initiated the project and guided me very well. In addition, Thomas Eissing who took over at a later stage has been a great support. Their experience and critical thinking were valuable during my candidature.

I would like to express my gratitude to the other colleagues in the former Competence Center for System Biology at Bayer Technology Services, who have always been willing to answer my questions.

I also thank Prof. Schmidt and the postdocs in his lab at the University of Florida for some great collaborations resulting in various contributions during the time of this work.

Despite the support of colleagues, a doctorate in an industrial setting comes along with limited contact to other doctoral students. Gladly I had two fellow sufferers in Markus and Stephan, to whom a close friendship developed. Likewise, there was always a close contact to Patricia and Achim in Bonn. I especially thank these four for proofreading of this work.

A special thank goes to the clinical pharmacy working group of Prof. Jaehde. Due to my sporadic presence, I appreciate the warm and friendly nature of all working group members among whom I never felt like a stranger.

I also thank all my friends, who I have missed out on one or the other occasion in recent years but they understandingly accepted this.

Finally but foremost, I thank my family, my parents, siblings and of course my wife Lena for their tremendous support during this time. My parents always backed me almost unconditionally in all my decisions in life although they may had doubts at one or the other move. Especially the fantastic support of my wife Lena during the entire candidature made this work happen. Seemingly major problems along the way appeared marginally due to her and our daughter Clara.

Für meine Familie

Table of Content

List of figures	I
List of tables	III
List of abbreviations	IV
List of original publications.....	VI
1 Introduction	1
1.1 Pharmacotherapy in elderly.....	1
1.2 Current status and need for clinical studies in elderly	2
1.3 Precision medicine approaches in the elderly	3
1.3.1 Expert consensus-based personalized medicine approaches.....	4
1.3.2 Genome-based personalization approaches for the elderly.....	6
1.4 Biomarkers	8
1.5 Quantitative personalized medicine approaches	9
1.5.1 Population pharmacokinetic/pharmacodynamic approaches	12
1.5.2 Physiologically based approaches	14
1.6 Development and qualification of an elderly PBPK database	16
1.6.1 Database development.....	17
1.6.2 Database qualification steps	18
2 Scope and objectives of this work	24
3 Methods	25
3.1 Software programs	25
3.1.1 Open Systems Pharmacology suite	25
3.2 Development of an elderly PBPK population model.....	28
3.2.1 Collection of data on anthropometric, anatomical and (patho-) physiological changes with age.....	28

3.2.2	Data processing	29
3.2.3	Workflow for elderly PBPK model development	30
3.2.4	Database qualification	33
3.3	Application of a lifespan PBPK population model for ciprofloxacin	35
3.3.1	Available data.....	35
3.3.2	PBPK model development of ciprofloxacin.....	38
3.3.3	PBPK model verification	40
3.3.4	Scaling of the adult model for predictions in pediatric and geriatric patients.	40
3.3.5	Sensitivity analysis.....	42
4	Results	44
4.1	Physiological changes in the elderly	47
4.1.1	Anthropometric measures	47
4.1.2	Muscle mass	48
4.1.3	Fat mass.....	48
4.1.4	Kidney weight	48
4.1.5	Liver weight	49
4.1.6	Brain	49
4.1.7	Heart.....	50
4.1.8	Bone	51
4.1.9	Gonads.....	52
4.1.10	Lung	52
4.1.11	Pancreas	52
4.1.12	Skin	52
4.1.13	Spleen.....	53
4.1.14	Cardiac output.....	53

4.1.15	Cardiac output distribution	54
4.1.16	Total body water distribution.....	59
4.1.17	Albumin	59
4.1.18	Alpha-1-acid glycoprotein	60
4.1.19	Hematocrit.....	60
4.1.20	Glomerular filtration rate (GFR).....	60
4.2	Predictability of PK data in the elderly	63
4.3	Application of a ciprofloxacin lifespan PBPK population model.....	70
4.3.1	Intravenous ciprofloxacin PBPK model simulations for adults	70
4.3.2	Oral ciprofloxacin PBPK model simulations for adults.....	73
4.3.3	PBPK model verification	74
4.3.4	Prediction of age-related impact on ciprofloxacin pharmacokinetics	76
4.3.5	Sensitivity analysis.....	80
5	Discussion.....	81
5.1	Database development.....	81
5.2	Database qualification	82
5.3	Application of the elderly PBPK population approach	84
5.4	Challenges and opportunities to streamline dosing regimens in the elderly ...	87
5.4.1	Current challenges.....	87
5.4.2	Opportunities.....	87
6	Conclusion and perspectives	90
7	Summary.....	93
	References	95
	Appendix	125

List of figures

Figure 1-1	Simvastatin clinical trials population compared to the prescription pattern for lipid-lowering medication for publicly insured patients in Germany stratified by age.	4
Figure 1-2	Interplay of qualitative pharmacokinetic approaches to inform and confirm geriatric dosing strategies during drug development.	11
Figure 1-3	Representation of the general building blocks which can be part of a PBPK model.....	15
Figure 1-4	Database qualification and verification steps.	21
Figure 3-1	Workflow for the knowledge-driven physiologically based pharmacokinetic (PBPK) ageing approach.....	31
Figure 3-2	Schematic workflow of the ciprofloxacin PBPK model building and.....	39
Figure 4-1	Distributions of mean organ weight from newborns to individuals up to 100 years of age.	44
Figure 4-2	Mean organ weights from early adulthood up to 100 years of age as percentage of body weight.	45
Figure 4-3	Age-dependent changes in body height, comparison between simulations and observations in females and males.	47
Figure 4-4	Simulated age distribution of brain weight compared to the nomogram of Hartmann <i>et al.</i>	50
Figure 4-5	Simulated age distribution for heart weight compared to the nomogram of Gaitskell <i>et al.</i>	51
Figure 4-6	Distribution of body water in females and males over the course of aging.....	59
Figure 4-7	Changes in kidney function in females and males over the course of ageing compared to literature values.	62
Figure 4-8	Predicted and observed plasma concentration-time profiles of morphine in younger adults vs. the elderly.	64
Figure 4-9	Trial individual observed vs. predicted values for volume of distribution at steady-state and the elimination half-life for the test compound morphine.....	65
Figure 4-10	Trial group observed vs. predicted values for volume of distribution at steady-state and the elimination half-life for the test compound morphine.....	65
Figure 4-11	Predicted and observed plasma concentration-time profiles of furosemide in younger adults vs. the elderly.	67
Figure 4-12	Trial individual observed vs. predicted values for volume of distribution at steady-state and the elimination half-life as well as the corresponding fold over/under prediction, for the test compound furosemide.	68

Figure 4-13	Trial group observed vs. predicted values for volume of distribution at steady-state and the elimination half-life as well as the corresponding fold over/under prediction, for the test compound furosemide.	69
Figure 4-14	Correlation matrix for parameter identification of distribution, metabolism and elimination parameters after intravenous administration.	72
Figure 4-15	Exemplary ciprofloxacin plasma concentration-time profile after a 200 mg intravenous administration and the respective goodness-of-fit plot.	72
Figure 4-16	Correlation matrix for parameter identification of oral absorption parameters.	74
Figure 4-17	Exemplary ciprofloxacin plasma concentration-time profile after a 500 mg oral administration and the respective goodness-of-fit plot.	75
Figure 4-18	Verification of the ciprofloxacin PBPK model for the investigated dose range by comparing simulation/observation ratios of pharmacokinetic measures.	76
Figure 4-19	Predictive performance of the ciprofloxacin PBPK model indicated by predicted versus observed mean plasma concentration data of pediatric and geriatric patients.	77
Figure 4-20	Comparison of predicted and individual observed plasma concentrations data for ciprofloxacin grouped by age.	79
Figure 4-21	Model predictions for AUC and C_{\max} following intravenous and oral administration.	79
Figure 4-22	Model predictions for AUC and C_{\max} following intravenous and oral suspension administration.	80
Figure A-1	Listing of the most sensitive parameters comprising 90 % of the entire variability in a descending order towards AUC_{inf} after intravenous administration.	131
Figure A-2	Listing of the most sensitive parameters comprising 90 % of the entire variability in a descending order towards AUC_{inf} after oral administration. ...	132
Figure A-3	Listing of the most sensitive parameters comprising 90 % of the entire variability in a descending order towards C_{\max} after oral administration.	133

List of tables

Table 3-1	Overview of input parameters for the PBPK models of furosemide and morphine	34
Table 3-2	Summary of clinical studies of ciprofloxacin	36
Table 4-1	Anthropometric measures, organ and tissue weights including blood as used in the elderly PBPK model	46
Table 4-2	Cardiac index and organ blood flow rates used in the elderly PBPK model	57
Table 4-3	Studies (including the numbers of subjects) utilized for model building to determine changes in organ volume and specific organ blood flow development over the course of aging in healthy European Caucasians	58
Table 4-4	Summary of clinical studies after intravenous dosing for the test compound morphine used to compare the simulated data	63
Table 4-5	Predictive performance analysis of the morphine PBPK model with and without the age-informed physiology	66
Table 4-6	Summary of clinical studies after intravenous dosing for the test compound furosemide used to compare the simulated data	67
Table 4-7	Predictive performance analysis of the furosemide PBPK model with and without the age-informed physiology	69
Table 4-8	Input data values and model parameters for ciprofloxacin PBPK model	71
Table 4-9	Results of the parameter identification for oral administration	73
Table A-1	Patient characteristics and mean pharmacokinetic parameters in ciprofloxacin studies using intravenous dosing reported in the literature	125
Table A-2	Patient characteristics and mean pharmacokinetic parameters in ciprofloxacin studies using oral dosing reported in the literature	127

List of abbreviations

AAG	Alpha-1-acid glycoprotein
ABC	ATP-binding cassette
ADE	Adverse drug event
ADME	Absorption, distribution, metabolism and elimination
$A_{\text{eff}}\text{Factor}$	Effective surface area enhancement factor
$AUC_{0-\tau}$	Area under the plasma drug concentration-time curve of one dosing interval
AUC_{inf}	Area under the plasma drug concentration-time curve from time point 0 to infinity
BDDCS	Biopharmaceutics Drug Disposition Classification System
BIA	Bioimpedance analysis
BID	Twice a day
BMC	Bone mineral content
BMD	Bone mineral density
CF	Cystic fibrosis
C_{max}	Maximum plasma concentration
CMR	Cardiac magnetic resonance
CT	Computer tomography
CYP	Cytochrome P-450
DXA	Dual energy X-ray absorptiometry
EMA	European Medicines Agency
EPA	United States Environmental Protection Agency
FDA	United States Food and Drug Administration
GFR	Glomerular filtration rate
GI	Gastrointestinal
GLP-1	Glucagon-like peptide 1
GWAS	Genome wide association studies
HbA _{1c}	Glycosylated hemoglobin
HCT	Hematocrit
ICH	International Conference on Harmonization
ICRP	International Commission on Radiological Protection
ME	Mean prediction error
MRI	Magnetic resonance imaging
OAT	Organic anion transporter
OSP	Open Systems Pharmacology
PAH	Para-aminohippuric acid

PBPK	Physiologically based pharmacokinetics
PD	Pharmacodynamics
PET	Positron emission tomography
P_{int}	Intestinal permeability
PK	Pharmacokinetics
PopPK	Population pharmacokinetics
RMSE	Root mean squared prediction error
SD	Standard deviation
SPECT	Single-photon emission computed tomography
START	Screening Tool to Alert to Right Treatment
STOPP	Screening Tool of Older People's Prescriptions
$t_{1/2}$	Elimination half-life
T2DM	Type II Diabetes Mellitus
TID	Three times a day
V_{ss}	Volume of distribution at steady-state

List of original publications

This thesis is based on the following publications, which are reprinted in the Appendix

- I. **Schlender JF**, Vozmediano V, Golden AG, Rodriguez M, Samant TS, Lagishetty CV, Eissing T, Schmidt S. Current strategies to streamline pharmacotherapy for older adults. *Eur J Pharm Sci.* 2018; 111:432-42.
- II. **Schlender JF**, Meyer M, Thelen K, Krauss M, Willmann S, Eissing T, Jaehde U. Development of a whole-body physiologically based pharmacokinetic approach to assess the pharmacokinetics of drugs in elderly individuals. *Clin Pharmacokinet.* 2016; 55(12):1573-89.
- III. **Schlender JF**, Teutonico D, Coboeken K, Schnizler K, Eissing T, Willmann S, Jaehde U, Stass H. A physiologically based pharmacokinetic model to describe ciprofloxacin pharmacokinetics over the entire span of life. *Clin Pharmacokinet.* 2018 [Epub ahead of print]

Sections 1 and 5.4 of this work, including the subsections thereof, originated from publication I. The contributions of the authors to the published article (doi:10.1007/s40262-017-0539-z.) were as follows: review conception and design: JS, VV, and SS; execution of literature search: JS and VV; drafting of the manuscript: JS, VV, MR and SS; discussion and correction of the manuscript: JS, VV, AG, MM, TS, CL, TS and SS.

Sections 3.2, 4.1, 4.2, 5.1 and 5.2 of this work, including the subsections thereof, originated from publication II. The contributions of the authors to the published article (doi: 10.1007/s40262-016-0422-3.) were as follows: study conception and design: JS, MM, KT, SW and UJ; execution of literature search: JS; analysis and interpretation of analyzed data: JS, KT and MK, critical revision: JS, MM, KT, MK, SW and UJ; drafting of the manuscript: JS; discussion and correction of the manuscript: JS, MM, KT, MK, TE and UJ.

Sections 3.3, 4.3 and 5.3 of this work, including the subsections thereof, originated from publication III. The contributions of the authors to the published article (doi: 10.1007/s40262-018-0661-6) were as follows: study conception and design: JS, DT and SW; execution of literature search: JS; PBPK model development and simulations JS, DT and KC; critical revision: JS, DT, KS, TE, SW, UJ and HS; drafting of the manuscript: JS; discussion and correction of the manuscript: JS, DT, KS, TE, SW, UJ and HS.

Additionally, the following original publications, book chapters and conference contributions were created during preparation of this thesis:

Publications

Kuepfer L, Niederalt C, Wendl T, **Schlender JF**, Willmann S, Lippert J, Block M, Eissing T, Teutonico D. Applied concepts in PBPK modeling: how to build a PBPK/PD model. *CPT Pharmacometrics Syst Pharmacol*. 2016; 5:516-31.

Bitter K, **Schlender JF**, Woltersdorf R. Drug-drug interactions in the elderly: Which ones really matter? *Internist*. 2016; 57:728-34.

Krauss M, Hofmann U, Schafmayer C, Igel S, **Schlender JF**, Mueller C, Brosch M, von Schoenfels W, Erhart W, Schuppert A, Block M., Schaeffeler E, Boehmer G, Goerlitz L, Hoecker J, Lippert J, Kerb R, Hampe J, Kuepfer L, Schwab M Translational learning from clinical studies predicts drug pharmacokinetics across patient populations. *NPJ systems biology and applications*. 2017; 11:1-11.

Lau SW, **Schlender JF**, Abernethy DR, Burckart GJ, Golden A, Slattum PW, Stegemann S, Eissing T. Improving Therapeutics to Better Care for Older Adults and the Young: Report From the American College of Clinical Pharmacology Workshop. *J Clin Pharmacol*. 2018; 58:277-80.

Book chapters

Schlender JF, Golden AG, Samant TS, Lagishetty CV, Schmidt S. The Personalization of Drug Therapy for Elderly Patients. In: *Developing Drug Products in an Aging Society 2016* (pp. 589-611). Springer, Cham.

Kuepfer L, Niederalt C, Wendl T, **Schlender JF**, Block M, Eissing T, Teutonico D. PBPK Modelling of Intracellular Drug Delivery Through Active and Passive Transport Processes. In: *Intracellular Delivery III 2016* (pp. 363-374). Springer, Cham.

Conference Contributions

Oral communications

Schlender JF, Eissing T. Pharmacometrics Approaches to Better Care for Older Adults and the Young, American College of Clinical Pharmacology (ACCP) Workshop 3, 2016 September 24, Bethesda, MD, USA

Schlender JS. Patient centric medicine development and pharmacokinetic considerations. 7th APS International PharmSci Conference, 2016 September 6, Glasgow, Scotland

Abstracts

Schlender JF, Krauss M, Block M, Eissing T, Jaehde U. A physiologically based pharmacokinetic approach to assess the impact of age on the pharmacokinetics of acetaminophen in elderly individuals. American Conference of Pharmacometrics (ACoP), 2016 October 23-26, Seattle, WA, USA

Schlender JF, Lautenbach N, Kanacher T, Block M, Eissing T. Simulating altered omeprazole kinetics in elderly individuals using physiologically based pharmacokinetic (PBPK) population modeling. American College of Clinical Pharmacology (ACCP), 2016 September 25-27, Bethesda, MD, USA

Kuepfer L, Niederalt C, Wendl T, **Schlender JF**, Willmann S, Lippert J, Block M, Eissing T, Teutonico D. Whole-body PBPK/PD modelling of ciprofloxacin and its anti-bacterial activity. 25th Population Approach Group Europe (PAGE), 2016 June 7-10, Lisboa, Portugal

Schlender JF, Samant TS, Meyer M, Thelen K, Willmann S, Eissing T, Schmidt S, Jaehde U. Impact of aging on bioavailability and multiple enzymatic elimination pathways using a lifespan physiologically based pharmacokinetic (PBPK) approach. American Association of Pharmaceutical Scientists (AAPS) Annual Meeting and Exposition, 2015 October 25–29, Orlando, FL, USA

Schlender JF, Werner N, Meyer M, Thelen K, Eissing T, Willmann S, Jaehde U. Application of an elderly PBPK model to specify age-dependent changes of active processes. 24th Population Approach Group Europe (PAGE), 2015 June 3-5, Heraklion, Greece

Schlender JF, Meyer M, Thelen K, Willmann S, Jaehde U. A physiologically based pharmacokinetic approach to assess the impact of age on the pharmacokinetics of acetaminophen in elderly individuals. American Conference of Pharmacometrics (ACoP), 2014 October 13-15, Las Vegas, NV, USA

Schlender JF, Thelen K, Meyer M, Willmann S, Jaehde U. Development of a whole-body PBPK approach to assess the pharmacokinetics of xenobiotics in elderly individuals. 23rd Population Approach Group Europe (PAGE), 2014 June 10-13, Alicante, Spain

Thelen K, Krauss M, **Schlender JF**, Diedrich C, Schuppert A, Burghaus R, Lippert J, Goerlitz L, Willmann S. Modeling Variability in Special Patient Populations. Bayer Scientific Symposium, 2013 November 2-3, Leverkusen, Germany

1 Introduction

1.1 Pharmacotherapy in elderly

Evidence of efficacy and safety of new drug products is based primarily on results of one or more randomized, placebo-controlled clinical trials, which generally derive “one-size-fits all” dosing regimens for new drug products [1]. However, patients respond differently to medications due to many reasons, which can either be intrinsic (e.g., age, weight, metabolic capacity, genetic constitution etc.) or extrinsic (e.g., comedication, comorbidity, etc.). Consequently, flat dosing regimens can have serious impact on efficacy and safety of the individual patient. In contrast, the purpose of “personalizing” drug therapy is to optimize the benefit and minimize the harm of medication interventions on a patient-by-patient basis [1]. Although personalized treatment regimens should be the first choice, initial drug labels often lack useful and explicit label information even for larger patient groups with special needs, e.g. for special population groups [2]. Individualization is then left to the physician, using the “art of medicine” based on experience, clinical judgment, and unique and frequently intangible factors related to a patient. The situation becomes even more complex in the case of elderly patients due to the lack of actual data from dedicated clinical trials in this heterogeneous population. In addition, optimal pharmacotherapy in elderly is hampered by highly variable organ functions, comorbidity, high drug-drug interaction potential, and lack of adherence to medication.

Provided that the Western society is growing increasingly older, there is a need for well controlled treatment strategies to improve the efficacy and safety of drug therapies in older adults. In particular, the impact of changes in body functions in elderly patients compared to healthy subjects needs to be better understood in order to provide optimal pharmacotherapy in this special patient population. For example, ageing is associated with changes in cellular, tissue, and organ function as well as an increased probability of suffering from multiple illnesses. Given this framework and the knowledge on age-related physiological and functional changes, it is important to tailor pharmacotherapy in the elderly to the age subgroups [3].

The International Conference on Harmonization (ICH) Efficacy Guideline E7 defines the elderly patient as a person of the standard retirement age 65 years or older [4]. In order to account for inter-individual variability in this large age group, the ICH purposes a further split of the elderly population into ‘young old’ (65 to 74 years), the ‘old’ (75 to 84 years), and the ‘oldest old’ (≥ 85 years). Within this framework, the classification of geriatric patients by age groups becomes important to account for differences related to physiological and functional changes observed in these patients with age [5].

However, a chronological age (years since birth) classification is often not ideally suited for designing pharmacotherapy for the elderly patient because it may or may not appropriately reflect the patient’s actual “biological age”. Age-related changes are highly heterogeneous due to the dynamic interplay between multiple, complex and poorly understood genetic, environmental, and disease-related risk factors. As a consequence, flat dosing regimens that fail to take the biological age into account are unlikely to appropriately meet the medication needs of the individual elderly patient [6].

1.2 Current status and need for clinical studies in elderly

To account for the increasing number of older adults and their special pharmacotherapeutic needs, the ICH E7 guideline recommends the inclusion of a meaningful number of geriatric patients (age 65 years of age and older) in phase III or phase II/III of clinical drug development. Even more ideal are exclusively dedicated geriatric trials in order to appropriately account for comorbidity and investigate the influence of polymedication in the elderly patient. In particular, the guideline arbitrarily recommends the inclusion of at least 100 geriatric patients to identify clinically relevant differences [4]. This allows for an assessment of deviating dose response and varying degrees of efficacy with increasing age. Based on this framework, the United States Food and Drug Administration (FDA) proposes to include data for elderly patients of all subgroups mentioned in ICH E7 for the marketing application of new drugs [7]. These subgroups should be considerable in size and comparable to respective patient numbers for the respective disease [8].

However, even if the intent behind present regulations is the inclusion of different groups of elderly patients in clinical trials, these recommendations are frequently not fully implemented. For example, in the phase II and III Type II Diabetes Mellitus (T2DM) trials, only one percent of the study population is older than 75 years of age [9]. In addition, the outcome of a typical trial may not accurately reflect clinical reality because elderly subjects included in clinical trials are mostly the ‘young old’, healthy older adults who have fewer and less severe comorbidity [10]. An exemplary case is shown in Figure 1-1 for simvastatin, where the clinical trial population [11] was compared to the actual target patient population for lipid-lowering medication among publicly insured patients in Germany [12]. Age distributions of these two populations clearly differ.

Older adults that are generally underrepresented in clinical trial settings include patients with dementia, non-native speakers, functionally dependent (nursing home or homebound) and those who are unable to consent to participate in a research study [13]. These patients live often geographically isolated from studies conducted at large medical centers. Similarly, patients with advanced comorbidity are also often excluded. It is not surprising that 61 % of new cancers are diagnosed in the elderly, whereas only 25 % of oncology trial participants can be assigned to this age group [14]. As a consequence, insufficient data is often available from geriatric clinical trials intended to develop geriatric-specific dosing information [15]. Therefore, ‘start low, go slow’ recommendations for pharmacotherapy are common. These empirical dosing approaches may lead to an increase in mortality as evident from over-treating hypertension and diabetes mellitus in older adults [16].

1.3 Precision medicine approaches in the elderly

This need for more precise dosing recommendations for older adults has been addressed at various levels of complexity ranging from expert consensus-based to physiologically based personalized medicine approaches.

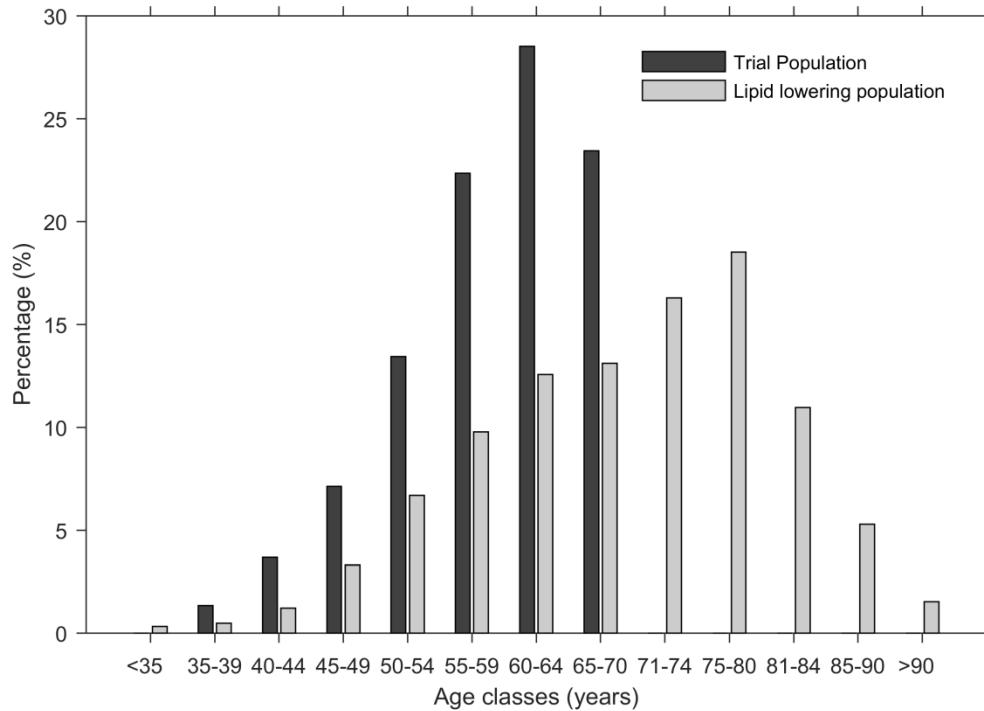


Figure 1-1 Simvastatin clinical trials population compared to the prescription pattern for lipid-lowering medication for publicly insured patients in Germany stratified by age. Trial population is shown in *dark grey bars* and was adopted from Martin *et al.* [11] whereas the German patient population is visualized in *light grey bars* [12].

1.3.1 Expert consensus-based personalized medicine approaches

Expert consensus-based personalized medicine approaches are intended to optimize medication use by guiding the avoidance of medications that place older adults at an increased risk of adverse events and for which safer alternatives exist.

Beers criteria

The Beers Criteria for inappropriate medications were developed by expert consensus in 1991 and have been updated in 1997, 2003, 2012, and 2015 [17-21]. These criteria identify medications with risks that may be greater than their benefits for people 65 years or older, and were developed to “guide” health care professionals prescribing for older adult patients. Although they have been used as a quality of care measure by many health care

systems, these criteria were not intended to imply that these medications are absolutely “contraindicated”. In addition, many newer medications are not included in the criteria and issues of inappropriate drug interactions or drug class duplications are not captured [22]. Studies to date have struggled to demonstrate a clear correlation between adherence to Beers Criteria recommendations and improved clinical outcomes.

STOPP/START criteria

The Screening Tool of Older People’s Prescriptions (STOPP) and the Screening Tool to Alert to Right Treatment (START) were first published in 2008 [23] and were updated in 2015 [24]. Like the Beers Criteria, STOPP Criteria were developed through expert review using the Delphi consensus methodology and are intended to identify medications to be avoided in older adults. The START Criteria were developed through a similar methodology to identify medication prescribing omissions. A comparison between the STOPP and the 2003 Beers Criteria found that patients taking a medication from the STOPP list were 85 % more likely to have an adverse drug event than those without a STOPP list drug. No association was found with the 2003 Beers criteria [25].

Priscus list

In order to facilitate a safe pharmacotherapy for older adults in Germany, an initiative of German physicians and scientists summarized potentially inappropriate medications for the German drug market and released it under the name Priscus list in 2010 [26]. As a starting point, the Beers criteria as well as similar lists from Canada [27] and France [28] were screened to identify overlaps with the German drug market, since specific prescription guidelines or habits as well as drug authorization may differ between countries. This list was extended by potentially harmful drugs for older adults available on the German market. Finally, this list was reviewed by experts using the Delphi consensus methodology.

FORTA list

The “Fit for the Aged” (FORTA) list is a clinical tool developed by the University of Heidelberg [29]. Similarly to the Priscus list, the FORTA list is tailored for German

geriatricians, but is the first classification system in which both negative and positive recommendations are combined. The list should aid geriatricians towards a safe prescription for individual indications instead of an assessment guided by a negative list. Similar to other lists, a two-round Delphi procedure was conducted for the FORTA list. A subsequent validation trial run suggests that the application of the FORTA list leads to an improvement of medication quality and a reduction of adverse drug reactions (ADRs).[30].

One of the major concerns about using a “hit list” approach includes lack of allowance for exceptions (e.g., palliative care). On the other hand, drugs that are considered beneficial may still present a high risk for adverse drug events in medically complex older adults. Budnitz *et al.* investigated hospital admissions due to ADEs and pointed out that only a few drugs cause the majority of hospitalizations [31]. Warfarin and insulins are the primary suspects for ADEs. However, the retrospective review of emergency room and hospital claims data may underestimate the true medication-related risks in older adults as many adverse-effects (i.e. dry mouth, incontinence, anorexia, confusion) are not captured in electronic health records [32].

1.3.2 Genome-based personalization approaches for the elderly

During the past two decades, the quest for identifying the genetic basis for ageing has sparked an entire field of research that focuses on cellular ageing processes. The study of nutrient signaling pathways, reactive oxygen species (i.e. “free radicals”), telomere length, DNA repair mechanisms, and mitochondrial dysfunction have been of particular interest because they represent cellular mechanisms for senescence and apoptosis [33]. Studies in centenarians (age ≥ 100 years) have gained prominence in evaluating the genetic basis for extreme longevity and the delay of frailty [34]. Several genes, such as APOE and FOXO3A, have been associated with ageing [35] in Genome Wide Association Studies (GWAS). GWAS determine statistical correlations between the genomic variability among individuals and the phenotypic variability among the same individuals [36]. The impact of the genomic variability of these “ageing genes” on the pharmacokinetics (PK) and pharmacodynamics (PD) of drugs in older adults remains unknown.

Genotype-guided dosing in the elderly

Genotype-guided dosing regimens are available for many drugs [37-39]. They are intended to enable safer and more effective drug treatment by identifying genetic sources of inter-individual variability needed to optimize dosing strategies by reducing toxicity and increasing efficacy of a given drug treatment. Regardless of the genotype, elderly patients may present higher drug levels than younger patients when the same dose is administered to both patient populations due to age-related reduction of intrinsic clearance capacity. In addition, the variance in Cytochrome P-450 (CYP) functionality with age may result in a multiplicative effect on metabolism [40]. As an example, venlafaxine plasma concentrations are 18-fold higher in elderly CYP2D6 poor metabolizers than in non-elderly poor metabolizers [40, 41]. In spite of the limited number of elderly poor metabolizers included in this study, an important observation was that all of them had serum venlafaxine and O-desmethylvenlafaxine (pharmacologically active compound) levels were above the upper recommended therapeutic limit [41].

Warfarin is another prominent example for genotype-guided (CYP2C9 and VKORC1) dosing regimens. Although age was not identified as the most significant covariate, a reduction of dose requirement of 0.2 mg per day per decade, independent of genotype and weight, was observed [42]. Because the impact of the CYP variation on the PK may be more pronounced and clinically meaningful in older adults, all possible covariates including age and genotype should be considered to develop a comprehensive dosing strategy regardless of its time-consuming and costly nature [43, 44].

The genome-based disease risk assessment

Certain diseases are associated with age or have an increased prevalence in the elderly. Based on genomic testing, estimates can conceptually be made for the incidence and/or prognosis of these diseases. However, the genetic basis for most diseases remains poorly understood. For example, the efforts invested to develop clinically useful genomic tests that can predict a higher risk for Alzheimer's disease in individual patients have not yet been fruitful and currently available results still remain elusive.

Whereas pharmacogenomic considerations for drug usage might not vary with increasing age, the benefit for a timely diagnosis will become more important for the elderly population. Similarly, understanding a patient's genetic variation is needed in order to optimize dosing strategies to reduce toxicity and increase efficacy of a particular drug treatment.

1.4 Biomarkers

The development of drug treatments in the elderly is limited by the lack of reliable biomarkers in this special patient population. For example, current efforts for developing effective medications for the prevention and treatment of Alzheimer's disease are hampered by the lack of established biomarkers, both for preclinical detection and for monitoring clinical treatment response [45].

Given that many body functions either change or lose physiologic capacity as subjects become older, it is still unclear which of the identified biomarkers in healthy adults are equally applicable to the elderly patient. In addition, elderly patients may have different disease progression, lifestyle, comorbidity and poly-medication which may require the combination of different biomarkers or scores to obtain more specific measures of the drug response in this population. Ideally, the dynamic interplay between all above factors should be quantified to establish appropriate dosing regimens and support precision medicine approaches in the elderly.

Type II Diabetes Mellitus is a good example for the complexity of factors involved in the identification of appropriate biomarkers in the older adults. The general guidelines for controlling T2DM in elderly patients recommend higher target levels of glycosylated hemoglobin (HbA_{1C}) than in younger adults [46]. This recommendation is in part the result of the ACCORD trial, where even though a premature termination was required after a median duration of 3.5 years because of higher mortality in the group targeting lower HbA_{1C} levels, it provided the first evidence that hypoglycemia and other adverse effects are more frequent in older patients [46, 47]. Hypoglycemia is related with serious morbid

outcomes in the elderly population, such as falls, cognitive decline, autonomic dysfunction, depression, recurrent hypoglycemia, poor adherence, and possible cardiac ischemia or arrhythmia, which may contribute to poor function and poor prognosis [46, 48]. In addition, the regulatory feedback mechanisms involved in the maintenance of glucose homeostasis are defective in older people, which lead to an increased risk of hypoglycemia. Antidiabetic drugs with lower glycemic variability should, therefore, be part of the first-line treatments of T2DM in older adults. In addition, ageing is related with a progressive impairment in carbohydrate tolerance (possibly due to disorderly insulin release), reduced insulin production and reduced glucagon-like peptide 1 (GLP-1) secretion, increased adiposity, sarcopenia, and physical inactivity [46, 47, 49, 50]. In elderly patients, the relative contribution of postprandial glucose to blood glucose levels is higher than that of fasting glucose. Therefore, selecting antidiabetic therapies that are more efficacious in postprandial glucose control for older adults may also be considered for these patients [46].

1.5 Quantitative personalized medicine approaches

Mathematical and statistical approaches that integrate information on the drugs' PK and PD as well as the disease at the population and the individual patient level have been increasingly used in drug development and regulatory decision making since the 1990s. Compared to the expert consensus-based approaches introduced earlier, quantitative approaches typically use information on the dynamic interplay between drug(s), pharmacology, disease pathogenesis, and intrinsic as well as extrinsic patient factors to characterize and predict age-dependent changes in elderly patients and to personalize drug treatments in this population. The highly variable organ function(s) in the elderly population and the resulting variability in absorption, distribution, metabolism and elimination (ADME) as well as in the PD processes need to be considered to develop appropriate dose-exposure-response relationships. The establishment of these relationships is typically more problematic in elderly patients, but is important for optimal dose selection for this population [51]. This challenge may be met by the combined use of quantitative

approaches (e.g., population pharmacokinetics (PopPK) or physiologically based PK (PBPK) models) and prospective clinical trials. This combined approach will allow to identify a trial design and treatment regimen with the highest probability of maximizing desired effects while minimizing undesired side effects and may thus help to reduce cost and burden to the elderly patient.

Figure 1-2 shows an example of how a combination of quantitative clinical pharmacology approaches (PopPK and PBPK models) and clinical trials can serve as a tool for establishing safe and effective dosing regimens for older adults. Both modeling methods complement each other and are adapted gradually. In a first stage, the preclinical information is used to facilitate the mechanistic understanding of the drug's PK/PD behavior and to develop a preliminary PBPK/PD model including the physiological pathways identified to play a major role. Model predictions can then be used to guide the design of the clinical studies in an iterative manner (learning and confirming cycles that are used to inform both modeling approaches) and used to assist dosing decision making. Once the PK/PD data from the clinical trials is available, PopPK/PD analysis can then be used to validate the predictions and to further confirm the PBPK/PD model assumptions. This step will allow a better understanding of the drug's behavior in humans together with its associated inter-individual variability, and can also be used as supportive evidence for drug labelling. The updated PBPK/PD model can then be used to bridge the PK/PD to the elderly population (geriatric PK/PD model) by informing the model on age-related physiological changes, alterations in the pathophysiology and to extrapolate the clinical response to streamline the design of a confirmatory trial in the population of older adults. Again at this stage, the PK or PK/PD data arising from a confirmatory trial can be used to evaluate the effects of age on the geriatric PK/PD parameters when data from different age populations are available, also confirming the PBPK/PD modelling outcomes, and allowing the selection of the most appropriate dosing regimens in different categories of older adults.

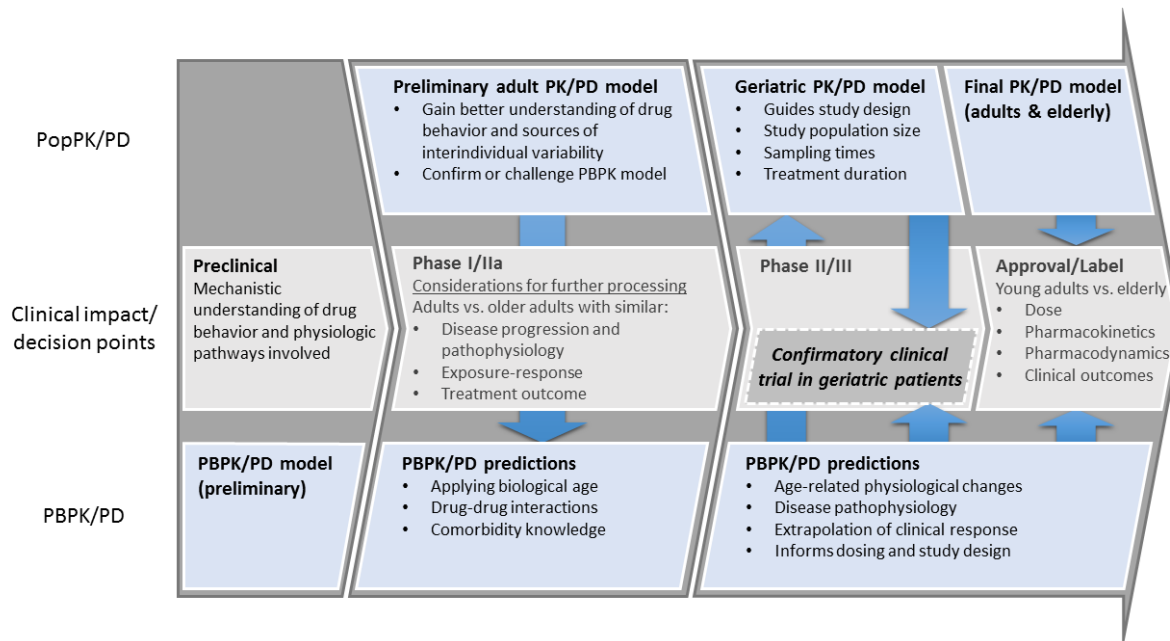


Figure 1-2 Interplay of qualitative pharmacokinetic approaches to inform and confirm geriatric dosing strategies during drug development. PBPK (lower stream) and PopPK (upper stream) model development run in parallel during early clinical development, the interplay can gain importance after certain decision points (main development stream) in order to inform and streamline subsequent trials (*dashed box*) or clinical decisions for older adults.

This approach has been extensively used in clinical drug development for children [52] and could also be used for extrapolation of adult dosing regimens to older adults.

It should be noted, however, that in isolation, information on PK is of limited clinical utility and needs to be linked to the corresponding PD response. Whereas the impact of age on a drug's PK is typically easier to assess, respective changes in PD remain understudied. Therefore, a robust understanding about the mode of action coupled with reliable appropriate measures is essential for the age-related PD assessment. Drug effects are most often based on a complex molecular cascade [53]. For example, the density of receptors can be reduced with increasing age as shown for α -adrenergic [54] or μ -receptors [55]. It also seems that there is increased sensitivity to various central nervous system drugs, including benzodiazepines, halothane, metoclopramide, and narcotic analgesics, as patients

become older [56]. Whereas some of these effects can be studied directly in elderly patients, our understanding of many PD effects relies on extrapolated animal data [57].

1.5.1 Population pharmacokinetic/pharmacodynamic approaches

The majority of the currently employed population approaches are descriptive (non-mechanistic or empirical) in nature and use statistically robust criteria to characterize the data. These methods, however, can be optimized by the inclusion of physiology-related processes to improve their predictive performance and further increase their applicability [58, 59]. As an example, PK scaling approaches are intended to extrapolate the dose-exposure relationship from a well characterized population to the special population of interest by defining specific physiological processes in the model. Whereas exposure matching using allometric scaling is most commonly employed in pediatrics [60], age- or organ function-based (e.g. creatinine clearance) scaling approaches are frequently employed in geriatrics [61]. For example, the FDA label for the anticoagulant apixaban [62] recommends age-, weight-, and serum creatinine-based dosing. The normal dose is 5 mg twice daily except for patients with two of the three factors: age ≥ 80 years, body weight ≤ 60 kg and serum creatinine ≥ 1.5 mg/dL. Under these circumstances, the dose is reduced to half of the normal dose. “Scaling by size only” (i.e. allometric scaling) approaches typically face limitations in the presence of non-linearity. For pediatrics, non-linearity is typically the result of enzyme ontogeny, whereas other factors, such as changes in body composition, play a bigger role among older adults. Ideal body weights based on age do not exist for geriatric patients and hypervolemic states from congestive heart failure, cirrhosis, and nephrotic syndrome are common. Even accurate height and weight measures may be unattainable in patients who are bedridden or have amputations, contractures or kyphosis. Therefore, a frail, medically complex 79 year-old would be more appropriate for the reduced dose of apixaban than a healthy 80 year old.

Although population approaches are typically descriptive and drug-centric in nature, they are routinely employed for dose selection and clinical trial design. They further allow for evaluation of covariates, both genetic and non-genetic, in order to account for inter-individual differences in patients’ dose-concentration-response relationships [63]. Once

established and qualified, population models can be used to address specific questions, either during drug development or in clinical practice [64]. During drug development, they can be applied to address specific questions on e.g. the dose-concentration-response (PK/PD) relationship of a drug or combination of drugs in a given patient population, which can then be prospectively qualified in a clinical trial setting. If linked to epidemiological, biological, clinical or real-world patient data, these methods can be used to simulate a virtual elderly patient population, which can be used to assess the benefit-risk relationship of a given treatment in a given patient population. One prominent example for the application of this innovative approach is the Alzheimer's disease progression simulator. This simulator integrates patient-level data with information from the neuroimaging initiative database and pooled literature data in a drug-disease trial model [65]. This model then allows simultaneously evaluating multiple factors that contribute to the heterogeneity of the disease and its manifestation, which can then be used to project an individual patient's disease progression. These approaches have gained popularity for characterizing the progression of highly heterogeneous diseases in the absence of distinct information on the onset and trajectory of an individual's disease. As such, this simulator provides a powerful approach for enriching our knowledge on patient cohorts with small sample sizes, i.e., chronically understudied elderly patients.

Given the practical limitations outlined earlier, this approach can be applied to optimize the clinical development of drugs in older adults, thus reducing the number of subjects to include in the study, as well as the number of samples per patient and the number of studies required to characterize drug PK/PD behavior. Combining these innovative simulation approaches with prospective clinical trials may therefore be helpful to establish respective geriatric dosing recommendations, whereas reducing cost and burden to the elderly patient. The use of sparse sampling designs may be a solution to improve the recruitment of the oldest study patients overcoming some of the barriers to participation (as time in the center by the accommodation of blood withdrawals in more flexible sampling windows, or the number of days required for participation).

Once in the clinic, especially for those drugs with narrow therapeutic index and high variability (i.e. difficult to be managed in clinical settings), population models can be

applied in combination with posterior Bayesian estimations to integrate the underlying PK or PK/PD mechanism of a drug along with patient specific covariates (characteristics) to aid in the prediction of the right dose for each individual patient [66-73]. Ideally, these individualization methods for complicated drugs should be applied during drug development to find the right dose for the right patient prior to market entry. However, such pharmaco-statistical methods have found limited application at the bedside to date. This is primarily due to a lack of practitioner-friendly decision support tool interfaces, which are needed to facilitate the translation of biomarker data and other patient-specific information into actionable treatment recommendations, without burdening practitioners with the underlying technical details [74].

1.5.2 Physiologically based approaches

PBPK models are set up to characterize and predict drug exposure at different target sites by dividing the biological system into a number of compartments, each representing a different organ or tissue. These organs or tissues are connected through arterial and venous blood flow. PBPK models consist of three distinct parts (Figure 1-3):

- 1) A drug-specific component that characterizes the physicochemical properties of the drug (e.g., pKa, molecular weight, log P), which can be predicted on the basis of *in vitro* assays.
- 2) A system-specific component that describes the functioning of the underlying physiological system, which can differ between and within species, e.g. between adult and elderly patients.
- 3) A trial design component that characterizes the impact of intrinsic (e.g. disease state, genetic constitution) and extrinsic (e.g. diet, smoking, drug-drug interactions) factors on the drug's PK as well as the trial design [60, 75].

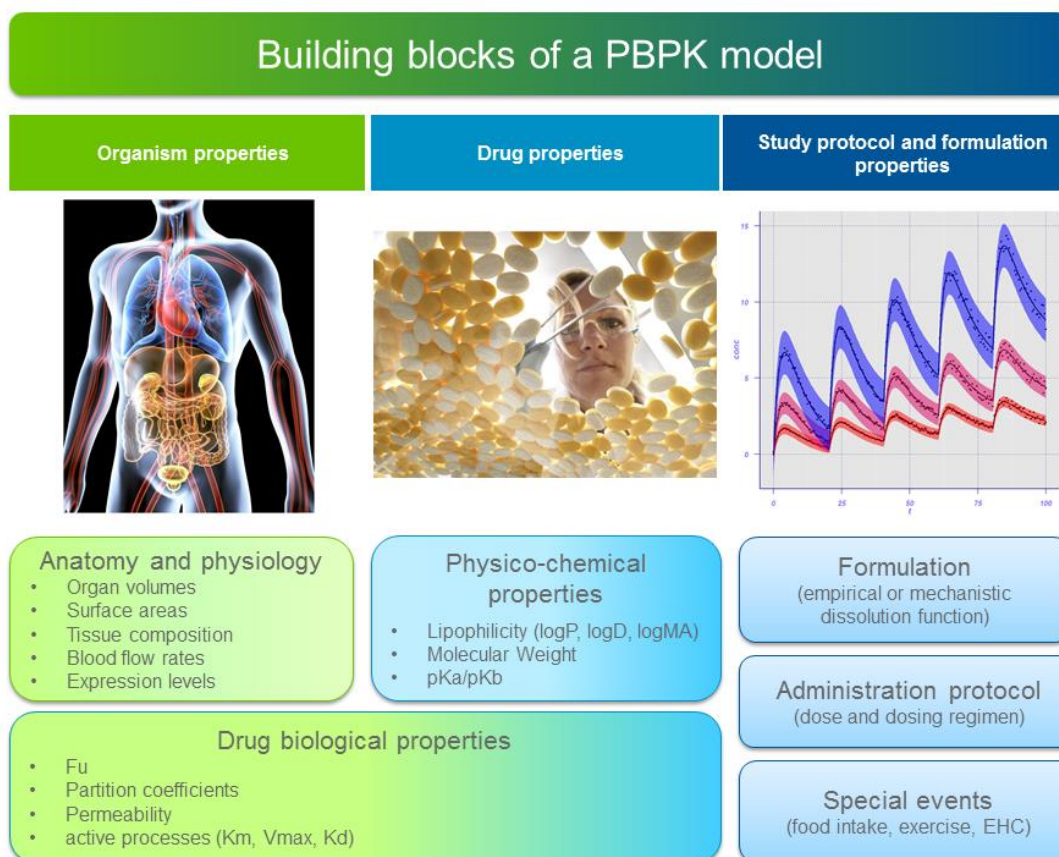


Figure 1-3 Representation of the general building blocks which can be part of a PBPK model. Some components may be optional depending on the model considered [75]. logP: octanol/water partition-coefficient, logD: octanol/water distribution-coefficient, logMA: membrane/water partition-coefficient, pKa: acid dissociation constant in log scale, pKb: basic dissociation constant in log scale, Km: Michaelis-Menten constant, Vmax: maximal rate of the reaction, Kd: dissociation constant, EHC: enterohepatic circulation.

Although PBPK models have been especially used in regulatory applications to characterize and predict the impact of drug-drug interactions, they are becoming popular for testing and understanding the PK in specific populations, such as pediatrics, but also to perform *in vitro* – *in vivo* extrapolations, to translate the PK cross-species and within-species as well as for pharmacogenomic purposes, evaluating the effect of organ impairment on drug elimination, investigations on drug absorption, and combinations thereof [76]. They may also serve as screening tools during early stages of drug

development to facilitate strategic decision-making to select those compounds with a more favorable PK and formulation properties [77].

Although PBPK approaches are uniquely positioned for evaluating the dose-exposure relationship in clinically understudied populations, such as pediatric patients, this approach has found little application for elderly patients thus far. There are some ongoing initiatives that attempt to expand PBPK modeling and simulation platforms to geriatrics by accounting for changes in the underlying physiology and for the age-related decline in the organ function, as well as for the influence of pathophysiological conditions [78, 79]. Once established and qualified, these expanded PBPK models may also serve as a platform to evaluate the impact of other clinically relevant factors, such as drug-drug interactions in elderly patients in the absence of actual clinical trial data, ideally as a basis for future confirmatory prospective studies.

The subsequent next step is the use of PBPK/PD models for integrating relevant information on PK (e.g., changes in metabolic capacity, or transporter expression) and PD (e.g., changes in receptor expression and activity) in order to select an optimal treatment and dosing regimen [80, 81]. Thus, these PBPK/PD models can be used for the individualization of drug and dosing regimens in the elderly by accounting for differences in e.g. organ function, genetic make-up, or general physiology [82]. However, it should be noted that both, implementation and predictive performance of these approaches, will rely on the use of clinically relevant biomarkers for the elderly patient as well as on the suitability of the physiological database used for model development.

1.6 Development and qualification of an elderly PBPK database

An elderly PBPK platform combined with age-related information on pathway or target abundance changes can be applied to develop novel treatment strategies. However, a comprehensive qualification upfront is essential in order to build confidence towards any PBPK application. Similar to pediatrics or the adult age range, a verified and/or qualified elderly PBPK database can be considered as the foundation for further consideration of

specific diseases in the elderly PBPK approach. Such a database allows a diversification of age- and/or disease-related physiological alterations. Although multimorbidity hampers a clear disease-related pathophysiological distinction, changes due to healthy ageing can clearly be separated with an elderly patient PBPK approach. Once the PK alterations with increasing age are physiologically informed, shifts in PD patterns can be explained by the plain exposure-response relationship.

1.6.1 Database development

The integrated use of PBPK/PD and their predictive performance relies on the concerted use of physiological, demographic, and genetic information. These PBPK/PD models consequently require the use of highly curated databases, which summarize our knowledge on human anatomy and (patho-) physiology as well as changes thereof with age. Jadhav *et al.* outlined the steps necessary to develop and qualify a model that appropriately characterizes the fate of a given drug in a particular patient population [2]. In addition to the fate of the drug, changes in the biological systems with age need to be considered in order to appropriately characterize and predict the dynamic changes in the interplay between drug, patient and potentially disease.

The establishment of databases for older adults is hampered by the fact that changes in the underlying physiology may or may not correlate well with chronological age and heavily depend on extrinsic and intrinsic factors. These factors are typically not normally distributed and can be significantly affected by comorbidity and comedication. For example, acute medical illness and hospitalization can profoundly affect biological ageing, whereas therapeutic or lifestyle interventions may lead to partial regeneration [83]. The rates at which anatomical, physical and cognitive impairment progresses with age differ in pace, which results in pharmacological heterogeneity in elderly patients. Finally, there are gender-specific differences in ageing that need to be considered. Whereas menopause represents a distinct event in women's lives, which is associated with distinct biological changes in the female body, ageing is a much more heterogeneous process in men [79, 84]. The World Health Organization (WHO) consequently recommends ten-year age bins for

ageing studies to capture the various degrees of physiological and biological changes in this patient group [6].

Whereas functional, physical or cognitive age-related changes are frequently monitored in sizeable study cohorts, anatomical and (patho-)physiological changes are primarily investigated in cross-sectional studies [85]. The general lack of longitudinal data also poses a challenge for our ability to compare results from different studies. This becomes particularly apparent when today's humans are compared to their age-matched counterparts from previous decades, who tended to be smaller and less obese than today's average adult [86]. The comorbidity and medication profiles are also different. This phenomenon is also referred to as 'secular trend' and needs to be considered when developing a database that includes data from previous decades.

1.6.2 Database qualification steps

Once a physiological database that accounts for age-related changes in physiology has been established, a rigorous qualification process is needed to ensure its broader validity and applicability. There has been a lot of controversy in the recent years on what is the best approach for qualifying PBPK platforms and models, highlighting the need for well-defined model development and qualification criteria [87]. However, this is not a new challenge and solutions are offered in the US Environmental Protection Agency (EPA) guideline [88], the European Medicines Agency (EMA) guideline [89], and the FDA guidance [90].

External model qualification is an overarching theme in all of the current best practices for PBPK model development and qualification. It refers to the use of one or more data sets that have not been used for model development to test the model's descriptive and predictive performance and, thus, the assumptions made during model development. The same concept also applies for associated model parameters [75]. A major advantage of PBPK models and associated databases is that this verification step does not have to be performed on a one off basis, i.e. for each drug, because the underlying anatomy and physiology of the biological system does not change with each drug. As a consequence, a distinction between biological system-specific and drug-specific model components can be

made. Whereas biological system specific model components characterize the functioning of the underlying biological system, drug-specific model components characterize the physicochemical properties of the drug.

Both model components can be qualified independently from one another. In other words, once a biological system has been characterized by biological system-specific model components, the PBPK model's setup is completed through the integration of system-independent, drug-specific parameters [91]. Of course, this concept also applies the other way around, e.g. by acknowledging changes in the biological system with age via the use of time-varying functions, while keeping the drug-specific model components constant. These time-dependent changes in the biological system are typically "mapped out" through the use of probe compounds. Changes in the probe compounds' distribution and elimination patterns serve as indirect measures of changes in e.g. metabolic capacity, perfusion or tissue composition.

Hence, PBPK models for selected probe drugs should be built for healthy young adults first and subsequently be scaled to the age-range of interest (see Figure 1-4). An appropriate step-by-step ADME process-driven qualification should consider the following elements and exclude subsequent characteristics when selecting the paradigm compounds:

- 1) The first test compounds should be characteristic for the extracellular space (e.g. aminoglycosides, ibuprofen). This property allows for a description and concomitant qualification of changes in blood volume and interstitial space with age. Preferably, the test compounds for this step should freely distribute in the absence of tissue binding.
- 2) Once this first task has been accomplished, the impact of plasma protein binding and changes therein with age can be verified in a second step through the use of probe compounds that show extensive plasma protein binding in the absence of tissue distribution. The latter will also provide an estimate of age-related changes in extracellular body water.
- 3) As tissue concentrations and biopsy studies in elderly are rarely performed, changes in drug tissue distribution need to be qualified by informing the

age-related changes of the accountable process. Here, the changes of the volume of distribution can be evaluated as a measure for altered tissue distribution. Turnheim *et al.* gathered literature information on the volume of distribution shifts between adults and elderly which can be used as a test set for these steps [84]. When the reported elderly to young ratio of volume of distribution was related to the compound's octanol/water partition-coefficient (Log P value), a tendency to a gradual increase of volume of distribution in elderly was observed for compounds with a Log P >2 [92]. The reversed tendency was inferred for more hydrophilic compounds. Volume of distribution qualification steps as parametrized for young adults will be governed by the age-related changes in organ size and blood flow.

- 4) Thereafter, the impact of age on elimination pathways can be qualified within an elderly PBPK approach. Firstly, characteristic single elimination pathway compounds should be selected for qualification to assess in a later stage the shifting extraction ratios of drugs with multiple elimination pathways.
 - Renal clearance mediated by a descending glomerular filtration rate (GFR) needs to be qualified by testing hydrophilic drugs solely eliminated by filtration without subsequent reabsorption or secretion processes.
 - Hepatic elimination can be governed by the hepatic perfusion in case of high extraction drugs (e.g. propranolol, metoprolol, morphine) or by the intrinsic clearance mediated by a certain enzymatic process besides shifts in the unbound fraction for low extraction drugs (CYP-paradigm substrates). Qualification should proceed via single-elimination pathway compounds. Multiple pathway elimination compounds can serve for additional assessments.
- 5) Once the major systemic processes driving distribution, metabolism and excretion have been qualified, the following step is to assess factors influencing the oral absorption. Gastric emptying and transit time or passive absorption due to alterations of the surface area may be qualified using

relatively small, Biopharmaceutics Drug Disposition Classification System (BDDCS) class I molecules such as paracetamol or caffeine [93]. In addition first pass effects, especially intestinal metabolism can be characterized.

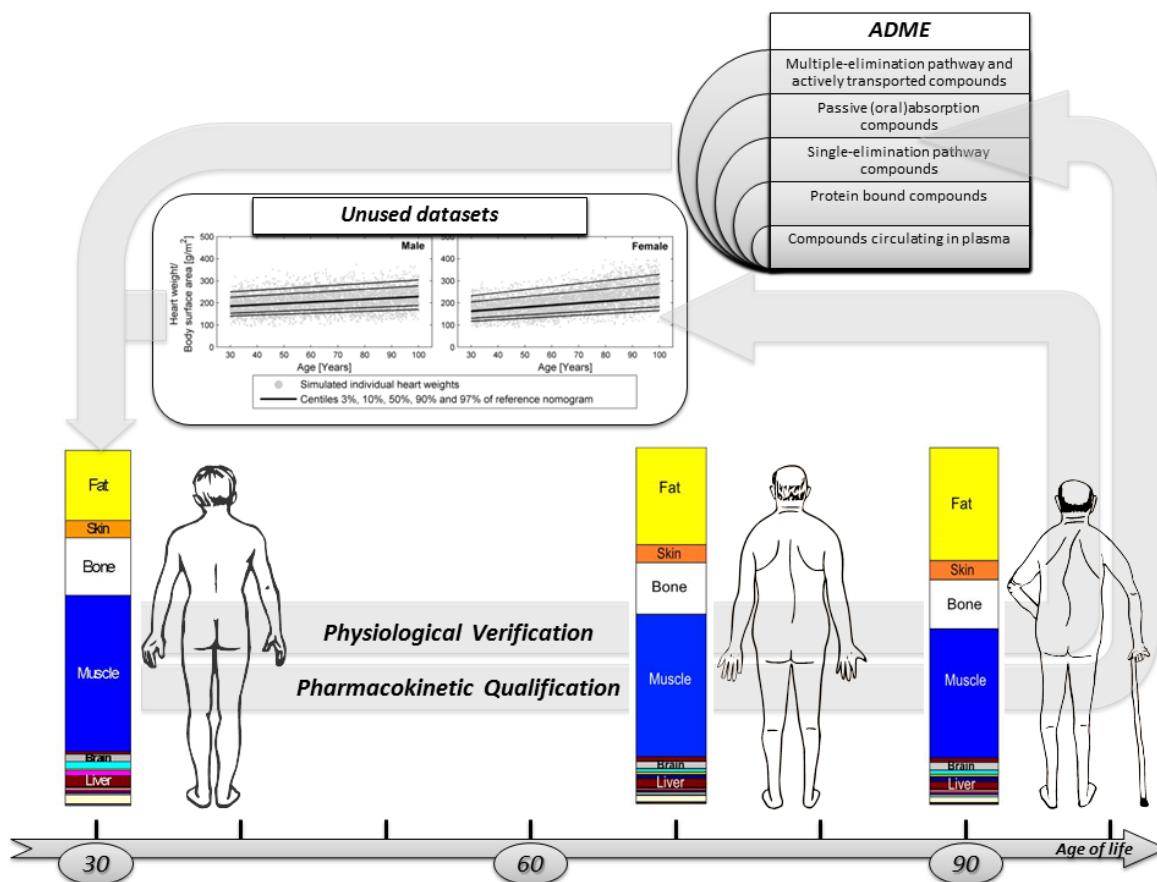


Figure 1-4 Database qualification and verification steps. Bars represent the body composition of a 30 year old individual, a septuagenarian, and a nonagenarian male with their relative organ volumes as part of the total body weight.

Once established and qualified, a major advantage of PBPK models is their ability to characterize and predict the dynamic interplay between multiple biological processes, such as the interplay between multiple metabolic enzymes. This ability can also be used to evaluate the impact of ageing on a drug's hepatic clearance. Clearance of drugs which are excreted to more than 70 % from blood or plasma upon passage through the liver (i.e., high extraction drugs) is mainly restricted by the liver blood flow, whereas clearance of low

extraction drugs (excreted to less than 30 %) is dependent on the metabolic capacity of the eliminating organ, in this case, the liver. Whereas the majority of studies does not report a significant impact of age on enzyme-mediated processes, the situation is heterogeneous for elimination via phase 1 and 2 metabolism [94]. One of the major CYP enzyme complexes, the 2C subfamily, is involved in the metabolism of frequently used drugs in elderly patients, such as anticonvulsants and non-steroidal anti-inflammatory drugs [95]. CYP2C19 is also needed for the enzymatic bioactivation of clopidogrel, a widely used anticoagulant, into its pharmacologically active metabolite [96]. Whereas the expression of CYP2C9 and CYP2C19 appears to be unaffected by age, the respective clearance values of drugs eliminated via these pathways seem to be decreasing. The CYP2D subfamily, on the other hand, seems to maintain its metabolic activity with increasing age [95, 97, 98]. The situation seems less clear-cut for the CYP3A4 subfamily since contradictory reports exist in the literature [95]. In addition, conjugation, acetylation, glucuronidation and sulfation are generally not influenced by age [99]. Whereas different metabolites can be formed in children compared to adults, this does not seem to be the case in the elderly [95].

The selection of probe compounds and the sequence described above is certainly idealistic. It is consequently possible that not all steps are applicable to all/other specific populations, e.g., due to the lack of appropriate data. However, it should be aimed for both, a general physiology verification and specific ADME process-driven qualification procedure once a new specific population PBPK database is established and prior to its use for modeling purposes. Qualification for intended use is especially important, when considering high impact applications [89]. Figure 1-4 depicts the database, as the backbone of a platform, qualification and verification steps. The described procedure defines criteria towards a fit-for-purpose characterization of a PBPK specific population database requiring a reliable standard PBPK framework. However, the qualification of the specific model for each compound should be predefined and considered with strong criteria mainly for drugs with narrow therapeutic index. For such purpose, the best practice of model assessment proposed by the WHO [100] is frequently applied. A recent investigation revealed a lack of consensus in the model qualification and verification practices for the majority of peer-reviewed PBPK models published between 2008 and 2015, where 56 % of the articles did

not pre-define the criteria to evaluate the successful performance of the model for its specific purpose [101]. Importantly, for narrow therapeutic index drugs, a 30 % or 2-fold deviation in the prediction of plasma concentrations or PK parameters were applied as qualification criteria but only in less than half of the studies whereas the other half had no criteria. These results highlight the need for consensus to decide on best practices to qualify PBPK models. In addition, the criteria actually used for model evaluation might be too soft for narrow therapeutic index drugs for which failures in the selection of the optimal dose can have fatal consequences. It is important to remark that the level of qualification determines the confidence into the extrapolative power, especially, when the prediction requires increased prior system knowledge. Moreover, when the model is going to be used to impact drug labelling, as for example to decide the dose recommendation for older adults, it is very important to ensure its adequate performance for this purpose, as the model-based decision taken will affect clinical practice and will have direct consequences for the patient.

2 Scope and objectives of this work

The goal of this study is the development, qualification and application of a PBPK population model for elderly individuals that considers typical (patho-) physiological conditions associated with ageing. This study was conducted in three projects.

In the first project, the literature was reviewed with a focus on age-related (patho-) physiological changes in European elderly subjects. The goal of this part was to extend an existing PBPK database for European adults based on the International Commission on Radiological Protection (ICRP) report [102] to encompass the full course of healthy ageing, through to the age of 100 years.

In the second project, paradigm compounds were identified to qualify the capability of the PBPK population model and to predict distribution and elimination of these compounds. The developed elderly PBPK database was used to predict plasma drug concentration over time profiles for the single elimination pathway drugs morphine and furosemide. Calculated PK parameters were compared to literature findings to statistically evaluate the predictive performance of the PBPK population model.

In the final project, reliability of predictions outside the simulated adult age range towards the extremes of ages for the multi-elimination pathway compound ciprofloxacin was assessed. Mean data of published clinical trials were identified and used for the ciprofloxacin PBPK model building, simulation and verification process. Whereas model simulations were conducted within the model building scenario, predictive performance on both ends of the age scale was assessed using data on individual patients from multiple trials.

3 Methods

3.1 Software programs

The PBPK modeling software Open Systems Pharmacology suite (OSP Suite, www.open-systems-pharmacology.org) was used for all whole-body PBPK models [75]. It comprises the PBPK software tool PK-Sim[®] version 7.2.0 and the systems biology platform MoBi[®], which allows in-depth mechanistic modeling. Parameter optimization was conducted with the MoBi[®] Toolbox for MATLAB[®] version 7.2.0, release 2013b (The MathWorks, Inc., Natick, MA, USA; www.mathworks.com/products/matlab.html) using the Monte Carlo algorithm of the statistical toolbox. MATLAB[®] was also used for data processing, statistical analysis, PK parameter calculation and the creation of graphics. Scan Data, an in-house developed software tool of Bayer Technology Services, was used to extract data from published figures.

3.1.1 Open Systems Pharmacology suite

The Open Systems Pharmacology suite is an open source PBPK software tool for which the source code is publicly available. This specialized software platform provides a generic PBPK model framework for the physiology of predefined species and populations. It includes physiological databases that are combined with compound-specific information as well as biometric data, and are used to parametrize a PBPK model on a whole-body level.

Anatomy and physiology

The generic PBPK software tool represents 18 organs and tissues and provides a large dataset for age-dependent anatomical and physiological parameters over the entire human life span [75]. The tissues and organs are characterized by its anatomical and physiological properties. Therefore, tissue size and composition, as well as perfusion rates are available within the software database. Within the PBPK framework, an organ is structurally represented in sub-compartments, namely the intracellular, interstitial and vascular space. The organs are connected by three blood pools. The arterial and venous blood pool

summarize the in- and outflux of each organ, whereas the portal vein adds up all blood flows emanating from the gastro-intestinal (GI) tract organs.

Drug properties

Drug-specific properties are mainly characterized by physicochemical parameters which can usually be obtained by *in vitro* measurements. Key parameters such as lipophilicity or molecular weight are used to estimate membrane permeability or distribution behavior. Drug solubility determines the availability for absorption of a compound in the GI tract, whereas pKa values are used to calculate pH-dependent solubility changes.

Formulation

In vitro dissolution profiles in biorelevant media, such as the Fasted State Simulated Intestinal Fluid (FaSSIF) and the Fed State Simulated Intestinal Fluid (FeSSIF), have been established. When used in standardized *in vitro* dissolution test methods, such media allow simulating the *in vivo* disintegration and dissolution behavior of orally administered dosage forms [103]. This dissolution profiles together with drug PK profiles can be used to establish an *in vitro–in vivo* correlation (IVIVC). The dissolution profiles can be represented by different kinetic functions, for which the Weibull function is the most common. This function is characterized by a shape parameter b corresponding to the dissolution shape and indicating the course of the dissolution being either exponential ($b = 1$), sigmoid ($b > 1$), or parabolic ($b < 1$). The dissolution time (50 % dissolved) defines the time after the start of dissolution, when 50 % of the administered dose is dissolved and, thus, corresponding to the scale parameter of the Weibull function.

Distribution models

Small molecules can generally distribute in all kinds of tissues in the body. Experimentally, the quantification of this compound-specific distribution is very labor-intensive. A major advance in PBPK modeling came with the use of calculation methods for organ/plasma partition coefficients describing the concentration ratios at steady-state between tissue and plasma. Various concepts for mechanistic correlations have been

developed for the *in silico* estimation of organ/plasma partition coefficients. Based on tissue composition, these coefficients can account for the distribution between drug-binding tissue constituents, such as proteins or lipids, on the one hand, and water on the other. Although the principles are very similar in all cases, the calculation methods deviate with respect to the kind of parameters used and resulting in different values of tissue concentration. All known partition coefficient models assume that tissue is composed of a limited number of components, and they all include partition coefficients for water/protein and lipid/water. These two partition coefficients are usually calculated from so-called surrogate *in vitro* measurements. The total organ/plasma partition coefficient is then calculated as a weighted sum of the partition coefficients for all of the components; the weights are the volume fractions of each component. Importantly, the distribution of a drug within aqueous and organic tissue components is always assumed to be homogenous and passive. The most widely used concepts for calculating organ/plasma partition are briefly introduced below:

- Poulin *et al.* calculate the lipo-hydrophilicity of tissue as a mixture of neutral lipids, phospholipids, and water [104, 105]. In addition to the volumetric tissue composition, fraction unbound (f_u), lipophilicity ($\log P$ and $\log D$), and pK_a are used as compound-specific input parameters. Here as well as in all the following concepts for the calculation of organ/plasma partition coefficients, f_u quantifies specific reversible binding to proteins in plasma and tissue, whereas lipophilicity accounts for nonspecific binding to lipids.
- Rodgers *et al.* extended the concepts of Poulin *et al.* to electrostatic interactions at physiological pH [106, 107]. These include binding of ionized and unionized drugs to acidic phospholipids and neutral lipids, respectively. Also electrostatic drug interactions with extracellular proteins are taken into account. Consequently, the partition coefficients are calculated taking into account the lipophilicity and pK_a value of the drug and the pH values of the tissues.
- Willmann *et al.* extended the concept of Poulin *et al.* by additionally considering proteins as a tissue component [108, 109]. Moreover, Willmann *et al.* use membrane affinity ($\log MA$) to quantify partitioning between water and an artificial

cellular membrane as a measure for lipophilicity by using an empirical equation [110]. This model is implemented in the PK-Sim software as the PK-Sim standard distribution model.

Parameter identification

In case experimental data are given, the reverse question for the true input parameters needed to achieve a simulation with output curves corresponding to the given experimental data might occur. This reverse problem is called parameter identification. Since the parameter identification run deals with an optimization problem, the residuals between observed data and corresponding simulation output should be minimized by varying the selected input parameters in a given range. A variety of algorithms exists to solve optimization problems, however, only the Monte Carlo algorithm was applied for the modelling tasks in this thesis. The required effort and the quality of the solution depend on several factors, e.g. number and bounds of the input parameters of interest, complexity of the model or the quality of start values for the input parameters.

3.2 Development of an elderly PBPK population model

3.2.1 Collection of data on anthropometric, anatomical and (patho-) physiological changes with age

The previously established database of Thompson *et al.* [85] provided a sound basis for establishing a PBPK model for the elderly age range, but needed extension. Exact data on sex, race and disease diversification, as well as details regarding covariates, are pivotal for establishing predictive PBPK models. Body weight and height or body mass index (anthropometric measures) as well as anatomical and (patho-) physiological parameters were searched for in PUBMED using the filters ‘Species-Human’ and ‘Ages-Aged: 65 + years’. Additional terms such as ‘age’, ‘ag(e)ing’, ‘elderly’ and ‘old’ were added for refinement where needed. For parameters that yielded only sparse literature in this initial search, an additional screen was performed in Google Scholar and MEDPILOT. Inclusion criteria were (a) clear assignment of sex, (b) clear assignment of race, (c) a comprehensible

statement regarding the method of analysis, and (d) ruling out of effects of medication or disease on subjects' physiology. Studies that included longitudinal surveillance were preferred. Since *in vivo* measurements of organ size are not directly comparable to measurements obtained from autopsy reports, the former were taken into consideration only for the evaluation of muscle, fat, and blood flow [111]. Furthermore, for each study cohort the available details about body composition, for example fat mass, fat-free mass and lean-body mass, as well as total body water were extracted and used as covariates. A second literature screen was performed for the ageing that occurs between 30 and 65 years of age (younger adults), in order to refine the existing physiological information and, thus, ensure that the data on ageing were continuous for the purpose of modeling.

In total, 19 studies from the database of Thompson *et al.* were used. After the second literature search data from 97 additional studies was added to build the ageing PBPK model.

3.2.2 Data processing

Since biological and chronological ageing differ, the data was analyzed in 10-year age bins, as recommended by the WHO [6]. The gathered literature was analyzed such that a polygonal function could be established, by defining ten-year standards for organ and blood-flow rates. In most cases values were reported as a geometric mean (\bar{x}_i), with the corresponding standard deviation (SD). Extracted organ weights were processed to an overall mean (\bar{x}) by applying the following equation:

$$\bar{x} = \frac{\sum_{i=1}^i n_i \bar{x}_i}{\sum_{i=1}^i n_i} \quad (\text{Eq. 1})$$

Here, \bar{x}_i is the mean of the i^{th} study and n_i represents the number of test persons in that study. In order to compute the overall standard deviation (SD) for a certain age bin, the following equation was used considering the standard deviations from each study (SD_i):

$$SD = \sqrt{\frac{1}{\sum_{i=1}^i n_i} \cdot \left(\sum_{i=1}^i ((n_i - 1) \cdot SD_i^2) + \sum_{i=1}^i (n_i \cdot (\bar{x}_i - \bar{x})^2) \right)} \quad (\text{Eq. 2})$$

In cases where the reported study mean and standard deviation define a lognormal distribution, the associated geometric mean value \bar{x}_i and standard deviation SD_i of the lognormal distribution were calculated to obtain comparable parameters, as follows:

$$\bar{x}_i = e^{\bar{x}_i + \frac{SD_i^2}{2}} \quad (\text{Eq. 3})$$

$$SD_i = \sqrt{(e^{SD_i^2} - 1) \cdot e^{2\bar{x}_i + SD_i^2}} \quad (\text{Eq. 4})$$

3.2.3 Workflow for elderly PBPK model development

The workflow for this study is described in Figure 3-1. Since biological and chronological ageing differ, the data was analyzed in 10-year age bins, as recommended by the WHO [6] and interpolated linearly. Thus, the data was pooled into 7 age bins covering the age range of 30 to 100 years, in order to derive the distinctive age-related body composition along the lifespan throughout the European dataset. In cases where the pooling did not lead to an acceptable description of the organ ageing process because of insufficient data, additional data from North American and Australian subjects were included.

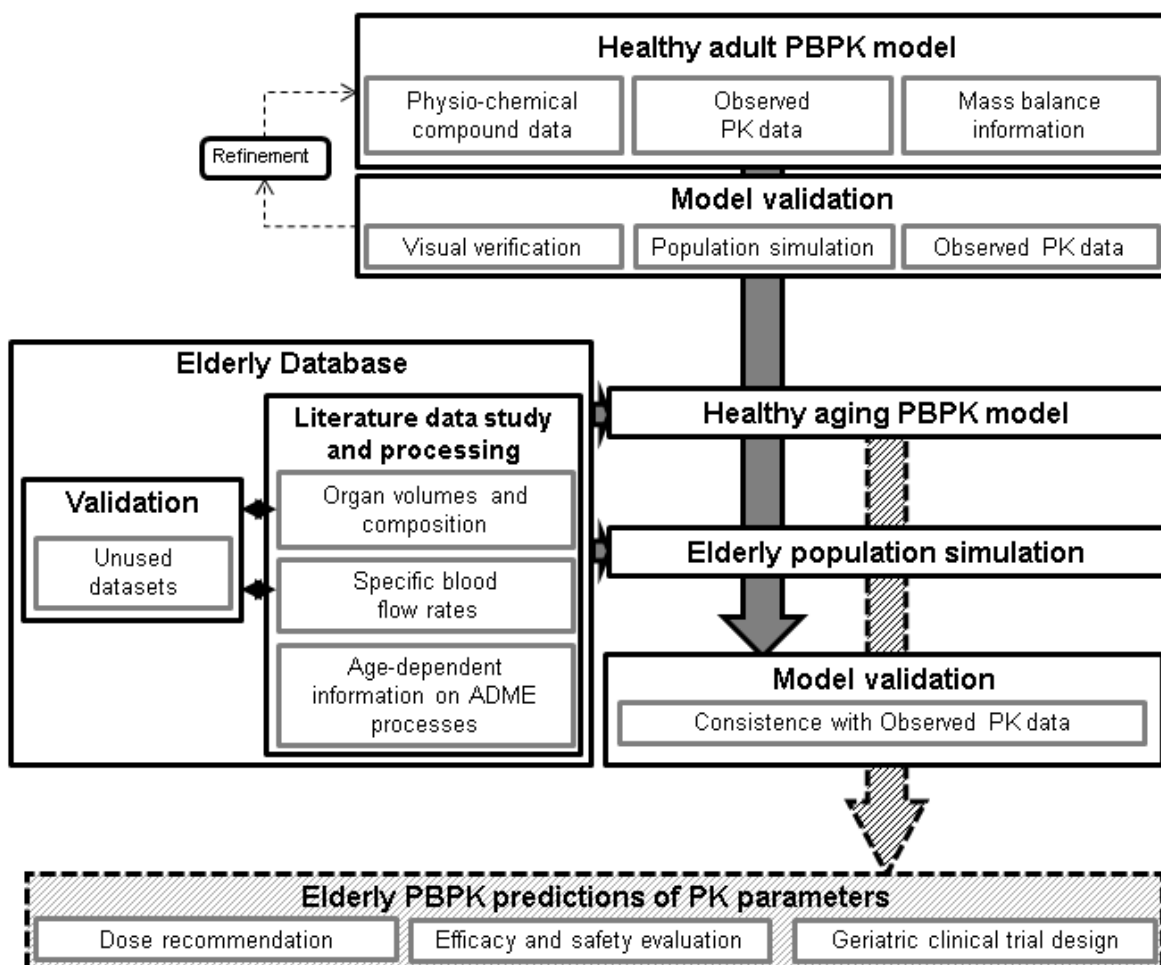


Figure 3-1 Workflow for the knowledge-driven physiologically based pharmacokinetic (PBPK) ageing approach. The *solid line* represents the work of the current study; the *broken line* depicts the potential usage of an ageing PBPK model. ADME: the absorption, distribution, metabolism and excretion processes; PK: pharmacokinetics.

Body composition for the same age might also vary between different historic time periods due to variations in anthropometric measures or potential impact of national nutrition [86]. In order to cope with these secular trends of study data published over the course of several decades, a reference anthropometric measure was generated for the age range of the ageing model considered for each 10-year time period over the past 60 years. It was applied whenever study data were stated without the corresponding subjects' anthropometric measures, to normalize organ weights for the scaling approach based on Willmann *et al.*

[112]. The underlying assumption of this approach is the correlation between organ sizes and their perfusion rates with body height, weight or mass index for a given age, gender and race. Starting from a mean individual, the anatomy and physiology of a target individual is scaled based on its anthropometric deviation from the mean individual.

The reported organ volumes originated mostly from autopsy studies, and thus represent cellular mass. They were used mainly in determining respective organ volumes, specific vascular fractions, the interstitial fractions, and the cytosolic proteins [113].

For each age bin the processed organ masses were summed up and found to reach 91-95 % of the body weight; the gap accounts for smaller organs not captured in this model, for example the adrenal glands, thyroid, tongue and prostate. In order to reach the final body weights, muscle and fat mass was increased in proportion to this gap.

Age-related changes in organ blood flow rates were accounted for as changes in cardiac output. Blood flow rates and cardiac output values were taken from the literature. The sum of all organ blood flows should be equal to the cardiac output. Thus, the unknown age-dependent organ blood flows were scaled with regard to their relative cardiac output contributions in adults as postulated by the ICRP report [102] to match the age-related changes in cardiac output. In these cases, the ratio between organ blood flow rate and cardiac output remained the same over the age span.

A virtual 30 year old individual was created using PK-Sim[®] [112]. Based on this individual, a virtual population [n=5000] for each sex was generated by only predefining the desired age range from 30 to 100 years. This population was used for checks of physiological consistency. Body water distribution and single, simulated sizes for each organ by the newly age-informed virtual population were compared to unused datasets or nomograms.

3.2.4 Database qualification

In order to assess the predictive ability of the knowledge-driven PBPK ageing approach, two compounds with different major elimination pathways were selected: the high-extraction drug morphine, which is eliminated up to 90 % by hepatic metabolism, and furosemide, which is eliminated mainly by the kidney. Model building parameters are listed in Table 3-1. The literature was screened for observed plasma concentration-time profiles and the corresponding PK parameters in healthy European volunteers ranging from young adults to the extremely elderly. Group data were preferred, but whenever individual data with a description of the subject's anthropometric measures was provided, corresponding virtual individuals were created. In case of missing anthropometric information, age-respective mean values were used. The reported intrinsic clearance values were used for the young adult simulation. Predictability of age-related impact on PK was then assessed in three steps. First, simulated plasma concentration-time profiles in the elderly were compared to observed profiles. In the second step, age-related changes in elimination were evaluated from shifts in elimination half-life ($t_{1/2}$). Finally, altered body composition and changes in the relationship between total body water and fat mass were assessed by calculating volume of distribution at steady state (V_{ss}) performing a non-compartmental analysis. Two-sided 1.25-fold and 2-fold levels of prediction accuracy for the ratio of predicted to observed values for plasma concentrations, $t_{1/2}$ and V_{ss} were applied for each compound.

Morphine

Morphine is a strong opioid analgesic indicated for cancer pain. Because of its basic alkaloid structure, morphine has a low lipid solubility. It is metabolized by several pathways leading to dihydromorphinone and normorphine. The plasma protein binding to albumin, globulin and glycoproteins of morphine is independent of its exposure. The drug has a high hepatic extraction ratio that is not affected by dose [114]. In the PBPK model, the metabolism of morphine was implemented as an intrinsic hepatic elimination process and thus affected only by age-dependent changes of hepatic blood flow and tissue size.

Furosemide

The loop diuretic agent furosemide induces the production of urine from water and sodium. It is moderately lipophilic and undergoes only minor metabolism in the liver, which is incorporated into the PBPK model as a non-specific intrinsic process. As furosemide is highly bound to albumin, renal elimination is driven mainly by tubular secretion, which delivers the compound to its site of action. Although clearance is transporter driven, the magnitude is accepted to be dose-linear for the therapeutic range [115]. Thus, tubular secretion was implemented as an intrinsic process in addition to passive glomerular filtration. Changes in kidney tissue and the vasculature are known to alter renal elimination of furosemide, and thus delivery to the target located at the luminal side of the sodium-potassium-chloride cotransporter in the loop of Henle [116].

Table 3-1 Overview of input parameters for the PBPK models of furosemide and morphine

Parameter	Furosemide	Morphine
Physicochemical		
Molecular weight (g/mol)	330.74	285.30
Log P	1.75 ^a	0.89 [117]
pKa	4.25 (acidic) ^a	7.90 (basic) ^a
Fraction unbound	0.03 [118]	0.80 [119]
Distribution		
Partition coefficient model	Willmann <i>et al.</i> ^b [108, 109]	Willmann <i>et al.</i> ^b [108, 109]
Cellular permeability model	Willmann <i>et al.</i> ^b [108, 109]	Willmann <i>et al.</i> ^b [108, 109]
Elimination		
GFR fraction	1	1
Renal clearance (mL/min/kg)	1.61 [120]	-
Hepatic clearance (mL/min/kg)	0.77 [120]	19.10 [119]

Log P: octanol-water partition coefficient, pKa: acid dissociation constant in log scale, GFR fraction: defines, if drug is only filtrated (1), reabsorbed (<1) or additionally secreted (>1)

^a Information obtained from Drugbank (<http://www.drugbank.ca>)

^b Willmann *et al.* is defined as the PK-Sim[®] standard

Statistical analysis

After the PBPK model was built using observed adult data, studies in the elderly were simulated by creating virtual individuals matching anthropometric measures of the clinical study populations or individuals. Virtual individuals were generated by two means: using either the physiology of a young adult as an uninformed simulation; or using the physiological information for the elderly gathered within this study as an age-informed simulation. The precision of simulated PK parameters was evaluated with the root mean squared prediction error (RMSE) and the bias based on the mean prediction error (ME) by weighing the residuals by the reciprocal concentration. In order to estimate the improvement when applying the age-informed physiology for the predictions of the elderly data set, a relative bias was calculated by subtracting the informed from the uninformed predictions (Δ ME). The same procedure was used to calculate the precision difference (Δ RMSE). The change was also set into relation to the uninformed predictions and expressed in percent.

3.3 Application of a lifespan PBPK population model for ciprofloxacin

3.3.1 Available data

At first, a comprehensive review of the published literature was performed focusing on pharmacokinetic information on ciprofloxacin following intravenous and oral administration in mainly healthy adults. Studies containing measured plasma concentration-time profiles, urinary excretion or the fractions for different elimination pathway contributions were gathered and extracted, respectively. In a second search step, pharmacokinetic studies in pediatrics and geriatrics were screened and analyzed. In case studies were conducted in patients, the impact of respective diseases or health condition on the pharmacokinetics in adults was reevaluated and excluded if confirmed. Since cystic fibrosis (CF) was identified as a covariate in a population pharmacokinetics analysis [121], studies including CF patients were excluded as well as studies in patients suffering from

sepsis [122, 123], organ impairment [124, 125], ectomy or observed during any other surgical procedures [126, 127]. Cancer patients were not considered due to contradicting observations derived from small study groups in this highly heterogeneous patient group [128, 129]. Furthermore, the study population should clearly represent a well-defined age group to allow an age-related PK assessment.

In total, 122 clinical studies reporting ciprofloxacin adult PK data published between 1983 and 2017 were screened, out of which 69 were considered in this study. The identified studies are listed in the Appendix (Table A-1 and Table A-2). For the pediatric age range, 4 studies were identified, whereas 14 studies were gathered for the geriatric age group. These studies are summarized in Table 3-2.

In addition to mean study data, individual plasma concentration-time profiles were gathered for pediatric and geriatric patients. Adult and geriatric individual plasma concentration-time profiles were obtained from three trials [130-132]. The 22 older adults were aged between 60 and 74 years of age and received 400 mg ciprofloxacin TID intravenously and a single 250 mg dose orally.

Table 3-2 Summary of clinical studies of ciprofloxacin sorted by dose in pediatrics and older adults used to define the prediction scenarios in this study and to assess the predictive performance of the ciprofloxacin PBPK model

Age [Years]	Population			n	Dosage			Reference	
	Females [%]	Weight [kg]	Height [cm]		Route	Formulation	Dose [mg]		Regime ^a
Pediatrics									
2-15	35			60	iv	suspension	10 ⁺	BID	[133]
0.7-7.1	54	14.3 (6.4-23.8)	90.5 (65-126)	16	iv	suspension	10 ⁺	TID	[134]
2-15	35	72.1 (66.8-78.8)		60	po	suspension	10 ⁺	BID	[135]
5-14*	43	5.5 (4.1-7.1)		7	po	unknown	15 ⁺		[136]
1-5	43	11.8 (8.3-17.3)		7	po	unknown	15 ⁺		[136]

Age [Years]	Population			n	Dosage			Reference
	Females [%]	Weight [kg]	Height [cm]		Route	Formulation	Dose [mg]	
Elderly								
66-90	78	66 (49.1-102.7)	168 (149-182)	9	iv	unknown	200	[137]
57-84	0	69 (52-80)	168 (155-175)	14	iv	unknown	200	[138]
67-83	0	72 (50-80)		14	iv	solution	200	[139]
65-87	35	65.6 (42-101)		17	iv	solution	200	BID [140]
44-96	95.5	67.09 (40-111)	160 (150-178)	44	iv	solution	200	BID [141]
63-76	0	76.9		8	iv	solution	250	[142]
67-83	0			6	iv	solution	400	TID [130]
67-83	100			6	iv	solution	400	TID [130]
60-73	40	65 (57-74)		10	po	tablet	250	[131]
71-86	0	65.1 (51-79)	161 (154-170)	12	po	tablet	500	[143]
63-76	0	76.9		8	po	tablet	500	[142]
65-87	35	65.6 (42-101)		17	po	tablet	500	BID [140]
63-76	0	76.9		8	po	tablet	500	BID [142]
68-76	0	62.1 (47.7-69.5)		6	po	tablet	750	BID [144]
61-82	0	70 (58-80)		15	po	tablet	750	[145]
64-92	40	56.5 (43.6-95.7)		20	po	tablet	750	BID [146]
58-77	10	64.3 (50-93)		10	po	unknown	750	[147]
66-90	78	63.4 (49.1-66.6)	168 (149-182)	6	po	unknown	750	[137]

Values are expressed with ranges (in parentheses)

^a Frequency of dose administration. BID twice a day; TID three times a day

* Age expressed in weeks

⁺ Dose in mg/kg bodyweight

For the children, a previously published data-driven population modelling dataset was used [121]. CF patients were discarded from the dataset resulting in 236 (143 male and 93 female) children included for this study. The individuals were treated for various infections and received 10 mg/kg twice a day (BID) orally or three times a day (TID) intravenously. In total, 763 plasma concentration-time data points sampled in non-CF children were available for this study.

3.3.2 PBPK model development of ciprofloxacin

Intravenous administration

The ciprofloxacin PBPK model building process was performed stepwise as depicted in the workflow scheme shown in Figure 3-2. First, physico-chemical data available in the literature were incorporated into an initial adult PBPK model. Reported mass balance data suggest 65.3% urinary and 11.4 % fecal excretion of unchanged ciprofloxacin after seven days following intravenous administration, whereas 19.6 % of the dose accounted for metabolites and 3.8 % were unaccounted [148]. Considering the reported mass-balance information, two first-order hepatic and two renal clearance processes were implemented in the model. Renal clearance processes include a passive GFR and an unspecific first-order tubular secretion to account for the renal clearance exceeding GFR. The active process was left unspecific although contribution of several transporters such as the ATP-binding cassette (ABC) drug efflux transporters [149] or organic anion transporters (OAT) [150] are discussed but not finally elucidated. Besides a first-order hepatic metabolism mediated by CYP1A2 [151], an additional active, unspecific GI-tract secretion was included. This process encounters the rapid GI transcellular and biliary secretion of ciprofloxacin [148, 152, 153]. The resulting luminal concentrations were consolidated by a continuous fraction of bile released into the gut. Less than 3 % of the mass balance information was not accounted for and proportionally distributed across all elimination processes.

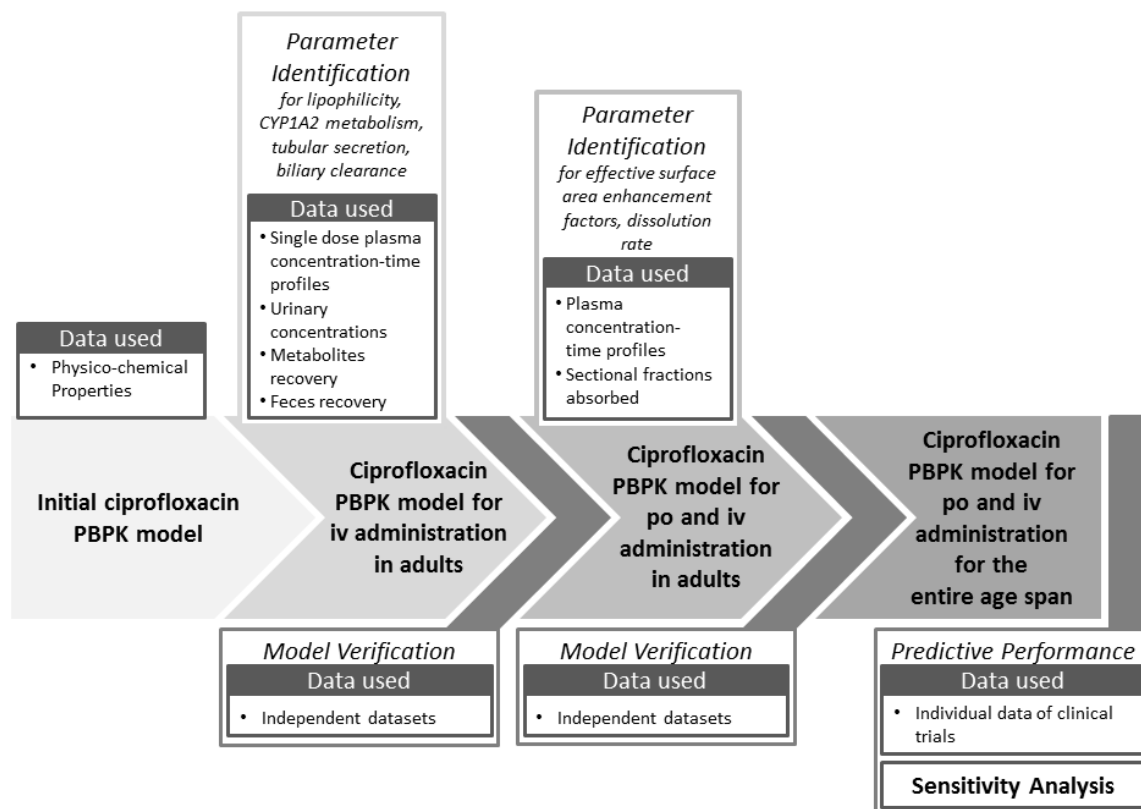


Figure 3-2 Schematic workflow of the ciprofloxacin PBPK model building and including estimated parameters, incorporated data and model verification. iv: intravenous, po: per os.

Oral administration and formulation

The mechanistic absorption model in PK-Sim[®] allows the identification of different factors contributing to the rate-limiting processes affecting the oral absorption of ciprofloxacin. Therefore, active uptake and dissolution profiles were estimated based on concentration-time profiles after oral administration of the solution, suspensions and immediate release formulations containing 100 to 750 mg active ingredient. Since the intestinal permeability (P_{int}) is a global parameter of the GI tract in PK-Sim[®], the effective surface area enhancement factor ($A_{effFactor}$), a multiplier of P_{int} in each intestinal segment of the GI tract [154], was estimated for each segment. By this, segmental net absorption impacted by active influx or efflux and deviating from the estimated passive absorption can be

accounted for by a respective increase or decrease of each $A_{\text{eff}}\text{Factor}$. Finally, *in vivo* dissolution was informed for each dosage form and dose level. The formulation and subsequent granulate disintegration and dissolution for each dosage form was estimated and assumed to follow a Weibull function. Similarly to parenteral administration, observed plasma concentration-time profiles following single and multiple administrations of oral doses were pooled for parameter identification. This allowed a separation of formulation- or GI tract-dependent influences.

3.3.3 PBPK model verification

In order to verify the adult intravenous and oral administration model of ciprofloxacin, population simulations in adult reference populations were compared to independent datasets (Table A-1 and Table A-2). Population simulations for each study and dosing scenario contained 1000 individuals matching the respective study characteristics. The performance of the adult ciprofloxacin PBPK model was assessed visually by goodness-of-fit plots of mean plasma concentration-time study data. Furthermore, the infinite and timely limited area under the plasma drug concentration-time curve (AUC_{inf} and $AUC_{0-\text{tau}}$) and, additionally for oral administration, the maximum plasma concentration (C_{max}) were determined using the non-compartmental approach of PK-Sim[®]. Mean model simulations were compared to mean literature observations. For the PK parameters ratio tests, model performance was evaluated by applying the bioequivalence criteria of 1.25-fold and the common 2-fold criteria [100] for simulation scenarios inside and predictions outside the model-building age range.

3.3.4 Scaling of the adult model for predictions in pediatric and geriatric patients

Once the final adult ciprofloxacin PBPK model was verified, exposure resulting from different dosing scenarios for both ends of the age scale outside of the previously simulated range were predicted by applying the underlying anatomical and physiological age-dependencies, as well as age-related clearance and protein binding information [79, 113, 155]. The predictions were carried out without any adjustment of substance-specific parameters defined for the adult reference ciprofloxacin model.

Scaling of the implemented clearance processes to the pediatric population age range was based on a previously published analysis [155]. For the scaling to the older adults, the active tubular secretion process was assumed to decrease proportionally to the GFR with increasing age. Therefore, the ageing function of the implemented unspecific tubular secretion was linked to the ageing GFR [79]. The hepatic elimination processes mediated by CYP1A2 and the unspecific biliary secretion were scaled in comparison with adult capability on a per-organ weight basis for the elderly population. This indirect scaling considered the age-dependent changes in liver size and perfusion, protein binding and hematocrit [79].

Formulation information derived during the model building process for adults were carried forward for the predictions in pediatrics and older adults. Age-dependent information on gastric emptying time, the pH of the GI tract, small intestinal transit times and the intestinal surface area were applied as defined in the underlying Open Systems Pharmacology database and published previously [156]. Since the specific transporters contributing to absorption and elimination of ciprofloxacin have not been fully elucidated yet, the effect of the maturation and ageing processes on these pathways is unknown. The resulting uncertainty can be minimized based on respective GI tract measure changes over age since transport processes are normalized to the surface area [154].

The scaled prediction scenarios were generated based on available literature data for clinical observations in children and older adults summarized in Table 3-2. Whenever the specific formulation administered was not stated in the respective study, the use of a single immediate-release tablet for the respective fixed dose and a solution for a body weight-based dose was assumed for the prediction.

The previously described model verification tests were also performed to allow a predictive performance analysis for scaling to the investigated age ranges. Additionally, AUC and C_{\max} predictions over the entire lifespan were compared to clinically observed data.

3.3.5 Sensitivity analysis

The impact of certain parameter changes was estimated in a sensitivity analysis for simulated C_{\max} following oral administration and AUC for representative individuals characterizing different regions in parameters' space. Investigating the influence of parameters on outputs provides valuable information on model performance, reliability, and significance of the results achieved.

The sensitivity analysis covered the entire age range assessed in this simulation study and was calculated for all 136 non-derived model parameters. The remaining parameters in the PBPK model were derived from these and were therefore investigated implicitly. Age classes were defined following the FDA binning [52] for the pediatric age range and continued with ten-year age steps from 30 years to the oldest old with testing the mean individual of each age bin.

The total sensitivity of the PBPK model is calculated by adding up each sensitivity of all parameters. In this analysis, parameters contributing to reach a cut-off defined by capturing 90 % of the cumulated total sensitivity were discussed. Therefore, parameter sensitivities were added up in a descending order starting with the parameter with the highest sensitivity until 90 % of the cumulated total sensitivity was reached. The more parameters needed to achieve the cut-off criteria, the better the robustness of a PBPK model. In case only a few parameters are needed, these should be well informed in order to rely on subsequent predictions.

Sensitivity analysis was performed numerically by varying each parameter separately with the factors 1/1.1, 1/1.05, 1.05, and 1.1. Individual sensitivity was then calculated as the slope of the linear regression line through the relative pharmacokinetic parameter changes in dependence of the different parameter variations. In other words, the sensitivity S was calculated for the representative virtual individuals detailed above as the average for the 4 perturbations Δ of different magnitude according to

$$S_{i,j} = \frac{\sum_{k=1}^n \frac{\Delta_k PK_j}{\Delta_k p_i} \cdot \frac{p_i}{PK_j}}{n} \quad (\text{Eq. 5})$$

with $n = 4$ and PK standing for the two (i.e. $j=1,2$) pharmacokinetic parameter outputs, p standing for the different parameters ($i=1,2,\dots,136$), and k representing the number of tested individuals. The p_i/PK_j -factor serves as normalization to the nominal values, which is important when comparing the influence of different characteristics and parameter values. Thus, the sensitivity values are dimensionless quantities. By this, a sensitivity of -1.0 implies that a 10% increase of the parameters, leads to a 10% decrease of the pharmacokinetic parameter value, and a sensitivity of +0.5 implies that a 10% increase of the parameters, leads to a 5% increase of the pharmacokinetic parameter value.

For each pharmacokinetic parameter output (PK_j) and parameter (p_i), maximal sensitivity values were defined as the maximum of the absolute sensitivity value for the set of all individuals Ind :

$$S_{Max,i,j} = \max_k \{|S_{i,j,k}| : k \in Ind\} \quad (\text{Eq. 6})$$

The parameters were then sorted in descending order according to $S_{Max,i,j}$. Mean parameter sensitivity values and their standard deviations were defined accordingly.

For each individual k , the variances of the sensitivity values were cumulated in order of their sorting defined above, according to

$$S_{Cum,k,l,j} = \frac{\sum_{i=1}^l |S_{i,j,k}|}{\sum_{i=1}^{136} |S_{i,j,k}|} \quad (\text{Eq. 7})$$

with $l=1,\dots,136$. The cumulated sensitivity as defined above includes normalization to the absolute total sensitivity. Therefore, the normalized total sensitivity $S_{total} = S_{Cum,k,136,j}$ equals to 1. A cut-off is defined by capturing 90 % of the cumulated total sensitivity. Since the sum of parameters needed to reach the cut-off as well as the identified parameters within this range might differ between the analyzed age groups, common and deviating parameters within this range were discussed.

4 Results

The overall body composition over the course of ageing as implemented in the PBPK population model for elderly is listed in Table 4-1, visualized in Figure 4-1 as progression of mean organ weights with ageing and in Figure 4-2 as distribution of mean organ weights over age as a fraction of body weight.

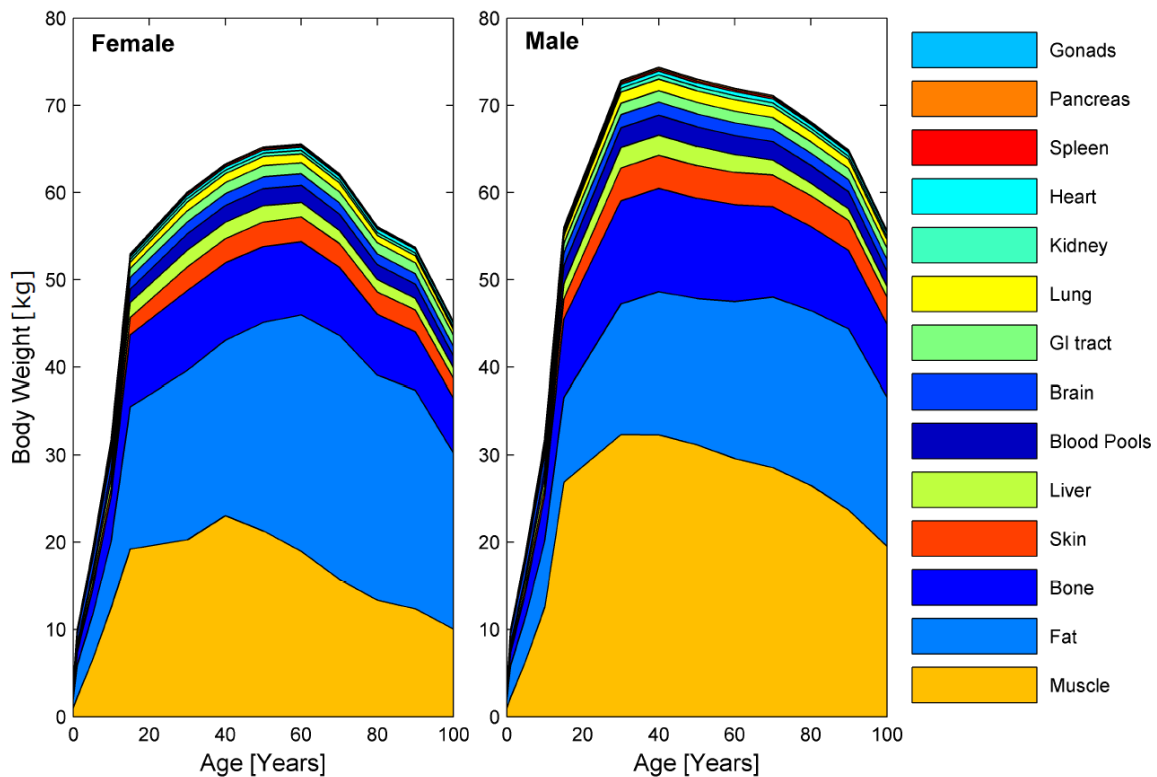


Figure 4-1 Distributions of mean organ weight from newborns to individuals up to 100 years of age. *Blood pools* represent arterial and venous blood, as well as blood in the portal vein, *GI-tract* summarizes the stomach, small and large intestine.

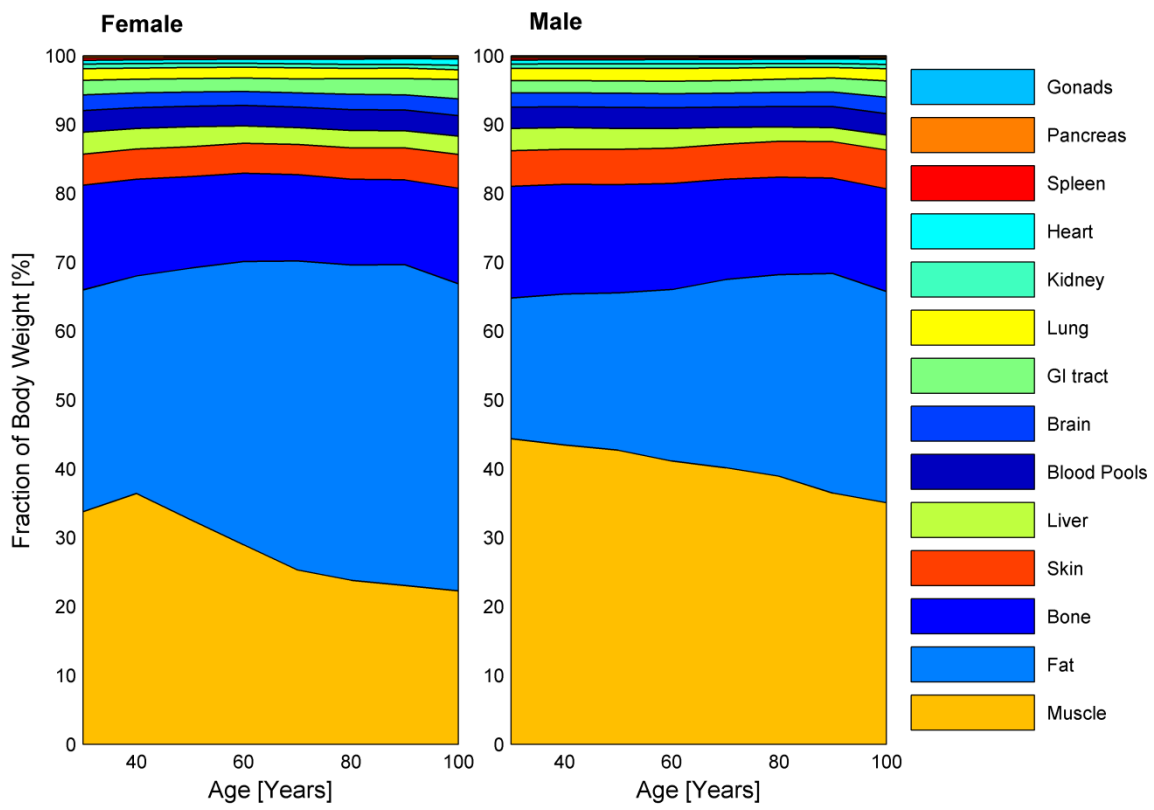


Figure 4-2 Mean organ weights from early adulthood up to 100 years of age as percentage of body weight. *Blood pools* represent arterial and venous blood, as well as blood in the portal vein, *GI-tract* summarizes the stomach, small and large intestine.

Table 4-1 Anthropometric measures, organ and tissue weights including blood as used in the elderly PBPK model

Parameter		Age [years]							
		30 ^c	40	50	60	70	80	90	100
Body weight (kg)	f	60.0	63.3	65.2	65.5	62.2	56.1	53.7	45.2
	m	73.0	74.4	73.0	72.0	71.1	68.1	64.9	55.6
Height (cm)	f	163.0	160.9	160.0	158.3	155.4	151.7	150.0	147.9
	m	176.0	175.1	173.9	171.2	167.4	165.5	163.8	157.6
Organ masses (g) ^a									
Blood Pools ^b	f	1899.4	1921.1	1961.2	1946.9	1847.7	1692.6	1634.5	1357.0
	m	2264.6	2269.5	2234.9	2180.2	2111.3	2042.5	1976.5	1739.5
Bone	f	9121.5	8886.3	8676.1	8401.8	7811.6	6981.4	6619.0	6263.5
	m	11817.8	11848.0	11481.6	11091.6	10355.0	9637.1	8969.0	8300.9
Brain	f	1357.0	1352.3	1347.6	1315.1	1287.3	1241.4	1169.4	1097.4
	m	1508.8	1506.9	1502.9	1463.3	1434.3	1400.1	1372.1	1344.2
Fat	f	19348.0	20002.5	23815.4	26993.0	27884.7	25694.5	25020.6	20171.4
	m	14868.0	16309.7	16676.5	17920.7	19447.4	19947.7	20691.0	17082.3
Gonads	f	13.1	13.0	6.6	5.3	5.2	5.1	5.1	4.9
	m	40.3	40.8	35.0	33.5	31.9	30.6	30.3	29.5
Heart	f	328.4	340.0	355.6	377.1	399.1	413.5	431.2	412.9
	m	417.2	434.3	439.1	454.6	464.8	441.4	437.9	425.1
Kidney	f	403.4	401.7	400.5	383.4	364.2	325.2	308.8	295.8
	m	437.7	475.9	468.1	455.6	441.7	395.7	366.7	355.9
Liver	f	1905.5	1881.0	1867.7	1679.8	1504.9	1423.4	1329.5	1189.4
	m	2357.8	2324.5	2206.0	2041.3	1714.6	1417.3	1324.0	1202.0
Lung	f	1009.5	1021.4	1038.8	1023.8	1005.4	849.1	804.5	637.3
	m	1294.3	1334.7	1337.4	1349.0	1271.8	1138.0	1007.4	978.0
Muscle	f	20276.2	23058.3	21300.1	18971.2	15746.4	13367.8	12394.3	10060.6
	m	32338.6	32318.2	31180.6	29600.0	28562.1	26524.8	23657.0	19534.0
Pancreas	f	169.5	170.3	163.8	158.7	148.5	131.9	128.0	122.6
	m	190.3	190.8	183.6	178.2	165.4	149.9	143.7	139.5
Skin	f	2723.5	2773.2	2836.2	2829.5	2725.8	2559.1	2493.8	2223.5
	m	3760.9	3790.2	3745.1	3692.0	3635.2	3537.0	3439.7	3122.6
Spleen	f	219.2	197.7	190.7	182.4	164.5	149.7	99.4	78.7
	m	243.4	221.9	208.2	197.0	186.6	160.4	133.4	108.4

f:female, m:male

^a Organ masses for GI organs were kept constant for females (1274.5 g) and males (1304.8 g) over the investigated age range^b Blood pools represent arterial and venous blood as well as blood in the portal vein^c Physiological and anatomical information of the 30 years old individual is derived from the ICRP reference man [102]

4.1 Physiological changes in the elderly

4.1.1 Anthropometric measures

Anthropometric measures were stated in almost every physiologic study. In addition, comprehensive European anthropometric studies were used, and coverage was dense for the age ranges of 30 to 100 years old [157-167].

In general, men tended to be taller and heavier than women at any age stage. Both sexes showed an increase in body mass to the age of 55 years, and then a progressive decrease. This decline starts at a 1.5 % decrease per decade and rises to nearly 10 % per decade between 90 and 100 years of age. Body height starts to decrease in early adulthood, after the age of 30 years, as visualized in Figure 4-3. As with body weight, the decrease sets on with a low rate of 1 % per decade and is comparable for men and women. In women this rate accelerates after menopause, culminating in a 4.2 % decrease of body height per decade in female nonagenarians. In males, height loss during the 10th decade averages only about 3.5 %.

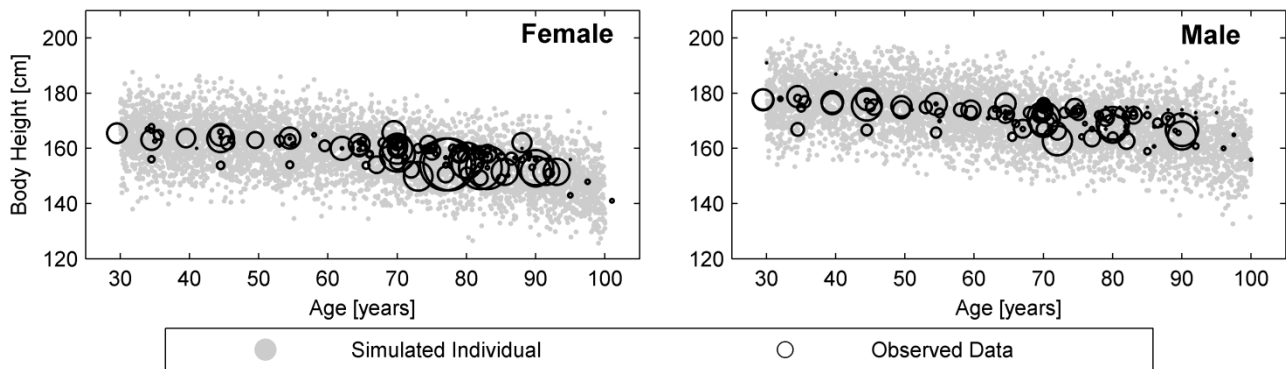


Figure 4-3 Age-dependent changes in body height, comparison between simulations and observations in females and males. Simulated individuals are represented in *grey dots* [n=5000] whereas observations of reference mean data are visualized in *black circles*. The reference data was gathered from anthropometric studies or studies where body height appeared as covariate. The sizes of the *black circles* indicate the relative numbers of subjects.

4.1.2 Muscle mass

Loss of muscle mass is assessed as part of the screening test for sarcopenia using the gold standards Computer Tomography (CT) and Magnetic Resonance Imaging (MRI) [168], but also using Dual energy X-ray Absorptiometry (DXA) [169-173] or Bioimpedance Analysis (BIA) [174-179] according to the European Working Group on Sarcopenia [180]. Janssen *et al.* introduced an equation enabling the calculation of skeletal muscle mass from BIA observations [181]. As decreases in muscle mass vary among different parts of the body, whole-body analysis was preferred for the data pooling. The decline of the maximum skeletal muscle mass from 37 % of body weight in female adults to 22 % in the centenarians follows a degressive trend and differs to the progressive reduction for males from 44% in adults to 34 % of body weight in the extremely old.

4.1.3 Fat mass

Similar to muscle mass, fat mass can generally be assessed using CT [182], MRI, BIA [165, 174, 183-187] or DXA [163, 188-200]. Estimations based on skinfold thickness and whole-body counter for total potassium content were not included due to the varying methods of calculation [201].

During aging, fat mass in females increases to an absolute maximum at the age of 70 years, whereas in males the peak is reached by the age of 65 years. Due to the diminished body weight and the severe loss of lean body mass from 70 to 100 years of life, the relative fat mass continues to increase, to as much as 45.8 % in female, and 31.5 % in male centenarians. Here, the increases are constant in males, with 0.98 kg fat mass /decade. Females, however, experience an accelerated gain of 3.5 kg fat mass /decade in the first two decades after menopause, and then a slower gain exhibiting the same rate as in males of the same age group.

4.1.4 Kidney weight

Four studies were included for model building [202-205]. These revealed that maximum kidney weight is achieved in the 4th decade and remains constant for almost 20 years before continuously declining. This decrease is associated with a loss of renal tissue and a

reduction in the number of nephrons, particularly in the renal cortex [206]. This results in a reduction of tubular and glomerular cells, and thus affects the GFR [207, 208].

4.1.5 Liver weight

The number of hepatocytes is reduced in the elderly, whereas the single-cell volume initially increases but subsequently decreases [209]. Thus, the number of hepatic lobules is constant over the course of aging, but the size of the liver declines, whereas collagen accumulation induces a widening of the perisinusoidal space [210]. In females liver mass decreases almost linearly, at the rate of 8.3 % per decade after the age of 40 years, whereas in males it proceeds in two steps: an initial decline of 6.1 % per decade to the age of 60 years, followed by a more rapid loss of 11.4 % per decade [203-205, 211, 212]. This tendency was determined from autopsy analysis, but was also detected in imaging studies [213-215].

4.1.6 Brain

Results of five studies in European subjects indicated that in both genders a minor decrease in brain weight begins in early adulthood and continues at a steady rate until the 5th decade, at which point the rate accelerates [204, 216-219]. These findings are in line with results from a large autopsy study on brains of white North Americans conducted by Dekaban *et al.* [220], as well as with recent longitudinal observations [221]. Also this tendency is consistent with findings from earlier studies in Europeans [222, 223]. These data were utilized to simulate the age distribution of brain weight, and subsequently verified using a nomogram developed by Hartmann *et al.* [224], as shown in Figure 4-4. Given that patients with Alzheimer's Disease show a severe cortical atrophy [225], they were excluded from the current analysis.

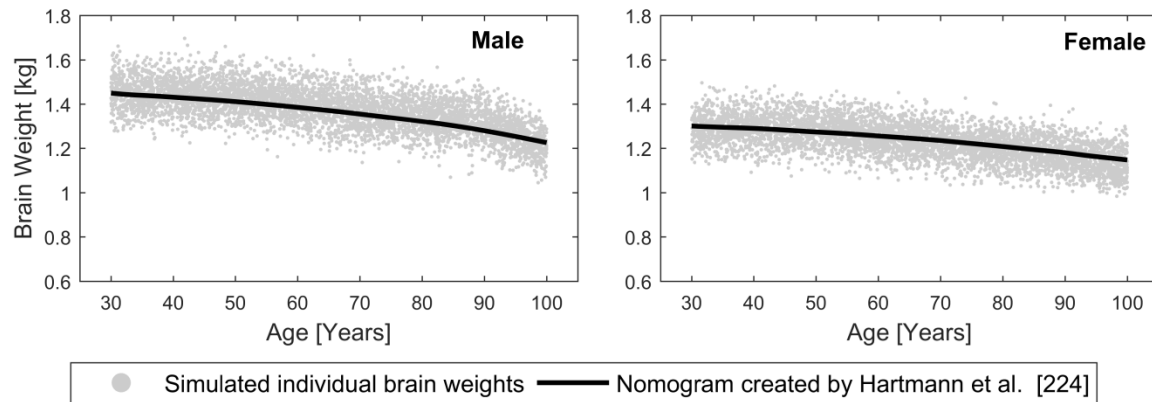


Figure 4-4 Simulated age distribution of brain weight compared to the nomogram of Hartmann *et al.* [224]. Simulated individuals are represented in *grey dots* [n=5000] whereas the nomogram is visualized with the *black line*.

4.1.7 Heart

Aging is associated with a loss of myocytes (which is particularly evident in males) and a concomitant increase in volume of the remaining myocytes [226, 227]. At the same time, amyloid disposition advances uniformly throughout the myocardium [228]. Ventricular mass thus increases continuously over the course of aging. Studies analyzing the volume and composition of heart tissue were carried out mainly by autopsy [203, 204, 229-235]. Analysis of the data in the literature was followed by verification of the results with the recent centile charts of Gaitskell *et al.* as shown in Figure 4-5 [236].

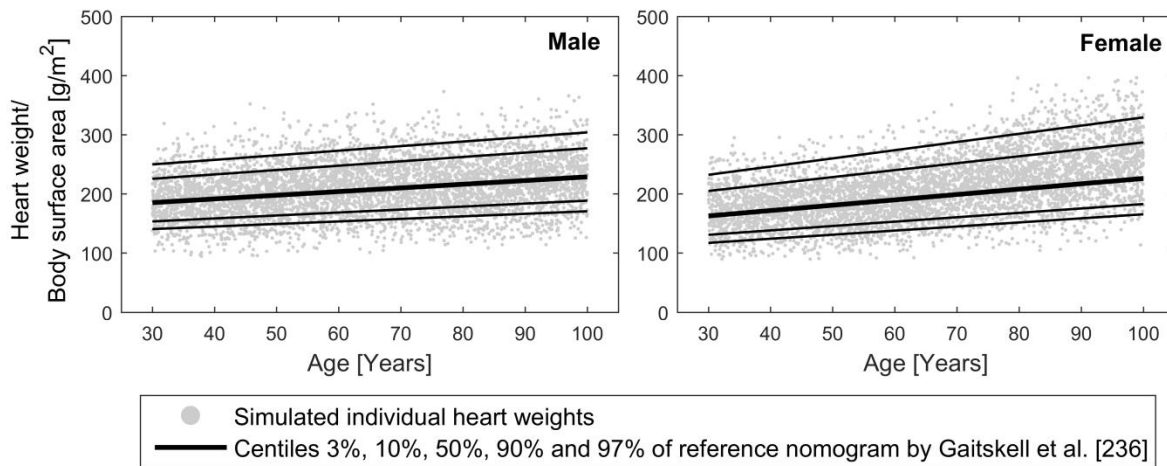


Figure 4-5 Simulated age distribution for heart weight compared to the nomogram of Gaitskell *et al.* [236]. Simulated individuals are represented in *grey dots* [n=5000] whereas the nomogram is visualized with the *black line*.

4.1.8 Bone

Bone mass is often described by the term bone mineral density (BMD), which is calculated by dividing the bone mineral content (BMC) by the bone area. Analysis of BMD indicates that body size has a marked influence on the bone mass, and thus is adequate for longitudinal assessment of the risk of osteoporosis and as an indicator of bone strength, but not for inter-individual comparisons [237]. Instead, analysis of whole-body BMC normalized to the surface area of the bone is usually used for a direct comparison over the course of maturation [238, 239] and in older adults [240], as well as for cross-sectional data. It is therefore applied in this analysis for inter-study comparison in elderly individuals.

European Caucasians gain bone mass through the age of 25 years and maintain this mass for at least a decade. In men, the loss of bone mass begins at the age of 40 years with a decrease of 0.54 % per year. In women, this rate increases to 1.41 % per year after menopause and is continuing at this rate over the following 5 to 10 years [163, 188, 196-200, 241-243]. In men, the rate of bone loss is constant and increases only slightly in old age. The rate in women reverts to one similar to that in men after the faster loss related to menopause, but during the 10th decade gradually increases in women to a rate of 6.75 %.

4.1.9 Gonads

Studies carried out in females on hormone replacement therapy were excluded, as this treatment has a dominant impact on uterine size following the menopause. The size of the uterus is markedly decreased during menopause due to atrophy. Volumetric decrease rates are highest during the initial decade after menopause, with a loss in weight of almost 50 %. After the age of 60 years, this rate is attenuated to a nearly constant decrease of 1.89 % per decade [223, 244].

Men undergo a gradual involution of the testis, at a rate of 3.40 % per decade. The size ratio of the tunica albuginea to rete testis is unaffected over the course of aging, and this is also true for the sizes of the two testes. [245-248].

4.1.10 Lung

Whereas the functional capability of the pulmonary system declines slowly but gradually after the age of 25 years, lung mass is not reduced in the same manner. In men lung tissue mass reaches its maximum at the age of 60 years, and in women it does so a decade earlier. In women, the subsequent decrease progresses gradually, at a rate of 50.3 g/decade. In men, however, the loss initiates at 77.1 g/decade and advances to 130.5 g/decade [205, 223].

4.1.11 Pancreas

The pancreas undergoes atrophy and fatty infiltration as well as intra-lobular fibrosis in older individuals. With a cellular weight of 140 g in adults, decline of weight initiates at 13.8 g/decade and continues at a rate of 5.85 g/decade between the ages of 80 and 100 years, mainly due to a loss of parenchymal tissue [111, 249-251].

4.1.12 Skin

The skin includes both the epidermis and the dermis, a deeper connective-tissue layer. Most common areas of skin thickness studied are the forearm and trunk or limbs, and this is analyzed by ultrasound. Only a few studies have examined the changes in skin thickness of more than two parts of the body and thus have visualized the overall changes in skin thickness during the aging process [252]. Changes in skin thickness and aging are driven

mainly by sun exposure and smoking but not pigmentation. Age has only a minor influence and can be described by a decrease in skin thickness in the cellular part of the epidermis and dermis after the age of 40 years in women, and after the age of 45 in men [253-256]. The stratum corneum remains unaffected [257, 258] with respect to thickness but undergoes a decrease in its moisture content. However, the skin barrier function is maintained even in extreme old age. In the basal layer, the number of cells per unit area decreases due to constrained proliferation. The abundance of microvilli, Langerhans cells and keratocytes declines, and thus the transdermal permeability to drugs altered [259]. In the dermis, the collagen fibers become reduced in number, thicker and less soluble. The decrease in collagen is linear [255, 260, 261].

4.1.13 Spleen

Studies of changes in splenic weight over the course of aging have produced inconsistent results. Autopsy studies reporting data for various age bins have concluded that spleen volume declines after early adulthood [203-205, 262]. Other autopsy and *in vivo* measurement studies have reported that spleen size is neither affected by age nor by gender; however, these do not describe the data that are the basis for this conclusion [263, 264]. An analysis of the available data suggested that in men a moderate absolute loss of cells (6.08 g/decade) occurs from adulthood to the age of 70 years, and that it progresses at a rate of 13.5 g/decade until the age of 100 years. In women, the initial decrease of cellular mass is 3.96 g/decade until the age of 60 years, and it rises to 8.45 g/decade thereafter until the age of 100 years. Thus, loss of spleen weight in relation to body weight can be up to two fold.

4.1.14 Cardiac output

Williams conducted a comprehensive literature analysis on changes over the course of aging in cardiac output and cardiac index, a parameter which relates the cardiac output to the BSA [265]. His study revealed that an initial decrease in cardiac index after the age of 20 years developed into a marked reduction after the 6th decade of life. Given that Williams summarized predominantly North-American reports and a large Japanese trial, European studies were screened to control for potential racial variations. The studies taken into

account for evaluating both changes in cardiac output [266-269] over the course of aging and the underlying distributions are listed in Table 4-2.

Females showed an almost linear decrease in cardiac index of 3.22 % per decade after the age of 30 years. The slowing of the cardiac blood circulation is more precipitous in males; whereas it starts out at 1.46 % per decade during early adulthood, followed by a stronger decrease of 8.30 % per decade in the elderly age range. These results have been confirmed by studies on stroke volume [270-272], assuming that heart rate remains constant over the lifespan. However, due to contradictory reports on changes in heart rate over the course of aging (some reports support a decrease in heart rate, due to the dropout of pacemaker cells [273, 274], whereas others indicate that heart rate increases in female subjects [275]), reports on isolated stroke volumes were not taken into account.

4.1.15 Cardiac output distribution

Kidney blood flow

In the kidney, the age-dependent decrease in absolute perfusion rate is more severe than weight loss. In comparison to the perfusion rate, the overall reduction in cardiac output proceeds at a slower rate. Correlation of kidney perfusion and filtration performance was shown in a larger population ranging from 20 to nearly 90 years of age [276]. Para-aminohippuric acid (PAH) is the marker substance of choice for the assessment of renal blood flow; in the past it was diodrast [277-279].

Hepatic and splanchnic blood flow

In healthy adults, the pre-portal organs, including the stomach, intestines, pancreas and spleen, provide about 75 % of the portal blood flow [113]. This relationship seems to be maintained over the course of aging, although the total flow rate decreases [280]. Additional shunting is negligible when blood flow rate is reduced and portal pressure remains constant. The hepatic blood flow itself is measured using the dye dilution method, where a subject is catheterized in the portal and the hepatic veins [214]. In order to

eliminate potential anastomosis, additional studies based on Doppler measurements were integrated into this analysis.

Although no absolute information is obtainable for splanchnic blood flow, relative alterations can be analyzed by Laser-Doppler flowmetry. Analysis of the blood flow in the superior mesenteric artery is the most common assessment of alteration in splanchnic perfusion [281-283]. Although the superior mesenteric artery is one of three vessels that contribute to the splanchnic blood supply, it is the major sustenance vessel of the small intestine, the duodenum and the colon. Alterations in perfusion of the stomach, pancreas and spleen can also be captured by this method. The ratio of splanchnic blood flow to cardiac output gradually decreases from 22.5 % in adults to 17.5 % during the tenth decade of life [284-287].

Adipose tissue blood flow

Only two studies have quantified absolute values for changes in blood flow to adipose tissue over the course of aging in humans [288, 289]. For this tissue, it is only possible to assess general decreases in specific blood flow rates; shifts in the disposition of body fat and in fatty tissue hydration during aging impede studies in single fat depots.

Cerebral blood flow

Cerebral perfusion decreases linearly over the course of aging. Age-associated regional differences of reduction in perfusion have been discovered recently by Chen *et al.* [290]. Although the results indicate that the reduction in older age is severe due to increasingly pronounced decreases in perfusion in the cortical area, this study failed to support a non-linear trend. However, studies that included data from additional sources revealed a linear reduction of 3.27 ml/year in female subjects, and a 3.01 ml/year decline in males [291-294].

Muscle blood flow

Although muscle mass is reduced with age, the blood flow to this tissue is unaffected over time [295-298]. However, the redistribution cascade initiated by physical load is altered in older adults, and is not adequate to support higher workloads [285].

Myocardial blood flow

Single-photon emission computed tomography (SPECT), cardiac magnetic resonance (CMR), and positron emission tomography (PET) are reliable methods for assessing the development of myocardial perfusion, and are used primarily to evaluate obstructive coronary artery disease [299]. Although diastolic relaxation is impaired during the progression of healthy aging, the myocardial blood flow increases only minimally [300-305]. Deviations by ethnicity have been observed [306], and multiethnic studies have confirmed this phenomenon [307]. Notably, although the myocardial blood flow is generally higher in women, the increase in flow rate over age is higher in men.

Skin blood flow

The decrease in blood supply to the dermal tissue layers is caused not only by the overall restriction in cardiac output; it has also been attributed to a diminished microvasculature. The loss of small vessels can be accelerated by photo damage, an effect that varies by body region [308]. For assessment of changes in skin blood flow, microdialysis in combination with Laser-Doppler flowmetry studies have predominated. Given that the results of these studies are reported in relative values with arbitrary units, it is not possible to interpret the data as a whole. Although the variability of the individual studies is high, no significant changes in cutaneous blood flow per unit were observed [309-312]. The response was impaired only in the context of exposure to heat or stress, due to reduced coverage of cutaneous tissue with capillary vessels.

In summary, information on blood flow alterations implemented into the elderly PBPK approach is listed in Table 4-2. The general lack of perfusion data impeded the computation of a robust variability for each blood flow rate, so that a 5 % coefficient of

variation was assumed as accepted for other approaches [313]. In total, 118 studies comprising 47029 male and 67419 female subjects were included to build the elderly PBPK database. All studies considered for the elderly PBPK population model and the total numbers of subjects comprised in these studies used to inform the changes in the respective organ are listed in Table 4-3.

Table 4-2 Cardiac index and organ blood flow rates used in the elderly PBPK model

Parameter		Age [years]							
		30 ^c	40	50	60	70	80	90	100
Cardiac index (L/m ²)	f	3.34	3.33	3.08	2.89	2.75	2.68	2.52	2.41
	m	3.23	3.22	3.09	2.86	2.58	2.36	2.18	2.04
Organ blood flow (ml/min)									
Adipose	f	501.1	528.2	578.0	655.3	684.7	630.2	607.0	491.5
	m	324.7	352.1	357.3	381.4	408.0	419.8	429.2	357.3
Cerebral	f	707.8	686.9	666.1	632.1	601.2	562.8	514.2	467.6
	m	779.7	747.6	727.9	692.9	650.6	623.8	594.4	536.1
Gonads	f	1.2	1.2	0.6	0.5	0.5	0.5	0.5	0.4
	m	3.2	3.3	2.8	2.7	2.6	2.5	2.4	2.4
Myocardial	f	295.0	311.2	313.2	363.1	376.3	445.8	464.8	445.2
	m	260.1	271.1	278.0	299.1	308.7	334.7	332.1	322.3
Renal	f	1121.0	1061.8	943.8	825.8	707.8	589.8	471.8	353.8
	m	1325.0	1339.3	1116.3	913.3	730.3	567.3	424.3	301.3
Splanchnic ^a	f	1239.0	1254.3	1187.2	1015.3	862.6	771.5	679.1	570.5
	m	1235.0	1241.9	1237.7	1056.7	813.1	610.6	512.9	413.5
Hepatic	f	383.4	388.1	367.3	314.2	266.9	238.7	210.1	176.5
	m	423.0	425.4	423.9	361.9	278.5	209.1	175.7	141.6
Muscle	f	665.1	774.8	636.6	568.4	479.8	405.6	369.0	298.8
	m	1105.7	1086.8	1036.8	975.0	922.3	861.7	751.9	625.9
Skeleton	f	294.9	287.3	280.5	271.6	252.6	225.7	214.0	202.5
	m	324.9	325.8	315.7	305.0	284.7	265.0	246.6	228.2
Skin	f	295.7	301.1	307.9	307.2	295.9	277.8	270.7	241.4
	m	325.1	327.7	323.8	319.2	314.3	305.8	297.4	270.0

f:female, m:male

^a Splanchnic blood flow rate combines gastro-intestinal, pancreatic and splenic blood flow and describes the portal blood flow

^b Cardiac output distribution information of the 30 years old individual is derived from the International Commission on Radiological Protection (ICRP) reference man [102]

Table 4-3 Studies (including the numbers of subjects) utilized for model building to determine changes in organ volume and specific organ blood flow development over the course of aging in healthy European Caucasians

Physiological measure	Number of Subjects				References
	Females 30-65 years	Males	Females >65 years	Males	
Anthropometry	2580	2514	12643	5283	[157-167]
Volumes					
Bone	1360	264	7896	105	[163, 188, 197, 199, 200, 241, 242]
Brain	672	1388	421	421	[204, 216-219, 221]
Fat	6548	5638	12824	2011	[163, 165, 174, 182-186, 188-194, 197]
Gonads	426	71	268	205	[223, 244-248]
Heart	1208	1739	2647	2852	[203, 204, 229-235]
Kidney	2300	3798	2635	3871	[202-205]
Liver	1226	2380	1419	2568	[203-205, 211, 212]
Lung	604	609	369	331	[205, 223]
Muscle	1829	2129	577	579	[174, 175]
Pancreas	521	336	1006	734	[111, 249, 251]
Skin	164	117	222	214	[253-256]
Spleen	1882	2775	2639	3223	[203-205, 262]
Blood flow rates					
Cardiac Output	97	174	79	97	[266-269]
Adipose	26	15	4	5	[288, 289]
Cerebral	130	197	59	48	[291-294]
Splanchnic	0	19	21	16	[284-287]
Kidney	0	39	3	14	[277-279]
Muscle	0	16	13	16	[295-297]
Myocardial	100	191	1	13	[300, 302, 304, 305]
Skin	0	7	0	7	[311]

4.1.16 Total body water distribution

Total body water remains stable throughout most of adulthood but decreases starting in the 6th decade of life. Race and sex have been associated with differences observed over the complete lifespan [314]. Normalization of total body water to body weight reveals that the ratio declines gradually during the aging process. This reduction is mainly due to the loss of intracellular water; the ratio of extracellular water to body weight is maintained during aging. These changes are visualized in Figure 4-6, together with observed data in healthy Caucasians [165, 185, 315-318].

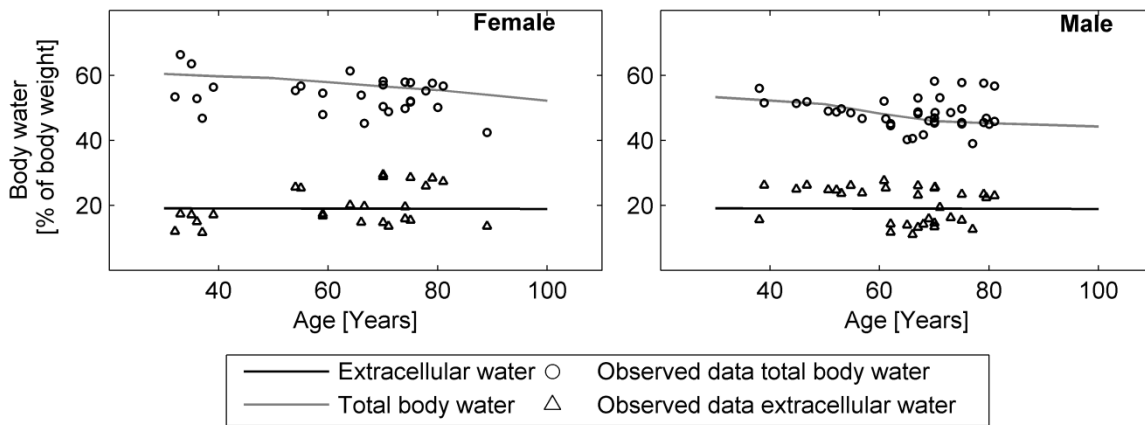


Figure 4-6 Distribution of body water in females and males over the course of aging. Extracellular (*dark grey lines*) and total (*light grey lines*) body water as percentage of body weight. Values reported in the literature for extracellular water (*triangles*) and total body water (*circles*) are shown for comparison.

4.1.17 Albumin

The mean serum albumin concentration decreases marginally with advancing age. Health conditions and nutritional status have a more pronounced impact [319, 320]. The decline of mean serum albumin is linear from 65 to 90 years, but becomes more severe thereafter [321-324]. No gender effect has been observed.

4.1.18 Alpha-1-acid glycoprotein

The acute-phase protein alpha-1-acid glycoprotein (AAG) is a predominant binding partner for basic lipophilic and neutral drugs. As its levels have large intra-individual variability, particularly in the context of disease and disease progression [325], estimates of changes in mean plasma levels over the course of aging have been inconsistent. However, a general stepwise regression analysis of available data for Europeans suggested that the mean AAG concentration was unchanged across the elderly age range, not differing between males and females [321, 323, 324]. This was consistent with data from healthy North Americans; there was no evidence for a difference between these groups.

4.1.19 Hematocrit

Similar to serum albumin levels, mean hematocrit (HCT) values in the elderly are only slightly lower than those in younger adults, although the range is amplified on the lower end [324, 326-328]. In the elderly age range, health conditions and nutritional status may account for the observed differences. Furthermore, the HCT range in Europeans does not differ from that in white Americans [320].

4.1.20 Glomerular filtration rate (GFR)

Although serum creatinine is widely used to predict GFR in the elderly population, it does not lead to reliable results. Due to the dependence on food intake [329], concentration of lipids [330], age, muscle mass and race [331], the variability in serum levels of this marker may lead to an under- or overestimation of GFR. Even small changes in serum creatinine levels can reflect major changes in GFR as the relationship is not linear. Furthermore, creatinine clearance is inversely correlated with blood pressure [332]. Moreover, a second endogenous marker of GFR, cystatin C, has its own pitfalls and is not sufficiently reliable in older people, especially in males, smokers, overweight individuals, tall individuals, or individuals with elevated levels of C-reactive protein [333].

A better but more time consuming method for assessing GFR is the use of exogenous markers, the gold standard being inulin [334]. However, this requires continuous inulin infusion, during which its clearance via the urine is measured. This procedure is not

feasible within large trials. However, results from analyses using non-radiolabeled markers should be interpreted carefully as they might slightly underestimate the GFR [335].

Another potential source of bias for GFR estimations is the standardization to BSA. Currently, different equations are in use for calculating the BSA, and only a few studies mention which equations were applied.

Almost as precise and more routinely used are the markers ^{125}I othalamate [335], $^{99\text{m}}\text{Tc}$ -diethylenetriamine-pentaacetate (Tc-DTPA) [336, 337], ^{51}Cr -ethylene-diamine-tetraacetate (Cr-EDTA) [336, 338] and iohexol [339]. In the case of the non-radioactive iohexol, measurements suggest that GFR decreases by about 1.0 mL/min/1.73 m²/year (157). Comparing the results obtained from all of these methods can lead to reliable results [340].

In order to generate population samples large enough to investigate GFR, most studies have been carried out in prospective renal transplant donors using exogenous markers [335, 336, 338, 341]. An analysis of the gathered and BSA-adjusted data for 1213 females and 1081 males was performed. This resulted in a slight reduction starting at the age of 30 years, and a more rapid reduction starting at the age of 40 years.

The GFR in PK-Sim[®] is linked to maturation of the kidney volume and described by a Hill function [342]. To describe the effect of aging on GFR, a new, reverse sigmoid hyperbolic maturation function was developed and optimized with the MATLAB function *lsqnonlin* starting (for both sexes) at the age of 30 years.

$$\text{Specific GFR}_{30-100y} = F_{PMA} \cdot \left(1 - \frac{V_{max} \cdot (\text{age} - 30\text{years})^{\text{Hill}}}{TA_{50}^{\text{Hill}} + (\text{age} - 30\text{years})^{\text{Hill}}} \right) \quad (\text{Eq. 8})$$

Here, F_{PMA} is the specific GFR derived from the sigmoid hyperbolic maturation function [342] after full maturation is achieved in the 40th week of gestation (26.6 ml/min/100 g kidney weight) [343]. In order to describe the effects of aging on kidney function, the maximal decreasing rate factor (V_{max}) was set to 0.9 ml/min/100 g kidney weight, the aging half-time (TA_{50}) to 59 years for females and 54 years for males. The Hill coefficient is parameterized at 1.5. The resulting function over the aging period is visualized in Figure 4-7. Whereas the specific GFR function is parameterized using the observed GFR values

and assuming the mean kidney weight at the respective age, the variability is entirely dependent on the deviation in kidney weight.

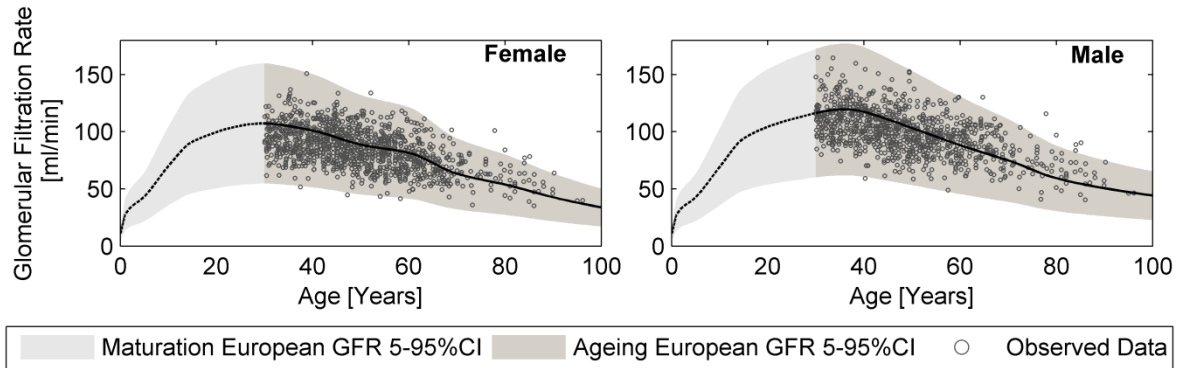


Figure 4-7 Changes in kidney function in females and males over the course of ageing compared to literature values. The *solid black line* represents the new GFR function in relation to kidney weight, whereas the *dashed black line* represents the maturation of GFR function according to Rhodin *et al.* [342]. The *grey shaded areas* represent the predicted 95% percentile range based on kidney size variability. The *black circles* depict the observed GFR rates [335, 336, 338, 341].

4.2 Predictability of PK data in the elderly

In the next step, the paradigm compounds furosemide and morphine were applied to qualify the capability of the PBPK population model and to predict drug distribution and elimination of drugs.

Morphine

The literature screen for observed PK data led to inclusion of several studies for morphine [344-353] as listed in Table 4-4.

Table 4-4 Summary of clinical studies after intravenous dosing for the test compound morphine used to compare the simulated data

Dose	Age [years]	n	Height [cm]	Weight [kg]	Reference
Morphine					
0.125 mg/kg	30.6 (24-40)	11		62.6 (47-85)	[344]
10 mg	27.4 (26-30)	8		67.6 ± 4.5	[345]
	74.0 (68-90)	9		66.4 ± 3.2	
5 mg	31 (26-40)	6			[346]
5 mg	30.2 (25-44)	10		72 (63-83)	[347]
5 mg	25.8 (20-40)	6		71.4 (49.2-102.1)	[348]
0.05 mg/kg	76.1 ± 4.5	16	167.4 ± 8.3	77.8 ± 16.9	[349]
10 mg	(22-29)	12		76.4 ± 7.4	[350]
10 mg	(20-39)	14		74.9 ± 11.0	[351]
7.5 mg	26 (23-30)	6	176 (165-187)	71 (54-98)	[352]
0.15 mg/kg	(22-54)	6			[353]

Values in curved brackets indicate the range; ± indicates standard deviation

The simulated plasma concentration-time profiles of morphine in healthy adults were consistent with the observed data, as visualized in Figure 4-8. Whereas 42 % of the simulations for young adults were outside the 1.25-fold range, only 18 % of the predicted plasma concentration-time points were outside this range for older adults. For both age groups, the number of under- and overpredicted plasma concentration-time points were

equally distributed to both sides of the 1.25-fold range. All plasma concentration-time points were predicted within the 2-fold range.

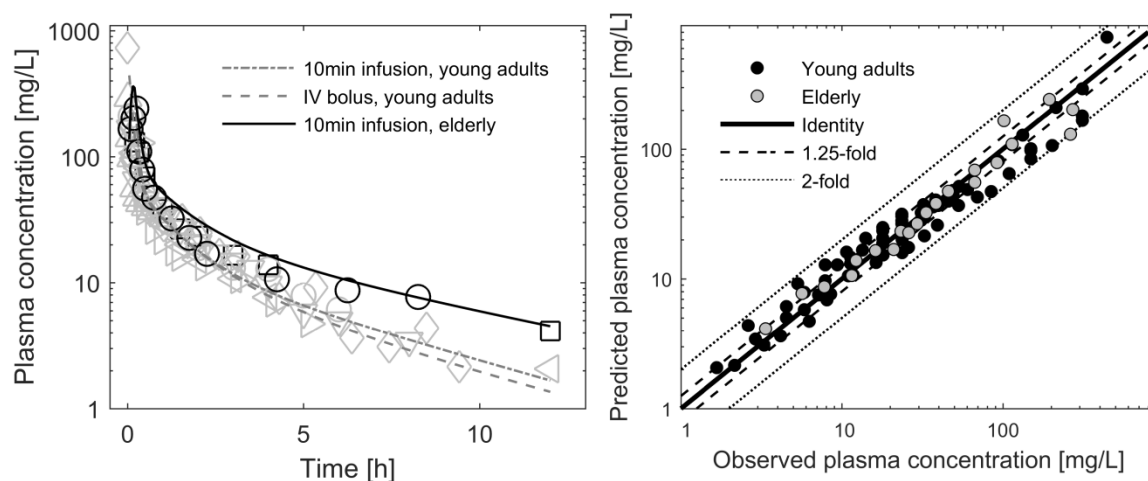


Figure 4-8 Predicted and observed plasma concentration-time profiles of morphine in younger adults vs. the elderly. Predicted mean plasma concentration-time profiles (left) for younger adults are visualized with a *grey dashed line* and with a *black line* for the elderly. The concentrations are normalized to a 10 g dose for morphine. Observed data are superimposed (*black open symbols* represent values for the elderly [345, 349]; *grey open symbols* represent values for younger adults [344, 345, 348, 351-353]). Goodness-of-fit plots (right) for model predictions in the adult (*black dots*) and elderly (*grey dots*) populations. *Solid line* indicates line of identity, 1.25-fold and 2-fold error ranges are indicated by *dashed lines* and *dotted lines*, respectively.

The scaling to higher ages reported in the above-mentioned drug studies led to an accurate description of the estimated PK parameters, as shown in Figure 4-9 for individual values and Figure 4-10 for average values from the included trials. Reliable predictions were obtained for the V_{ss} and $t_{1/2}$ of morphine. Only 3 individual values for V_{ss} and 2 of 8 individual values for $t_{1/2}$ were outside of the 1.25-fold level without any age-related pattern. For the trial group predictions, both PK parameters were predicted within the 2-fold range.

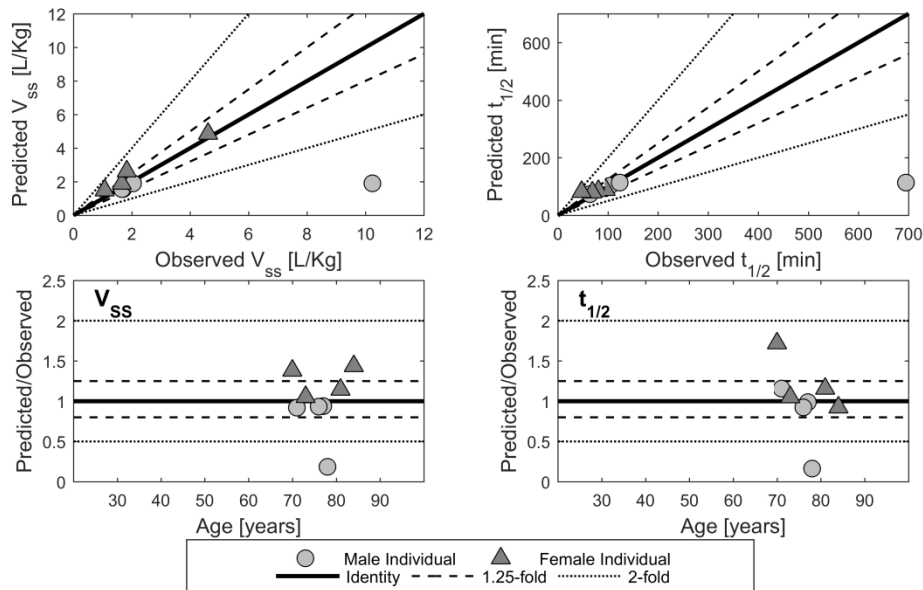


Figure 4-9 Trial individual observed vs. predicted values for volume of distribution at steady-state and the elimination half-life for the test compound morphine. The *solid black lines* represent the line of identity; the *dashed black lines* represent the 1.25-fold level and the *solid grey lines* represent the 2-fold level of accuracy.

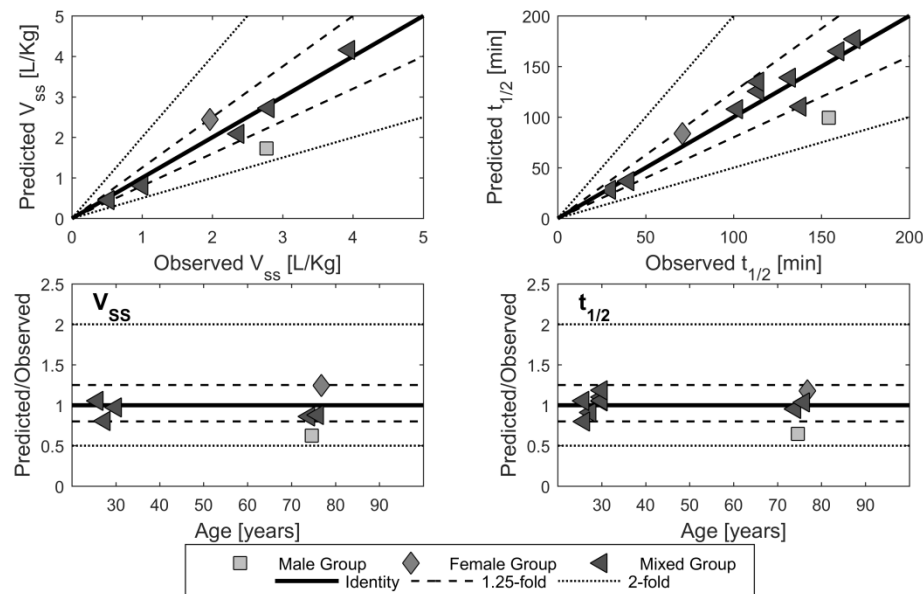


Figure 4-10 Trial group observed vs. predicted values for volume of distribution at steady-state and the elimination half-life for the test compound morphine. The *solid black lines* represent the line of identity; the *dashed black lines* represent the 1.25-fold level and the *solid grey lines* represent the 2-fold level of accuracy.

The predictive performance of the PBPK model for morphine is summarized in Table 4-5. The precision for the predictions of plasma concentrations improved by 0.212 for morphine when using the age-informed physiology for the simulations of the elderly studies. This is a relative improvement in prediction by 49 % for morphine. The plasma concentrations were under-predicted in the absence of consideration of age-informed physiology. The bias was considerably reduced when age-informed physiology was applied.

Table 4-5 Predictive performance analysis of the morphine PBPK model with and without the age-informed physiology

	Adult	Adult physiology Elderly	Age-informed physiology Elderly
Morphine			
Bias			
ME	0.082 (0.001, 0.163)	-0.093 (-0.231, 0.045)	0.050 (-0.072, 0.172)
Precision			
RMSE	0.286 (0.189, 0.358)	0.437 (0.001, 0.656)	0.224 (0.004, 0.384)
Δ RMSE			0.212 (0.001, 0.635)
Relative Δ RMSE			49 %

ME: mean prediction error, RMSE: root mean squared prediction error, Δ RMSE: Difference in RMSE
Values [mg/L] are stated with the 95 % confidence interval in parentheses

Furosemide

The literature screen for observed PK data led to inclusion of several studies for furosemide [120, 354-357] as listed in Table 4-6. Only for two doses, plasma concentration-time profiles were available.

The simulated plasma concentration-time profiles of furosemide in healthy adults were consistent with the observed data, as visualized in Figure 4-11. Only 13 % of the simulations for young adults were outside the 1.25-fold range, with no predicted plasma concentration-time point outside this range for older adults. The majority of these outliers

were underpredictions especially for later time-points. All plasma concentration-time points were predicted within the 2-fold range.

Table 4-6 Summary of clinical studies after intravenous dosing for the test compound furosemide used to compare the simulated data

Dose	Age [years]	n	Height [cm]	Weight [kg]	Reference
Furosemide					
80 mg	27.1 (20-35)	10		71.4 ± 6.7	[120]
80 mg	27 ± 4.8	8		71 ± 6.7	[354]
	64 ± 4.0	8		76 ± 7.3	[354]
40 mg	30 (20-45)	7			[355]
20 mg	76	1		70	[356]
40 mg	74 (64-84)	20		73.1 ± 12.8	[357]

Values in curved brackets indicate the range; ± indicates standard deviation

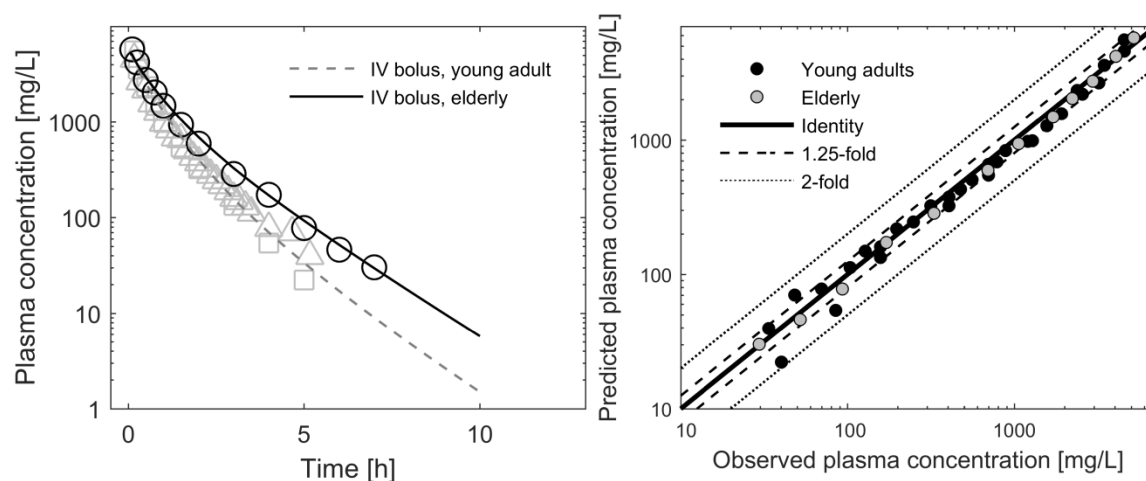


Figure 4-11 Predicted and observed plasma concentration-time profiles of furosemide in younger adults vs. the elderly. Simulated mean plasma concentration-time profiles (left) for younger adults are visualized with a *grey dashed line* and with a *black line* for the elderly. The concentrations are normalized to a 40 mg dose for furosemide. Observed data are superimposed (*black open symbols* represent values for the elderly[354]; *grey open symbols* represent values for younger adults[354, 355]). Goodness-of-fit plots (right) for model predictions in the adult (*black dots*) and elderly (*grey dots*) populations. *Solid line* indicates the line of identity, 1.25-fold and 2-fold error ranges are indicated by *dashed lines* and *dotted lines*, respectively.

The scaling to higher ages reported in the above-mentioned drug studies led to an accurate description of the estimated PK parameters, as shown in Figure 4-12 for individual values and Figure 4-13 for average values from the included trials. All but 4 of 36 predicted V_{ss} value of furosemide were within the 1.25-fold level of the experimental values. The $t_{1/2}$ values for furosemide for individuals with a longer half-life were underpredicted. Here, 8 of 36 values for $t_{1/2}$ were not within the 1.25-fold range including two values outside the 2-fold range. On trial population level, all predicted values were within the 2-fold and only a single $t_{1/2}$ value predicted outside the bioequivalence criteria.

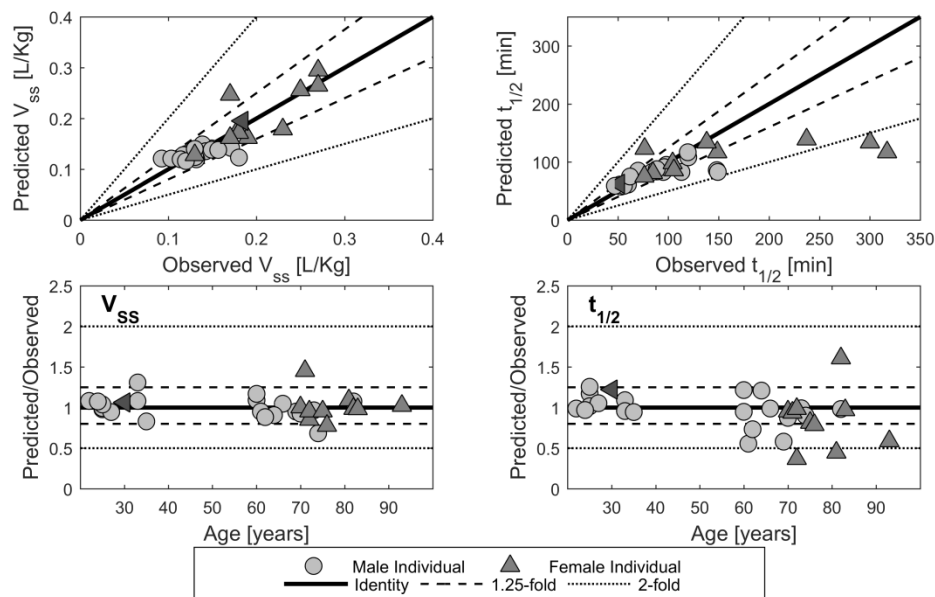


Figure 4-12 Trial individual observed vs. predicted values for volume of distribution at steady-state and the elimination half-life as well as the corresponding fold over/under prediction, for the test compound furosemide. The *solid black lines* represent the line of identity; the *dashed black lines* represent the 1.25-fold level and the *solid grey lines* represent the 2-fold level of accuracy.

The predictive performance of the PBPK model for furosemide is summarized in Table 4-7. The precision for the prediction of plasma concentrations improved by 0.132 when using the age-informed physiology for the simulations of the elderly studies. This is a relative improvement in prediction by 32 %. The plasma concentrations were underpredicted in the absence of consideration of age-informed physiology. The bias was considerably reduced when age-informed physiology was applied.

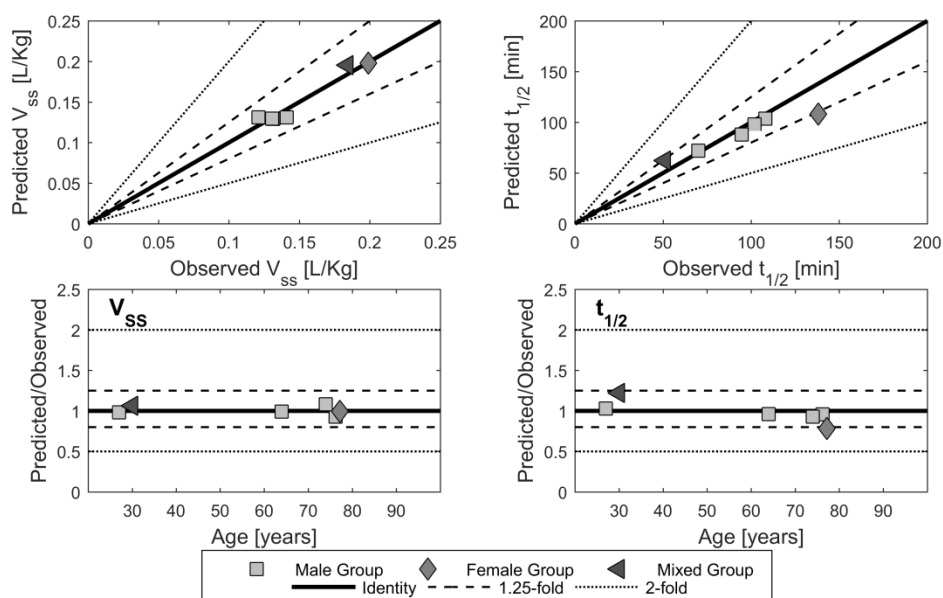


Figure 4-13 Trial group observed vs. predicted values for volume of distribution at steady-state and the elimination half-life as well as the corresponding fold over/under prediction, for the test compound furosemide. The *solid black lines* represent the line of unity; the *dashed black lines* represent the 1.25-fold level and the *solid grey lines* represent the 2-fold level of accuracy.

Table 4-7 Predictive performance analysis of the furosemide PBPK model with and without the age-informed physiology

	Adult physiology		Age-informed physiology
	Adult	Elderly	Elderly
Furosemide			
Bias			
ME	0.032 (-0.034, 0.010)	-0.339 (-0.621, -0.057)	0.076 (-0.015, 0.137)
Precision			
RMSE	0.180 (0.141, 0.212)	0.408 (0.004, 0.721)	0.276 (0.185, 0.343)
Δ RMSE		0.132 (0.005, 0.695)	
Relative Δ RMSE		32 %	

ME: mean prediction error, RMSE: root mean squared prediction error, Δ RMSE: Difference in RMSE
 Values [mg/L] are stated with the 95 % confidence interval in parentheses

4.3 Application of a ciprofloxacin lifespan PBPK population model

According to the previously defined PBPK model building, verification and scaling workflow in Figure 3-2, the model was parametrized based on experimental data in adults for intravenous and oral administration of ciprofloxacin. The model was then scaled to the pediatric and geriatric age range considering age-dependent physiological changes. For both ends of the age-scale, previously studied dosing scenarios were predicted based on prior knowledge and subsequently compared to the observed exposure.

4.3.1 Intravenous ciprofloxacin PBPK model simulations for adults

Parameters describing the drug distribution (octanol-water partition coefficient Log P), metabolism (mediated by CYP1A2) and excretion (tubular secretion and biliary clearance) processes were identified based on human plasma concentration-time data (octanol-water partition coefficient Log P), mass-balance information (CYP1A2 metabolism, tubular secretion and biliary clearance) and urinary excretion profiles (tubular secretion) following single or multiple intravenous administrations with doses ranging from 25 to 400 mg using the parameter identification process. Studies applied for this step are indicated in Table A-1. The results of the multi-parametric fit to inform the lipophilicity as well as the metabolism and elimination processes are listed in Table 4-8. The correlation matrix for this fit shown in Figure 4-14 revealed no or weak correlations among the three processes and lipophilicity, but a stronger correlation between the two hepatic pathways. Since mass balance information applied to run the parameter identification clearly defined the fraction of administered dose metabolized and the unchanged fecal excretion, the retrieved pathway kinetic parametrization for hepatic metabolism and biliary clearance was accepted for further application.

Table 4-8 Input data values and model parameters for ciprofloxacin PBPK model

Parameter	Ciprofloxacin PBPK model	
	Model input value	Source
Physicochemical		
Molecular mass (g/mol)	331.3	Drugbank (http://www.drugbank.ca)
Log P	0.95	Estimated using parameter identification
pKa	6.09 (acidic)	Experimentally determined [358]
	8.62 (basic)	Experimentally determined [358]
Fraction unbound	0.67	Experimentally determined [359]
Aqueous solubility at pH 7 (mg/ml)	38.4	Experimentally determined [360]
Absorption		
Enhancement factor		
Duodenum	255.8	Estimated using parameter identification
Upper and lower jejunum	10.4	Estimated using parameter identification
Upper and lower ileum	11.0	Estimated using parameter identification
Large intestine	2.3	Estimated using parameter identification
Distribution		
Partition coefficient model	PK-Sim [®] standard	Willmann <i>et al.</i> [108, 109]
Cellular permeability model	PK-Sim [®] standard	Willmann <i>et al.</i> [108, 109]
Metabolism		
CYP1A2 mediated clearance (L/min)	0.067	Estimated using parameter identification
Excretion		
GFR fraction for passive renal clearance	1	
Tubular secretion clearance (L/min)	0.706	Estimated using parameter identification
Biliary clearance (mL/min/kg)	1.286	Estimated using parameter identification

Log P: octanol-water partition coefficient, pKa: negative decadic logarithm acid dissociation constant in log scale, GFR fraction: defines, if drug is only filtrated (1), reabsorbed (<1) or additionally secreted (>1)

In a subsequent application, the developed ciprofloxacin PBPK model for intravenous administration in adults was able to describe the plasma concentration-time profiles following different intravenous administration protocols. An exemplary profile is shown in Figure 4-15.

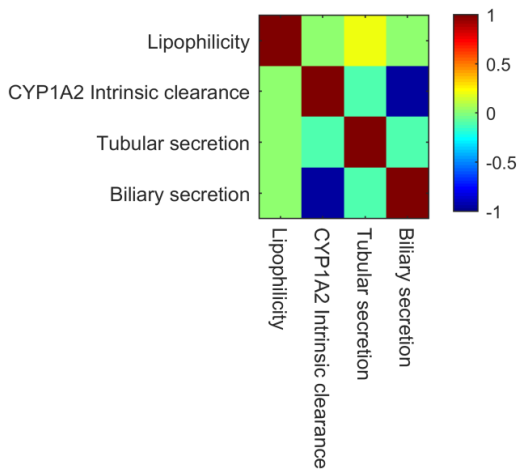


Figure 4-14 Correlation matrix for parameter identification of distribution, metabolism and elimination parameters after intravenous administration.

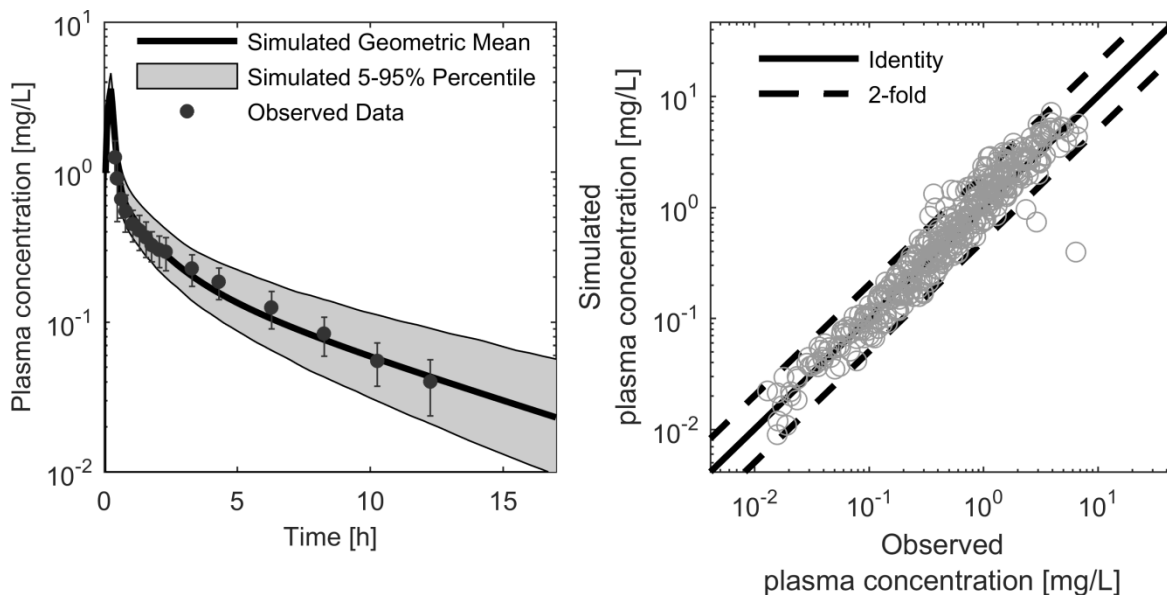


Figure 4-15 Exemplary ciprofloxacin plasma concentration-time profile after a 200 mg intravenous administration and the respective goodness-of-fit plot. The symbols (*black dots*) represent the median of the observed plasma concentration with the corresponding standard deviation indicated with error bars [359] for the plasma concentration-time profile (left). The *thick black line* represents the simulated population median and the *grey shaded area* covers the 5th to 95th percentile prediction interval of simulated plasma concentration-time profiles. The simulated versus reported study population mean plasma concentration-time points (right) were used for model verification in the adult age range. Here, the *thick black line* represents the line of identity, the *dashed lines* indicate the 2-fold range.

4.3.2 Oral ciprofloxacin PBPK model simulations for adults

After the ciprofloxacin PBPK model was parametrized for intravenous administration in adults, the model was expanded to simulate oral absorption from the GI tract. Following the multi-parametric fit, the respective parameters were adjusted as shown in Table 4-8 and Table 4-9, where estimated parameters were not or only weakly correlated (Figure 4-16).

Table 4-9 Results of the parameter identification for oral administration

Parameter name	Best value
Dissolution shape	
Sucrose suspension	0.53
100 mg tablet	0.30
250 mg tablet	0.70
500 mg tablet	0.81
750 mg tablet	0.65
Dissolution time	
Sucrose suspension	73.49 min
100 mg tablet	43.54 min
250 mg tablet	60.68 min
500 mg tablet	44.75 min
750 mg tablet	60.85 min
Solubility change per charge	1212.64

The subsequent simulations of plasma concentration–time profiles following oral administration of ciprofloxacin doses ranging from 50 to 1000 mg were sufficiently reliable compared with experimental data. Although the in vivo dissolution profile of each formulation for a certain dose strength was identified, the fraction dissolved was almost complete and a fraction absorbed of nearly 80 % was achieved allowing a bioavailability around 70 % across all formulations. The formulations differed in the initial phase after absorption leading to differences within the bioequivalence range for the time at which maximum plasma concentration occurred. An exemplary profile is shown in Figure 4-17.

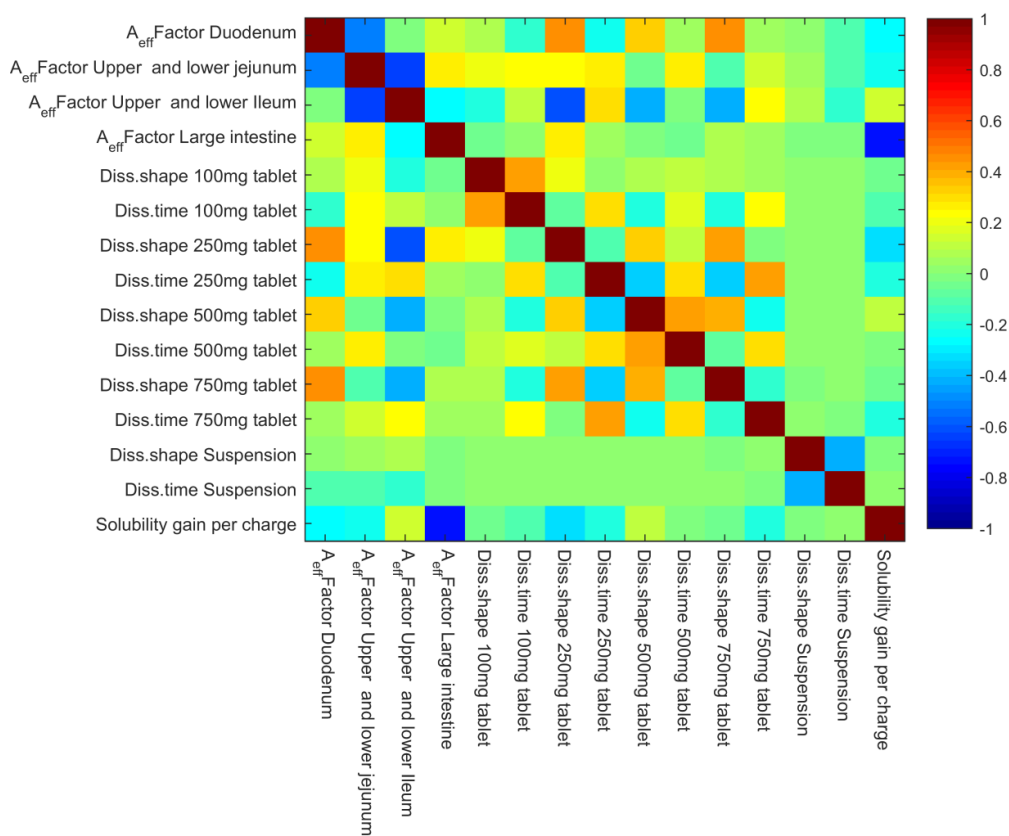


Figure 4-16 Correlation matrix for parameter identification of oral absorption parameters.

4.3.3 PBPK model verification

The ciprofloxacin PBPK model for adults was verified by comparing independent datasets that were not used for model building with corresponding simulations. Reliable simulations were obtained for the mean plasma concentration-time data after intravenous and oral administration as visualized in Figure 4-15 and Figure 4-17. Only 4.82 % of the reported mean data points for intravenous and 12.13 % for oral administration were outside the simulated 2-fold range with no concentration-related bias.

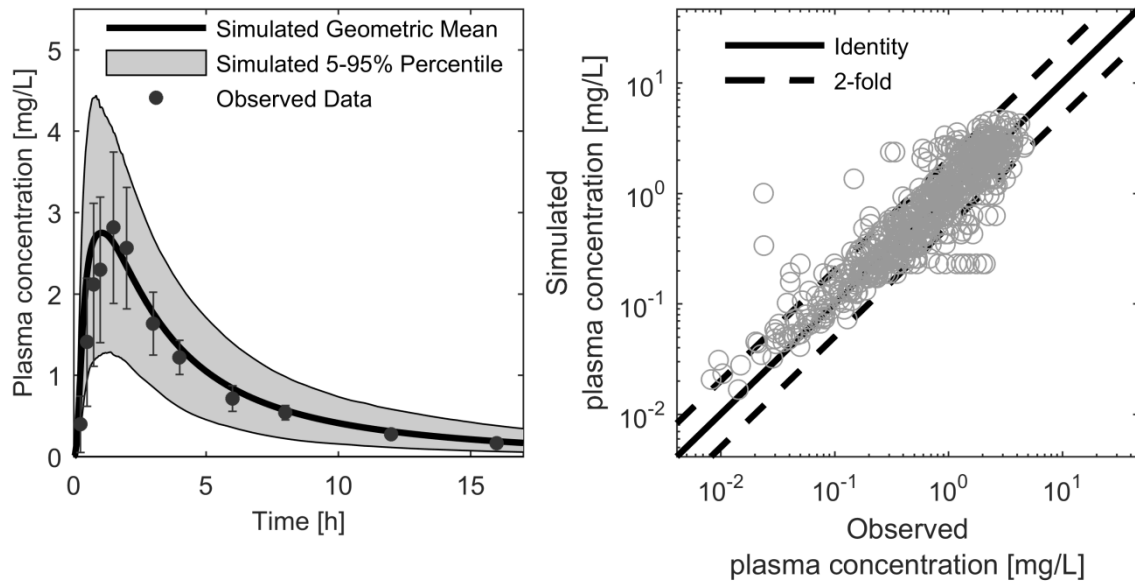


Figure 4-17 Exemplary ciprofloxacin plasma concentration-time profile after a 500 mg oral administration and the respective goodness-of-fit plot. The symbols (*black dots*) represent the median of the individually observed plasma concentration with the corresponding standard deviation indicated with error bars [361] for the plasma concentration-time profile (left). The *thick black line* represents the simulated population median and the *grey shaded area* covers the 5th to 95th percentile prediction interval of simulated plasma concentration-time profiles. The simulated versus reported study population mean plasma concentration-time points (right) were used for model verification in the adult age range. Here, the *thick black line* represents the line of identity; the *dashed lines* indicate the 2-fold range.

The comparison of AUC and C_{\max} to literature observations showed no bias for the respective doses (Figure 4-18). Figure 4-18 illustrates that variability in AUC is higher in oral compared to intravenous dosing: 4 simulated to observed AUC ratios were outside the 1.25-fold range after intravenous dosing compared to 21 out of 44 after oral dosing. Still, all C_{\max} ratios for oral administration were within the 2-fold range, whereas 10 out of the 21 ratios were outside the 1.25-fold range. These results showed that, overall, the PBPK model is well suited to describe the pharmacokinetics of ciprofloxacin after intravenous and oral administration in adults.

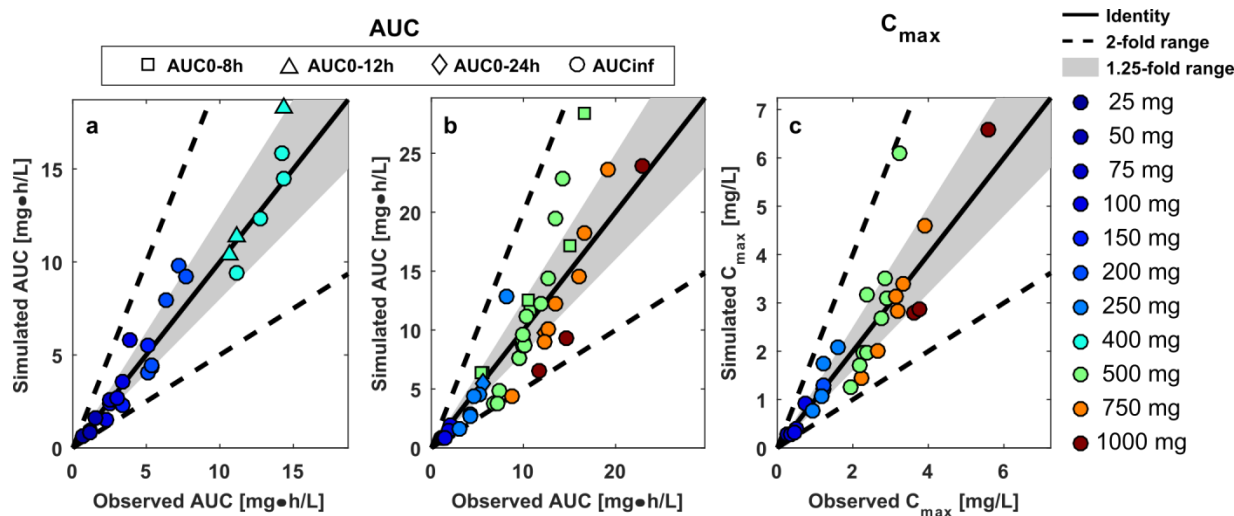


Figure 4-18 Verification of the ciprofloxacin PBPK model for the investigated dose range by comparing simulation/observation ratios of pharmacokinetic measures. The plots show the mean area under the curve (AUC) following intravenous (a) and oral (b) administration and maximum plasma concentration (C_{\max}) following oral administration (c) of ciprofloxacin from various clinical studies in healthy adults at indicated doses. The *thick black line* represents line of identity (sim./obs. ratio = 1); the *grey shade* represents the 1.25-fold window, the *dashed lines* indicate the 2-fold range.

4.3.4 Prediction of age-related impact on ciprofloxacin pharmacokinetics

Considering the physiological changes related to maturation and aging of the human body, the ciprofloxacin PBPK model was scaled to both ends of the age-span. The model successfully predicted the ciprofloxacin plasma concentration-time profiles from 3 month to 90 years of age. Mean data points for intravenous and oral administration were well predicted with only 7.61 % and 5.56 % of the predictions outside the 2-fold range with no concentration-related bias (Figure 4-19). No observed plasma concentration-time points following intravenous administration were available in the literature for pediatric patients, which allowed only an evaluation of the predictions for geriatric patients for this route of administration.

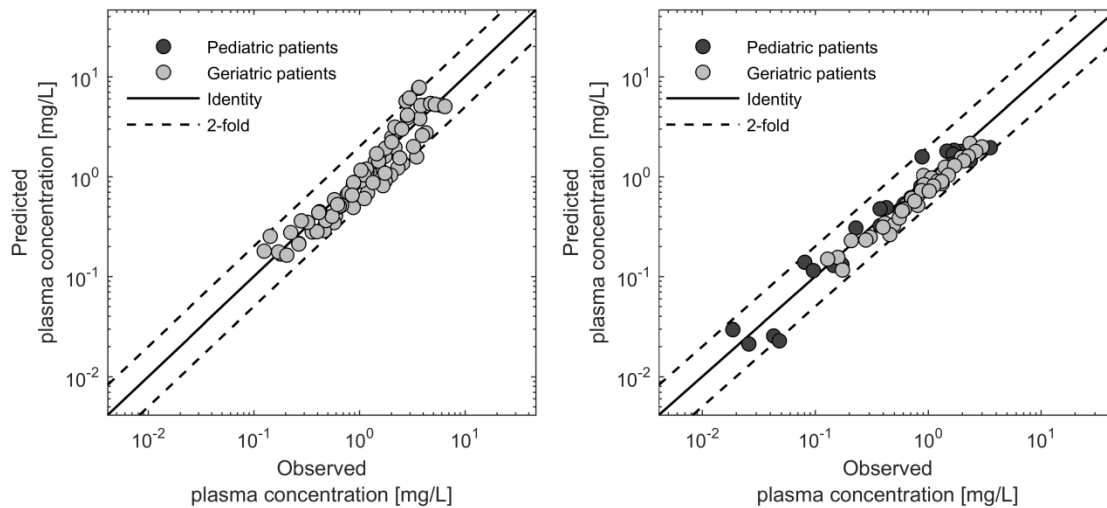


Figure 4-19 Predictive performance of the ciprofloxacin PBPK model indicated by predicted versus observed mean plasma concentration data of pediatric and geriatric patients. Data are stratified by age group and represented as *diamonds* for pediatric [134, 136] and *squares* for geriatric [130, 137-139, 142, 143] patients following intravenous (left) and oral (right) administration. The *thick black line* represents the line of identity; the *dashed lines* indicate the 2-fold range.

Predicting the exposure following several dosing schemes in different pediatric age groups and overlay plots with observed data revealed a wider variability for the clinical observations. Towards younger ages, C_{\max} was well predicted for the population mean but the observed data also showed some extremely high concentrations in these age groups. However, the model was able to cover these concentrations with the predicted maximum plasma concentration range. The deviation was less pronounced for the adult and geriatric population following oral administration (Figure 4-20). Overall, on a population level, the ciprofloxacin PBPK model was able to predict the exposure and the respective shifts over the entire lifespan well as shown in Figure 4-21 and Figure 4-22.

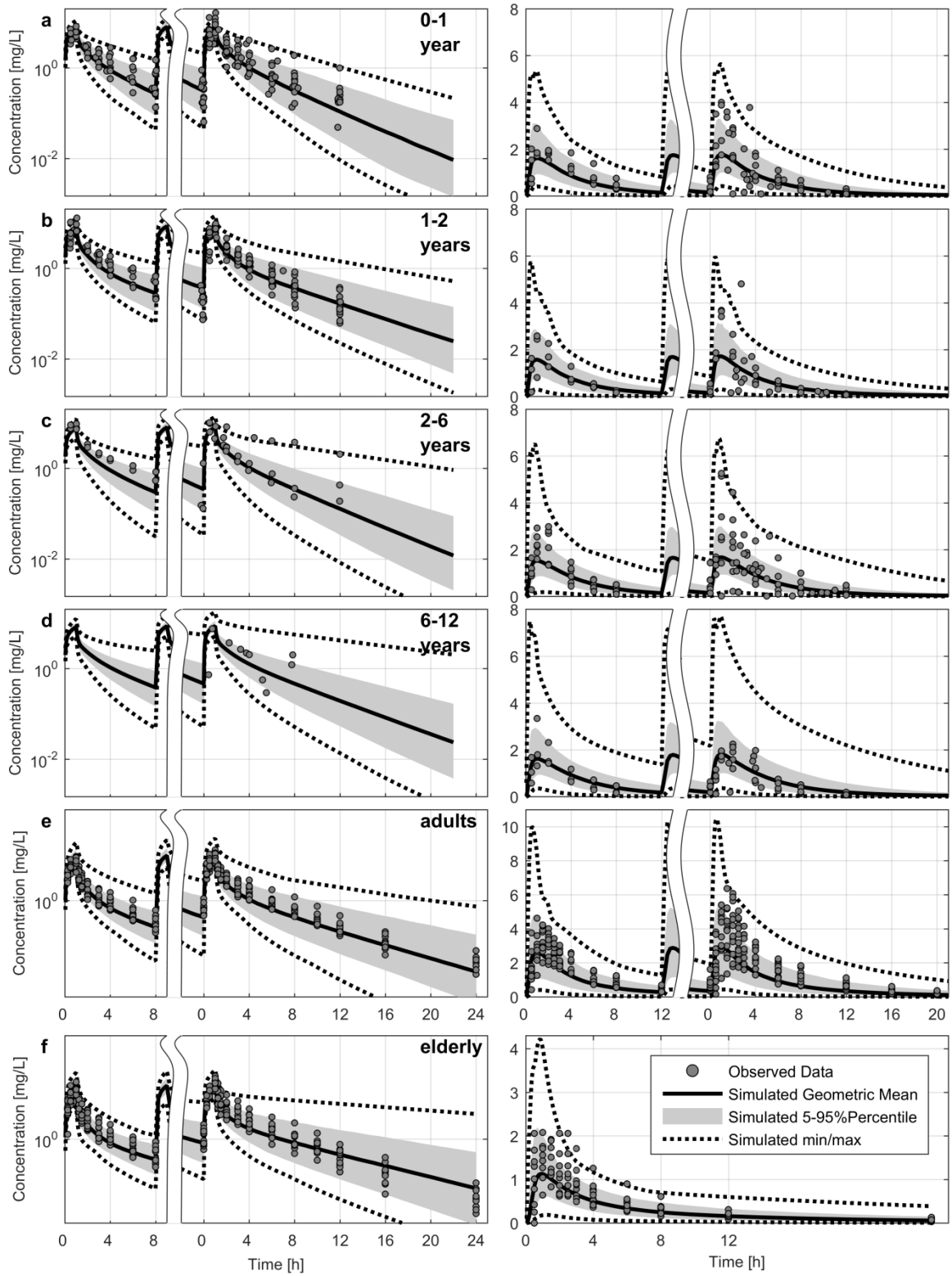


Figure 4-20 Comparison of predicted and individual observed plasma concentrations data for ciprofloxacin grouped by age. Predicted profiles are indicated by *solid lines* for the geometric mean, *shaded area* for the 5–95th percentiles deviation and *dashed lines* for minimum and maximum. Individual study data (*dots*) after intravenous (left panel) and oral (right panel) administration of 10mg/kg ciprofloxacin every 8 h in pediatric patients of different age are visualized for 0-1 year (a), 1-2 years (b), 2-6 years (c) and 6-12 years (d). Intravenous doses in adults (e, left) and geriatric patients (f, left) were 400 mg, whereas oral dosing in adults was 750 mg (e, right) and 250 mg in geriatric patients (f, right). The time indicates the time after the first dose (*before axis break*) and at steady-state (*after axis break*). Observed data are based on previous studies [121, 130-132, 134, 362].

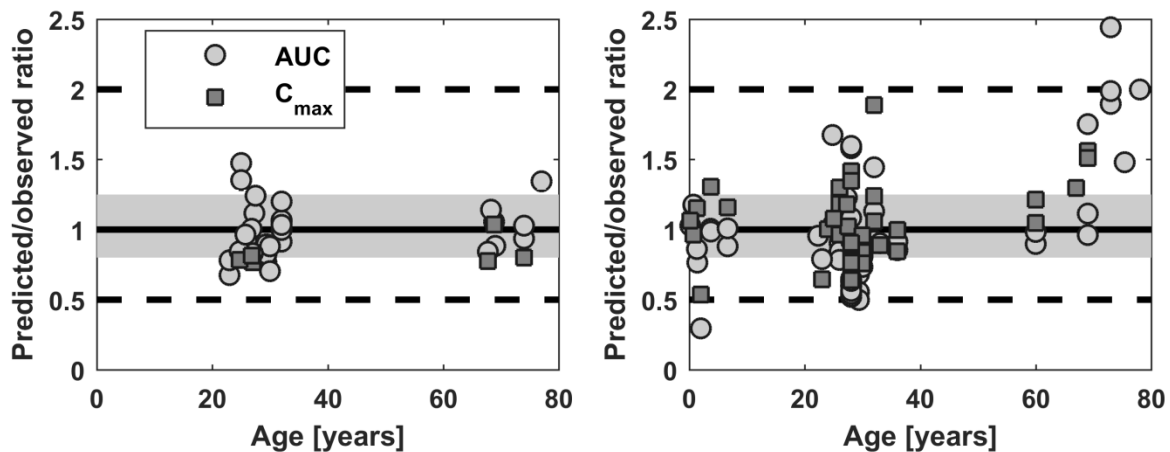


Figure 4-21 Model predictions for AUC and C_{max} following intravenous and oral administration. Predicted/observed ratios over age for both parameters following intravenous (left side) and oral (right side) administration. Here, a *solid line* represents the line of unity; the *grey shaded area* represents the 1.25-fold level and *dashed black lines* represent the 2-fold level of predicted accuracy.

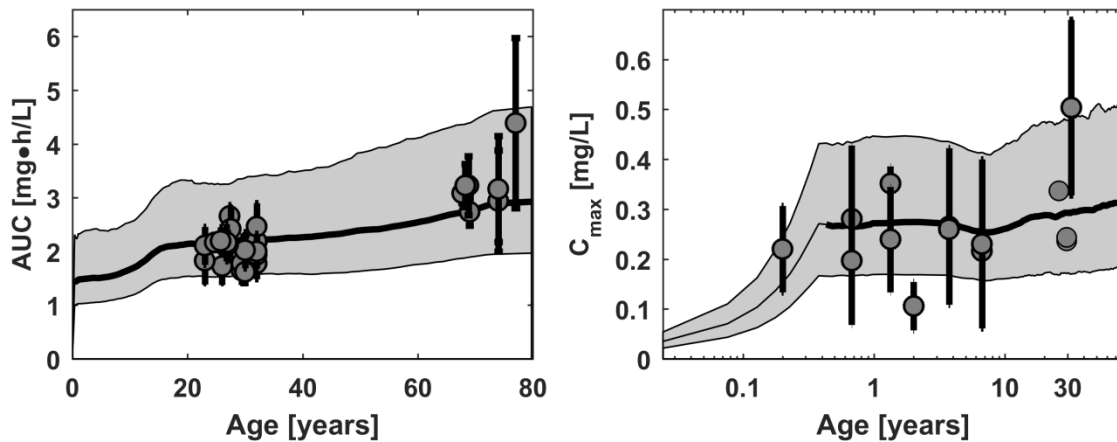


Figure 4-22 Model predictions for AUC and C_{\max} following intravenous and oral suspension administration. AUC after intravenous (left) and C_{\max} after oral (right) suspension dosing prediction over age for a dose of 1 mg/kg. Here, predicted population data are represented as geometric mean (*thick black line*) and 90 % prediction interval (*grey shaded area*). Observed, dose-normalized pharmacokinetic measures indicate reported means (*dots*) and standard deviations (*error bars*).

4.3.5 Sensitivity analysis

The parameter sensitivity analysis shown in Figure A-1 to Figure A-3 revealed that, among all model parameters, dose had the highest and equal impact on the pharmacokinetic measures AUC_{inf} and C_{\max} for all age groups followed by the unbound fraction and parameters related to elimination pathways. For the AUC_{inf} , age-related patterns were observed for the impact of metabolism and excretion. Whereas the impact of the mainly hepatically located CYP metabolism and biliary secretion increased towards younger age groups, the renal tubular secretion had a greater impact towards older age groups. More model parameters contributed to achieve 90 % of the cumulated total sensitivity for C_{\max} . Besides parameters related to metabolism and elimination, distribution-related parameters were more important with increasing age. Generally, most parameters showed a similar impact of age, whereas only the dose has the same sensitivity for all age groups.

5 Discussion

5.1 Database development

The PBPK elderly database described here summarizes anatomical and (patho-) physiological changes from early adulthood to extreme old age. Data were extracted from the peer-reviewed literature for all relevant PBPK parameters, and analyzed in order to describe the systemic changes that occur with age.

Only a few studies have attempted geriatric PBPK modeling by including ageing considerations in their databases. The recent approach by McNally *et al.* [313] included detailed considerations for age-related changes in brain weight and bone mass. Also, the implementation of muscle mass alterations according to Janssen *et al.* [168], as well as the analysis of change of the cardiac output by Luisada *et al.* [363], have proven to be useful for PBPK modeling for the elderly. By informing bone and muscle mass, this approach considers changes in fat mass indirectly. However, alterations in cardiac output distribution and changes in major organs (such as liver and kidney) were not captured by data from the literature [313, 363].

The gathering of data from the literature for PBPK application is a serious challenge. Some organs, such as the brain, are well described over the entire age range, due to advances in analytical methods and enhanced focus on research in these areas. This enables investigations on secular trends and tracking of longitudinal aging trends. For other organs, however, the available data are sparse or outdated. One of the main cited studies referring to changes in liver weight over the course of ageing is from Boyd from 1933 [364]; this study included severely diseased individuals. Generally, due to the higher survival rate of women, data yield for extreme old age was less representative for men. Another hurdle is the research on massive blood-containing organs like the lung and the spleen. Here, an infection prior to death can cause high variability in the reported weight at autopsy. Furthermore, contrary to gestation and maturation, which involve highly predictable biological changes over a defined time scale, the classification of individuals beyond the

age of 65 years has no physiological basis. This impedes the generation of a clear reference interval for a certain chronological sequence, and thus increases variability.

In contrast to studies on changes in organ volume during the ageing process, studies on blood flow rates and cardiac output distribution were sparse or used questionable analytical methods. In these cases, our data collection included information from studies on North Americans and Australians, and linear regression was performed. Since no study covered the topic of gonadal perfusion, specific blood flow was kept constant and only volumetric change in this organ was taken into account. Moreover, the last data point for muscle blood flow was for a group of 73 year-old subjects, allowing only a linear regression from young adulthood up to 100 years of age. Similarly, no studies on body water distribution were available for females above the age of 80 years. Besides lack of data, the predicted variability for the GFR based on kidney size variability was too high along the course of ageing as it can be seen in Figure 4-7. Since the GFR is linked to the kidney size in this PBPK modelling framework, the propagation of kidney size variability causes a wider spread of simulated compared to estimated GFR values. Alternative approaches such as the correlation of GFR and renal plasma flow have been proposed by others [276] due to the uncertain extent of glomerulosclerosis. However, since the renal blood flow rate also scales with the kidney size and underlies an additional variability, a coupling of the GFR and renal blood flow rate would increase the simulated GFR variability.

5.2 Database qualification

In the current study, parameters relevant to a PBPK approach were gathered by a comprehensive review of the literature, and for the first time they were integrated into a knowledge-driven PBPK ageing approach that captures whole-body physiology. This methodology enables an age-dependent description of plasma concentration-time profiles for young adults and elderly (Figure 4-8 and Figure 4-11). Importantly, the clinically observed increasing plasma concentrations in elderly for furosemide and morphine are reflected by the ageing PBPK model. Along with this, this approach allows description of the shifts in V_{ss} and $t_{1/2}$ for the paradigm compounds furosemide and morphine for on a

population (Figure 4-10 and Figure 4-13), but also on an individual level (Figure 4-9 and Figure 4-12). Unfortunately, only a few studies providing plasma concentration-time profiles were available, and thus an age-grouped analysis was not feasible. Especially for the age range 40-60 years and 85-100 years there is hardly any stratified PK data. When the underlying physiological changes were used the predictions were reasonably precise over the investigated age range. There was an underprediction of higher $t_{1/2}$ values for furosemide, which can be due to the temporary decrease of the kidneys hydrodynamic observed in several patients in the first 2-3 hours after intravenous administration [116]. Since the GFR initially increases after administration of furosemide, a subsequent fluid retention inside the nephron lumen and an increase in the intracapsular hydrostatic pressure lead to a temporary reduction in GFR. This effect is considered to be dose-dependent [365] and could be assessed with an additional pharmacodynamic model.

Although predictive performance was generally increased towards the older adult age range by applying the developed age-informed physiological database, mispredictions in certain cases can be explained by peculiarities of morphine PK. Variability in morphine PK is associated with variation in protein concentrations. Perturbed levels of albumin and alpha-1-acid glycoprotein may occur in patients suffering from acute or chronic pain as a result from immobility. This, in turn, will strongly impact the extent of morphine binding to plasma proteins [119]. Due to the high extraction ratio, the age-related changes in the vasculature and hepatic tissue are more descriptive for the fate of morphine [119, 366].

The developed PBPK approach for elderly individuals is of high clinical relevance as this group receives the greatest number of drug prescriptions. With this approach, knowledge on anatomical and (patho-) physiological age-dependencies can be used to predict alterations in PK from early adulthood through extreme old age. This will improve the prediction of effective starting drug dosages for healthy elderly patients, as depicted in Figure 3-1 and emphasized by Jadhav *et al.* [2]. Further disease implementations are encouraged in order to distinguish between age- and/or disease-related physiological alterations in drug usage. In general, this knowledge-driven approach is expected to be effective for increasing the efficiency of clinical trial designs, as well as for optimizing drug therapy in the elderly population.

5.3 Application of the elderly PBPK population approach

The PBPK approach for elderly individuals was used to perform the first lifespan pharmacokinetic predictions for ciprofloxacin. Furthermore, a model assessment for predictions based on a large-scale sensitivity analysis was introduced and performed.

After development of a ciprofloxacin adult PBPK model for intravenous administration based on *in vitro* and adult pharmacokinetic data, the model was verified for extended simulations in a subsequent step. Visual prediction checks for mean plasma concentration-time data revealed a successful description of the observed data. The assessment of the estimated pharmacokinetic parameters led to an equally well description over the investigated dose range verifying the distribution-, metabolism- and elimination-related parametrization. This also confirmed the underlying dose linearity of ciprofloxacin since the PBPK model was built solely with linear elimination processes.

The model application for an exposure simulation following intravenous administration for adults was then extended by gastrointestinal absorption following oral administration. Similarly to a recent study by Martinez *et al*, effective surface area enhancement factors were estimated to describe the impact of segmental absorption [367]. Generally, the model-based net absorption needed to be increased in all segments, showing a large uptake in the duodenum and jejunum. This is in line with previous observations following an administration of a Remote-Control Capsule [368]. A saturated absorption with increasing doses discussed previously was not observed in the estimation steps [369]. The previous observation might be due to an administration of multiple tablets to achieve higher dose levels and thereby causing limitations in tablet dissolution rather than in absorption. For the mean plasma concentration-time data, only 4.82 % after intravenous and 12.13 % after oral administration of the simulation to observation ratios were outside the 2-fold range (Figure 4-15 and Figure 4-17). The resulting simulation to observation ratio values for AUC and C_{\max} were evenly distributed across the line of identity.

Subsequent scaling to both ends of the age scale revealed a robust estimation of age-related exposure changes. Trends in AUC changes reported in literature were adequately predicted for intravenous and oral dosing. Prediction to observation ratios revealed a similar

accuracy for the mean plasma concentration-time data compared to adults. The increasing variability in C_{\max} towards younger age groups was captured by the model predictions. Since small intestinal transit time has a notable impact on C_{\max} based on the sensitivity analysis, but was shown to be barely age-dependent [370], an even higher net absorption for some individuals in the duodenum or jejunum might explain the scattered instances of elevated maximum plasma exposure. Although pharmacokinetic observations of ciprofloxacin in neonates are published, these data were not considered in this analysis since neonates in the respective studies were pooled with other pediatric age-groups [371] or treated with varying dosing schemes [372, 373].

In this thesis, distribution and elimination parameters for intravenous administration as well as *in vivo* dissolution and segmental absorption parameters for oral administration had to be identified simultaneously. The influence of these initially uncertain parameters was later on assessed in a sensitivity analysis, which helped to identify model uncertainties and foster the communication between the model developer and the clinical pharmacologist, who gains a better understanding of the applicability of a model in a clinical setting. The sensitivity analysis was conducted to scrutinize how age-dependent changes affect systemic exposure and assess the impact of identified parameters on the model performance. Mainly, parameters related to the kinetics of metabolism and excretion were found to be crucial for the simulated pharmacokinetic profiles (Figure A-1 to Figure A-3). However, the metabolism and excretion kinetic rates for each pathway were informed by previously reported mass-balance studies which support the confidence in the identified rates [148].

Several PBPK models for ciprofloxacin have been published over the recent years with different grades of complexity depending on the purpose of the respective studies. First, a preliminary whole-body PBPK approach of the applied model in this thesis was published to exemplify the best practice in model building by following simple model learning steps which allowed already reasonable pharmacokinetic approximations but lacked generality [75]. Later, Sadiq *et al.* parametrized an ordinary differential equation system in NONMEM[®] based on plasma observations in intensive care patients in order to predict target tissue concentrations and the time-course of bacterial killing at different sites of

infection [374]. Ball *et al.* and Navid *et al.* evaluated the drug-drug interaction potential using ciprofloxacin as a perpetrator drug for renal transporters [375] and CYP1A2 [376]. In the latter case model verification was not described, whereas the only verification dataset used for the Ball *et al.* study was under-predicted after single dose administration. Only Ball *et al.* developed a full-PBPK model on a commercial PBPK platform which potentially allows for age-dependent ADME scaling using the underlying databases on physiology and ontogeny. Navid *et al.* conducted drug-drug interaction predictions in elderly by adjusting the unspecific clearance without taking general physiological changes in older adults into account.

A mechanistic description of the oral absorption of ciprofloxacin has been covered by two publications. First, Martinez *et al.* investigated the peculiarities of the oral absorption of ciprofloxacin with dedicated clinical trials and sophisticated stepwise information of model processes [367]. Recently, Hansmann *et al.* focused on the dosage form dissolution mechanisms and tried to inform *in vivo* behavior with *in vitro* dissolution, transfer and two-stage experiments [377]. Both approaches were conducted using a commercial platform, but described systemic exposure with a (non-)compartmental approach. Unevaluated model predictions by Hansmann *et al.* towards the older age range showed a lower C_{\max} than in adults, which is opposed to the published clinical observations [142] and the predictions presented here. All these PBPK models allocate between renal and non-renal clearance without a precise distinction of separate processes. This limits potential pharmacokinetic evaluation of age- or disease-related impact on these specific processes, which is explicitly considered and informed in the hereby presented PBPK model.

In summary, this developed and verified ciprofloxacin lifespan PBPK model comprises a thoroughly informed basis for a mechanistic representation of the compound's absorption, distribution, metabolism and excretion processes, which allows a reliable scaling to both ends of the age scale. Therefore, such a model can be used to support clinical trial designs or optimize dose regimens. Special pharmacokinetic-related questions triggered by certain clinical scenarios can be responded adequately for this multi-pathway drug over the entire age span. Further pharmacokinetic assessments in other special population groups or an evaluation of biopharmaceutical issues during formulation development are potential

application scenarios and support subsequent pharmacodynamic model extension. This work also demonstrates the importance of an adequately established and verified PBPK model incorporating profound prior knowledge to allow a scientifically sound prediction.

5.4 Challenges and opportunities to streamline dosing regimens in the elderly

5.4.1 Current challenges

The inclusion of older patients in the testing of new medications as outlined in the ICH E7 guidelines is not mandatory for pharmaceutical industry as long as reasonable justification for an evasion is provided. In addition, a comprehensive representation of the elderly in clinical trials remains hindered by the complex nature of this patient population including the heterogeneity in comorbidity, poly-medication, socio-economic backgrounds, and physiological state. It also disqualifies a direct comparison of the elderly population in its entirety to healthy adults. The situation is particularly challenging for narrow therapeutic index drugs, where small changes in PK and/or PD have the potential to change the benefit/risk profile of the drug, consequently warranting close assessment in older adults. In addition, adherence to medication and off-label use due to poly-medication, complex dosing regimens, cognitive and functional disabilities are major challenges in geriatric pharmacotherapy in general and individualization in particular. As discussed in greater detail in the previous sections of this thesis, the lack of geriatric information can be supplemented by the application of informative pharmacometric modeling and simulation methods.

5.4.2 Opportunities

Personalization of drug therapy holds tremendous potential to change the way drug therapies could be used in the elderly to better care for these patients. Over the past decade, FDA and other regulatory authorities have been on the forefront of establishing approaches that increase the benefit of drug therapies, while minimizing their risk in this vulnerable patient population. While pediatric guidelines have been frequently updated over the past

decade [378, 379], respective regulatory documents are not yet available for the elderly even when the concepts outlined for pediatrics may be used as reference point for geriatrics as well.

Whenever possible, clinical trials should include elderly subjects in order to establish appropriate dosing regimens for this special patient population. The conduct of these trials can be supported through the use of modeling and simulation approaches that account for the dynamic interplay between genetic and non-genetic factors in older adults as well as their impact on the drug's PK/PD as a function of age. These quantitative approaches can be used to optimize study designs based on sparse sampling strategies to overcome some of the practical limitations of performing clinical trials in older adults. The success and failure of these approaches is closely linked to the identification of reliable biomarkers of ageing. Whereas the identification of age-appropriate biomarkers is currently primarily subject to academic research [61], an increase in research efforts can be expected over the next decade given the importance of this growing patient population. In addition, to these "hard" endpoints, the impact of socio-economic factors and patient behavior on drug therapy needs to be better understood when attempting to optimize treatment on a patient-by-patient basis. To that end, a promising approach was recently promoted by Novartis in order to personalize clinical development in the field of oncology. The program was for a couple of compounds associated with certain mutations independent from the affected tissue [380]. Based on a hierarchical Bayesian approach, information gained in one subgroup can verify the potency of a compound in another subgroup [381]. This approach can, for example, be used in elderly cancer patients who are highly variable in their tumor set of mutations. It is already feasible with small study groups and, thus, could facilitate and personalize geriatric clinical development. The development of large databases and big data management that integrate prescription payment and medical claims information provide an opportunity for post-marketing geriatric pharmacovigilance. Database analysis allows for pharmacovigilance of older generic medications that may no longer be under active investigation. The data mining of these large health care databases does not prove a medication-related adverse effect but shows association that could be used to generate the hypotheses for future studies.

Therapeutic drug monitoring (TDM) approaches are nowadays a useful tool to individualize the dose of compounds with a narrow therapeutic window in clinical settings. Whereas this approach is usually based on population pharmacokinetic knowledge, PBPK applications in patient care will help to individualize dosing for initiating a drug treatment once the approach is clinically robust. Knowledge of exposure and response under a certain medication can be translated and applied to introduce a new treatment in this patient or individually help to balance the potential hazard against the possible benefit by understanding specific system capabilities.

The selection of the best quantitative approach to optimize and/or personalize drug therapies in the elderly should be evaluated on a case-by-case basis. The success depends on the available knowledge on the drug based on the drug development stage and the biological systems. Whereas PBPK models can be useful to establish dosing regimens in population subgroups based on specific patho-physiological conditions during drug development, Bayesian approaches usually aim at individualizing the dose at the patient level in the clinical environment. Both approaches can be used in combination to understand the underlying mechanism of age-related physiology and their impact on drug PK/PD and to establish the most appropriate dosing regimens for each population subgroup since the early drug development phases. In any case, the development and application of these approaches is complex and requires high-level training. Additionally, for those drugs that require a more precise selection of the dose due to a narrow therapeutic index and high variability, the development of practitioner-friendly decision support tool interfaces is needed to simplify their clinical application [74].

6 Conclusion and perspectives

This study was set up to develop, qualify and apply a physiologically based pharmacokinetic (PBPK) population model for elderly individuals that considers typical (patho-) physiological conditions associated with ageing and allows reliable exposure estimations for all ages. Elderly people are more likely to experience adverse drug reactions due to poly medication and the impact of age-related physiological changes that do not occur in younger adults typically recruited in clinical trials. Due to this knowledge gap, pharmacokinetics (PK) and pharmacodynamics (PD) of drugs administered to elderly patients are difficult to estimate.

The onset and course of ageing for different organs is highly heterogeneous due to the dynamic interplay between multiple, complex and poorly understood genetic, environmental, and disease-related risk factors as well as the difference between chronological and biological age. This results in a pharmacological heterogeneity in elderly patients. In this thesis, the anatomical and physiological changes with healthy ageing were analyzed from the literature and assembled to a PBPK database. Since this whole-body PBPK database is publicly accessible in the Open Systems Pharmacology Suite (<https://github.com/open-systems-pharmacology>), an open source platform, further research is encouraged and promoted by direct interaction of researchers on the platform.

When analyzing the literature data, several knowledge gaps and inconsistencies were identified. Additionally, age-related process-specific information such as enzyme and transporter activities was not considered in this study. Therefore, the database allows distinguishing between functional capability and physiological changes. The open source platform enables the user to update and adapt the compiled database presented in this thesis once new information has become available. Furthermore, this study describes mechanistically the data processing from literature findings towards a PBPK population database. Since the approach provides the ability to differentiate between age- and disease-related physiological alterations, the database facilitates an implementation of additional patho-physiological implications of certain disease states.

Both physiological qualification with unused datasets and pharmacokinetic verification with single elimination pathway compounds were successfully performed. With such stringent model qualification this work took into account the increasing awareness of model qualification during the development of new PBPK approaches in the scientific community. Statistical evaluation of PBPK population model performance for elderly showed a clear improvement compared to age-uninformed simulations. To allow a judgement on the confidence in a PBPK model, a global sensitivity analysis for every parameter of each simulated age-group was conducted. This analysis quantifies the uncertainty in a PBPK model due to the unknown underlying biology or mechanisms. Although this procedure is technically complex for generic whole-body PBPK models with usually more than 130 parameters per simulation, it will become common practice in PBPK model development, not least due to the recently issued European Medicines Agency (EMA) guideline [89].

In a final step, the predictive performance of the PBPK approach was assessed by scaling a comprehensively informed ciprofloxacin whole-body PBPK model to the elderly. The study showed reliable predictions outside of the tested adult age range towards the extremes of ages. The analysis indicated that the current dosing scheme for ciprofloxacin ensures a consistent exposure for the entire age-range. Furthermore, the established and verified ciprofloxacin model can be applied for further pharmacokinetic assessments in other special population groups or for the evaluation of biopharmaceutical issues during formulation development.

Although exposure changes with increasing age were analyzed in this thesis by a thorough literature investigation on anatomical and physiological changes, guidance for pharmacotherapy in older adults will inevitably be driven by changes in drug response. However, alterations in pharmacodynamics with increasing age are poorly understood in many cases. In order to understand changes in drug response following a certain dose, exposure is a reliable link. The hereby presented approach supports drug exposure estimations at the target site and by that encourage additional research on target alterations in elderly patients.

In conclusion this model represents a valuable tool for the assessment of drug exposure in the elderly. Further, it facilitates the optimization of dosing regimens and clinical trials with regard to the safety and efficacy profile of a given compound. This would improve pharmacotherapy and increase drug safety, thereby reducing costs resulting from adverse events caused by inappropriate dosing.

7 Summary

Clinical drug development is traditionally focused on young and middle-aged adults. The elderly are often underrepresented in clinical trials, even though persons aged 65 years and older receive the majority of drug prescriptions. Consequently, there is a knowledge gap on dose-exposure relationships in elderly subjects. This thesis aimed at contributing to a better understanding of the age-related mechanisms governing the pharmacokinetics (PK) in this clinically understudied population.

First, a physiologically based pharmacokinetic (PBPK) database for the course of healthy ageing was successfully established. For parameterization of the PBPK model for healthy ageing individuals, anthropometric and physiological data were identified in the literature, which were incorporated into the PBPK software PK-Sim[®]. Although age-related changes occurring from 65 to 100 years of age were the main focus of this work, data on anatomical and physiological changes beginning from early adulthood to the elderly age range were also included for a sound and continuous description of ageing humans. In total, 118 studies comprising 47029 male and 67419 female subjects were included to build the elderly PBPK database.

As next step, the capability of the elderly PBPK approach to predict the distribution and elimination of drugs was verified using the test compounds morphine and furosemide administered intravenously. Both drugs are cleared by a single elimination pathway. PK parameters for the two compounds in younger adults and elderly individuals were obtained from the literature. Matching virtual populations – with regard to age, gender, anthropometric measures and dosage – were generated. Profiles of plasma drug concentration over time, volume of distribution at steady-state (V_{ss}) and elimination half-lives ($t_{1/2}$) from the literature were compared to those predicted by PBPK simulations, for both younger adults and the elderly. Based on age-informed physiology, the predicted PK profiles described age-associated trends well. The root mean squared prediction error (RMSE) for the prediction of plasma concentrations for furosemide and morphine in the elderly was improved by 32% and 49%, respectively, compared to predictions without age-informed physiology. The majority of the individual V_{ss} and $t_{1/2}$ values of the two model

compounds furosemide and morphine were well predicted in the elderly population, except for long furosemide half-lives.

Finally, the reliability of predictions outside the tested adult age range towards the extremes of ages was assessed using the multi-elimination pathway compound ciprofloxacin as probe drug. Mean data of 69 published clinical trials were identified and used for model building, simulation as well as the verification process. The predictive performance on both ends of the age scale was assessed using individual data of 236 pediatric and 22 geriatric patients observed in clinical trials. Ciprofloxacin model verification demonstrated no concentration-related bias and accurate predictions for the adult age range with only 4.8 % of the mean observed concentrations following intravenous and 12.1 % following oral administration outside the simulated 2-fold range. Predictions towards both extremes of ages for the area under the plasma concentration–time curve (AUC) and the maximum plasma concentration (C_{max}) were reliable.

The results of this thesis support the feasibility of using a knowledge-driven PBPK ageing model to predict PK alterations throughout the entire course of ageing, and thus to optimize drug therapy also in older adult individuals. Overall, the predictive power of a thoroughly informed middle-out approach towards older adults to potentially support the decision making process for pharmacotherapy in the elderly was demonstrated. These results indicate that medication safety in geriatric patients may be greatly facilitated by the information gained from PBPK predictions.

References

1. Lesko LJ, Schmidt S. Individualization of drug therapy: history, present state, and opportunities for the future. *Clin Pharmacol Ther* 2012;92:458-66.
2. Jadhav PR, Cook J, Sinha V, Zhao P, Rostami-Hodjegan A, Sahasrabudhe V, et al. A proposal for scientific framework enabling specific population drug dosing recommendations. *J Clin Pharmacol* 2015;55:1073-8.
3. Patki KC, von Moltke LL, Harmatz JS, Hesse LM, Court MH, Greenblatt DJ. Effect of age on in vitro triazolam biotransformation in male human liver microsomes. *J Pharmacol Exp Ther* 2004;308:874-9.
4. ICH. E7 studies in support of special populations: Geriatrics. International Conference on Harmonisation of Technical Requirements for Registration of Pharmaceuticals for Human Use (ICH); 1993
5. Swanlund SL. Successful cardiovascular medication management processes as perceived by community-dwelling adults over age 74. *Appl Nurs Res* 2010;23:22-9.
6. de Onis M, Habicht JP. Anthropometric reference data for international use: recommendations from a World Health Organization Expert Committee. *Am J Clin Nutr* 1996;64:650-8.
7. FDA. E7 Studies in Support of Special Populations: Geriatrics U.S. Department of Health and Human Services Food and Drug Administration (FDA); 2012
8. EMA. Studies in Support of Special Populations: Geriatrics, Questions and Answers. European Medicines Agency (EMA); 2010
9. Beers E, Egberts TC, Leufkens HG, Jansen PA. Information for adequate prescribing to older patients : an evaluation of the product information of 53 recently approved medicines. *Drugs Aging* 2013;30:255-62.
10. Masoudi FA, Havranek EP, Wolfe P, Gross CP, Rathore SS, Steiner JF, et al. Most hospitalized older persons do not meet the enrollment criteria for clinical trials in heart failure. *Am Heart J* 2003;146:250-7.
11. Martin K, Begaud B, Latry P, Miremont-Salame G, Fourier A, Moore N. Differences between clinical trials and postmarketing use. *Br J Clin Pharmacol* 2004;57:86-92.
12. Schaufler J, Telschow C. Arzneimittelverordnungen nach Alter und Geschlecht. In: Schwabe U, Paffrath D, editors. *Arzneiverordnungs-Report 2016: Aktuelle Daten, Kosten, Trends und Kommentare*. Berlin, Heidelberg: Springer Berlin Heidelberg; 2016. p. 763-73.
13. Golden AG, Tewary S, Dang S, Roos BA. Care management's challenges and opportunities to reduce the rapid rehospitalization of frail community-dwelling older adults. *Gerontologist* 2010;50:451-8.

14. Lewis JH, Kilgore ML, Goldman DP, Trimble EL, Kaplan R, Montello MJ, et al. Participation of patients 65 years of age or older in cancer clinical trials. *J Clin Oncol* 2003;21:1383-9.
15. Herrera AP, Snipes SA, King DW, Torres-Vigil I, Goldberg DS, Weinberg AD. Disparate inclusion of older adults in clinical trials: priorities and opportunities for policy and practice change. *Am J Public Health* 2010;100 Suppl 1:S105-12.
16. Cherubini A, Del Signore S, Ouslander J, Semla T, Michel JP. Fighting against age discrimination in clinical trials. *J Am Geriatr Soc* 2010;58:1791-6.
17. Beers MH, Ouslander JG, Rollinger I, Reuben DB, Brooks J, Beck JC. Explicit criteria for determining inappropriate medication use in nursing home residents. UCLA Division of Geriatric Medicine. *Arch Intern Med* 1991;151:1825-32.
18. Beers MH. Explicit criteria for determining potentially inappropriate medication use by the elderly. An update. *Arch Intern Med* 1997;157:1531-6.
19. Fick DM, Cooper JW, Wade WE, Waller JL, Maclean JR, Beers MH. Updating the Beers criteria for potentially inappropriate medication use in older adults: results of a US consensus panel of experts. *Arch Intern Med* 2003;163:2716-24.
20. Fick DM, Semla TP. 2012 American Geriatrics Society Beers Criteria: new year, new criteria, new perspective. *J Am Geriatr Soc* 2012;60:614-5.
21. Radcliff S, Yue J, Rocco G, Aiello SE, Ickowicz E, Hurd Z, et al. American Geriatrics Society 2015 updated beers criteria for potentially inappropriate medication use in older adults. *J Am Geriatr Soc* 2015;63:2227-46.
22. Golden A, Silverman M, Daiello L, Llorente M. Inappropriate Medication Prescribing: Going Beyond The Beer's Criteria. *Long-Term Care Interface* magazine 2005;6:31-4.
23. Gallagher P, O'Mahony D. STOPP (Screening Tool of Older Persons' potentially inappropriate Prescriptions): application to acutely ill elderly patients and comparison with Beers' criteria. *Age Ageing* 2008;37:673-9.
24. O'Mahony D, O'Sullivan D, Byrne S, O'Connor MN, Ryan C, Gallagher P. STOPP/START criteria for potentially inappropriate prescribing in older people: version 2. *Age Ageing* 2015;44:213-8.
25. Hamilton H, Gallagher P, Ryan C, Byrne S, O'Mahony D. Potentially inappropriate medications defined by STOPP criteria and the risk of adverse drug events in older hospitalized patients. *Arch Intern Med* 2011;171:1013-9.
26. Holt S, Schmiedl S, Thurmann PA. Potentially inappropriate medications in the elderly: the PRISCUS list. *Dtsch Arztebl Int* 2010;107:543-51.
27. McLeod PJ, Huang AR, Tamblyn RM, Gayton DC. Defining inappropriate practices in prescribing for elderly people: a national consensus panel. *CMAJ* 1997;156:385-91.

28. Laroche ML, Charmes JP, Merle L. Potentially inappropriate medications in the elderly: a French consensus panel list. *Eur J Clin Pharmacol* 2007;63:725-31.
29. Kuhn-Thiel AM, Weiss C, Wehling M, members Faep. Consensus validation of the FORTA (Fit fOR The Aged) List: a clinical tool for increasing the appropriateness of pharmacotherapy in the elderly. *Drugs Aging* 2014;31:131-40.
30. Wehling M, Burkhardt H, Kuhn-Thiel A, Pazan F, Throm C, Weiss C, et al. VALFORTA: a randomised trial to validate the FORTA (Fit fOR The Aged) classification. *Age Ageing* 2016;45:262-7.
31. Budnitz DS, Lovegrove MC, Shehab N, Richards CL. Emergency hospitalizations for adverse drug events in older Americans. *N Engl J Med* 2011;365:2002-12.
32. Golden A, Beers MH, Fick DM. Is it safe to conclude that Beers criteria medications led to few adverse events? *Ann Intern Med* 2008;148:628-9; author reply 9.
33. Golden A, Troen B. Biology of aging. In: Hirth V, Wieland D, Dever-Bumba M, editors. *Case-Based Geriatrics*. New York: McGraw Hill; 2010.
34. Butler RN, Sprott R, Warner H, Bland J, Feuers R, Forster M, et al. Biomarkers of aging: from primitive organisms to humans. *J Gerontol A Biol Sci Med Sci* 2004;59:B560-7.
35. Brooks-Wilson AR. Genetics of healthy aging and longevity. *Hum Genet* 2013;132:1323-38.
36. Miles C, Wayne M. Quantitative trait locus (QTL) analysis. *Nature Education* 2008;1:208.
37. Oztaner SM, Taskaya Temizel T, Erdem SR, Ozer M. A Bayesian Estimation Framework for Pharmacogenomics Driven Warfarin Dosing: A Comparative Study. *IEEE J Biomed Health Inform* 2015;19:1724-33.
38. Mallal S, Phillips E, Carosi G, Molina JM, Workman C, Tomazic J, et al. HLA-B*5701 screening for hypersensitivity to abacavir. *N Engl J Med* 2008;358:568-79.
39. FDA. Table of Pharmacogenomic Biomarkers in Drug Labeling. U.S. Department of Health and Human Services Food and Drug Administration (FDA); 2015
40. Winner J. Pharmacogenomic Treatment Support. *Today's Geriatric Medicine* 2014;4:20.
41. Waade RB, Hermann M, Moe HL, Molden E. Impact of age on serum concentrations of venlafaxine and escitalopram in different CYP2D6 and CYP2C19 genotype subgroups. *Eur J Clin Pharmacol* 2014;70:933-40.
42. Miao L, Yang J, Huang C, Shen Z. Contribution of age, body weight, and CYP2C9 and VKORC1 genotype to the anticoagulant response to warfarin: proposal for a new dosing regimen in Chinese patients. *Eur J Clin Pharmacol* 2007;63:1135-41.
43. Gage BF, Eby C, Johnson JA, Deych E, Rieder MJ, Ridker PM, et al. Use of pharmacogenetic and clinical factors to predict the therapeutic dose of warfarin. *Clin Pharmacol Ther* 2008;84:326-31.

44. Sconce EA, Khan TI, Wynne HA, Avery P, Monkhouse L, King BP, et al. The impact of CYP2C9 and VKORC1 genetic polymorphism and patient characteristics upon warfarin dose requirements: proposal for a new dosing regimen. *Blood* 2005;106:2329-33.
45. Bor JS. The search for effective Alzheimer's therapies: a work in progress. *Health Aff (Millwood)* 2014;33:527-33.
46. Du YF, Ou HY, Beverly EA, Chiu CJ. Achieving glycemic control in elderly patients with type 2 diabetes: a critical comparison of current options. *Clin Interv Aging* 2014;9:1963-80.
47. Kirkman MS, Briscoe VJ, Clark N, Florez H, Haas LB, Halter JB, et al. Diabetes in older adults: a consensus report. *J Am Geriatr Soc* 2012;60:2342-56.
48. Bonaventura A, Montecucco F, Dallegri F. Update on strategies limiting iatrogenic hypoglycemia. *Endocr Connect* 2015;4:R37-45.
49. Meneilly GS, Ryan AS, Veldhuis JD, Elahi D. Increased disorderliness of basal insulin release, attenuated insulin secretory burst mass, and reduced ultradian rhythmicity of insulin secretion in older individuals. *J Clin Endocrinol Metab* 1997;82:4088-93.
50. Geloneze B, de Oliveira Mda S, Vasques AC, Novaes FS, Pareja JC, Tambascia MA. Impaired incretin secretion and pancreatic dysfunction with older age and diabetes. *Metabolism* 2014;63:922-9.
51. Leong R, Vieira ML, Zhao P, Mulugeta Y, Lee CS, Huang SM, et al. Regulatory experience with physiologically based pharmacokinetic modeling for pediatric drug trials. *Clin Pharmacol Ther* 2012;91:926-31.
52. FDA. General Clinical Pharmacology Considerations for Pediatric Studies for Drugs and Biological Products. U.S. Department of Health and Human Services Food and Drug Administration (FDA); 2014
53. Hammerlein A, Derendorf H, Lowenthal DT. Pharmacokinetic and pharmacodynamic changes in the elderly. Clinical implications. *Clin Pharmacokinet* 1998;35:49-64.
54. Borst SE, Scarpace PJ. Reduced high-affinity alpha 1-adrenoceptors in liver of senescent rats: implications of assessment at various temperatures. *Br J Pharmacol* 1990;101:650-4.
55. Morley JE, Flood JF, Silver AJ. Opioid peptides and aging. *Ann N Y Acad Sci* 1990;579:123-32.
56. Kane R, Ouslander J, Abrass I, Resnick B. *Essentials of Clinical Geriatrics*, 7th ed. New York: McGraw-Hill; 2013.
57. Van Dam D, De Deyn PP. Drug discovery in dementia: the role of rodent models. *Nat Rev Drug Discov* 2006;5:956-70.
58. Vozmediano V, Ortega I, Lukas JC, Gonzalo A, Rodriguez M, Lucero ML. Integration of preclinical and clinical knowledge to predict intravenous PK in human: bilastine case study. *Eur J Drug Metab Pharmacokinet* 2014;39:33-41.

59. Encinas E, Calvo R, Lukas JC, Vozmediano V, Rodriguez M, Suarez E. A predictive pharmacokinetic/pharmacodynamic model of fentanyl for analgesia/sedation in neonates based on a semi-physiologic approach. *Paediatr Drugs* 2013;15:247-57.
60. Samant TS, Mangal N, Lukacova V, Schmidt S. Quantitative clinical pharmacology for size and age scaling in pediatric drug development: A systematic review. *J Clin Pharmacol* 2015.
61. Lagishetty C. Covariates in Pharmacometrics [PhD thesis] Chapter 1; p.26-27: University of Otago; 2013.
62. BMS-Pfizer. Eliquis (apixaban) - Summary of Product Characteristics. Bristol-Myers Squibb (BMS) Pfizer European economic interest grouping (EEIG); 2013
63. Mueck W, Stampfuss J, Kubitzka D, Becka M. Clinical pharmacokinetic and pharmacodynamic profile of rivaroxaban. *Clin Pharmacokinet* 2014;53:1-16.
64. Saeed MA, Vlasakakis G, Della Pasqua O. Rational use of medicines in older adults: Can we do better during clinical development? *Clin Pharmacol Ther* 2015;97:440-3.
65. Rogers JA, Polhamus D, Gillespie WR, Ito K, Romero K, Qiu R, et al. Combining patient-level and summary-level data for Alzheimer's disease modeling and simulation: a beta regression meta-analysis. *J Pharmacokinet Pharmacodyn* 2012;39:479-98.
66. Oteo I, Lukas JC, Leal N, Suarez E, Valdivieso A, Gastaca M, et al. Tacrolimus pharmacokinetics in the early post-liver transplantation period and clinical applicability via Bayesian prediction. *Eur J Clin Pharmacol* 2013;69:65-74.
67. Hennig S, Norris R, Kirkpatrick CM. Target concentration intervention is needed for tobramycin dosing in paediatric patients with cystic fibrosis--a population pharmacokinetic study. *Br J Clin Pharmacol* 2008;65:502-10.
68. Valdivieso N, Oteo I, Valdivieso A, Lukas JC, Leal N, Gastaca M, et al. Tacrolimus dose individualization in "de novo" patients after 10 years of experience in liver transplantation: pharmacokinetic considerations and patient pathophysiology. *Int J Clin Pharmacol Ther* 2013;51:606-14.
69. Oteo I, Lukas JC, Leal N, Suarez E, Valdivieso A, Gastaca M, et al. Pathophysiological idiosyncrasies and pharmacokinetic realities may interfere with tacrolimus dose titration in liver transplantation. *Eur J Clin Pharmacol* 2011;67:671-9.
70. Sanchez A, Cabrera S, Santos D, Valverde MP, Fuertes A, Dominguez-Gil A, et al. Population pharmacokinetic/pharmacogenetic model for optimization of efavirenz therapy in Caucasian HIV-infected patients. *Antimicrob Agents Chemother* 2011;55:5314-24.
71. Karafoulidou A, Suarez E, Anastasopoulou I, Katsarou O, Kouramba A, Kotsi P, et al. Population pharmacokinetics of recombinant factor VIII:C (ReFacto) in adult HIV-negative and HIV-positive haemophilia patients. *Eur J Clin Pharmacol* 2009;65:1121-30.

72. Krauss M, Tappe K, Schuppert A, Kuepfer L, Goerlitz L. Bayesian Population Physiologically-Based Pharmacokinetic (PBPK) Approach for a Physiologically Realistic Characterization of Interindividual Variability in Clinically Relevant Populations. *PLoS One* 2015;10:e0139423.
73. Krauss M, Burghaus R, Lippert J, Niemi M, Neuvonen P, Schuppert A, et al. Using Bayesian-PBPK modeling for assessment of inter-individual variability and subgroup stratification. *In Silico Pharmacol* 2013;1:6.
74. Zineh I, Huang SM. Biomarkers in drug development and regulation: a paradigm for clinical implementation of personalized medicine. *Biomark Med* 2011;5:705-13.
75. Kuepfer L, Niederalte C, Wendl T, Schlender JF, Willmann S, Lippert J, et al. Applied Concepts in PBPK Modeling: How to Build a PBPK/PD Model. *CPT Pharmacometrics Syst Pharmacol* 2016;5:516-31.
76. Huang SM, Abernethy DR, Wang Y, Zhao P, Zineh I. The utility of modeling and simulation in drug development and regulatory review. *J Pharm Sci* 2013;102:2912-23.
77. Jones HM, Dickins M, Youdim K, Gosset JR, Atkins NJ, Hay TL, et al. Application of PBPK modelling in drug discovery and development at Pfizer. *Xenobiotica* 2012;42:94-106.
78. Polasek TM, Patel F, Jensen BP, Sorich MJ, Wiese MD, Doogue MP. Predicted metabolic drug clearance with increasing adult age. *Br J Clin Pharmacol* 2013;75:1019-28.
79. Schlender JF, Meyer M, Thelen K, Krauss M, Willmann S, Eissing T, et al. Development of a Whole-Body Physiologically Based Pharmacokinetic Approach to Assess the Pharmacokinetics of Drugs in Elderly Individuals. *Clin Pharmacokinet* 2016;55:1573-89.
80. De Buck SS, Sinha VK, Fenu LA, Nijssen MJ, Mackie CE, Gilissen RA. Prediction of human pharmacokinetics using physiologically based modeling: a retrospective analysis of 26 clinically tested drugs. *Drug Metab Dispos* 2007;35:1766-80.
81. Sinha VK, Snoeys J, Osselaer NV, Peer AV, Mackie C, Heald D. From preclinical to human-prediction of oral absorption and drug-drug interaction potential using physiologically based pharmacokinetic (PBPK) modeling approach in an industrial setting: a workflow by using case example. *Biopharm Drug Dispos* 2012;33:111-21.
82. Schaller S, Willmann S, Lippert J, Schaupp L, Pieber TR, Schuppert A, et al. A Generic Integrated Physiologically based Whole-body Model of the Glucose-Insulin-Glucagon Regulatory System. *CPT Pharmacometrics Syst Pharmacol* 2013;2:e65.
83. Vidal EI, Mayoral VF, Villas Boas PJ, Jacinto AF, Fukushima FB. Physical Frailty As a Clinical Marker of Biological Age and Aging. *J Am Geriatr Soc* 2015;63:837-8.
84. Turnheim K. Drug dosage in the elderly. Is it rational? *Drugs Aging* 1998;13:357-79.
85. Thompson CM, Johns DO, Sonawane B, Barton HA, Hattis D, Tardif R, et al. Database for physiologically based pharmacokinetic (PBPK) modeling: physiological data for healthy and health-impaired elderly. *J Toxicol Environ Health B Crit Rev* 2009;12:1-24.

86. Kawamura H. Development of the Japanese reference man model for age-specific phantoms. *Radiat Prot Dosimetry* 2012;149:28-34.
87. Shepard T, Scott G, Cole S, Nordmark A, Bouzom F. Physiologically Based Models in Regulatory Submissions: Output From the ABPI/MHRA Forum on Physiologically Based Modeling and Simulation. *CPT Pharmacometrics Syst Pharmacol* 2015;4:221.
88. EPA. Physiologically-Based Pharmacokinetic (PBPK) Modeling White Paper: Addressing the Use of PBPK Models to Support Derivation of Acute Exposure Guideline Levels. US Environmental Protection Agency (EPA); 2010
89. EMA. Draft guideline on the qualification and reporting of physiologically based pharmacokinetic (PBPK) modelling and simulation. European Medicines Agency (EMA); 2016
90. FDA. Physiologically Based Pharmacokinetic Analyses — Format and Content U.S. Department of Health and Human Services Food and Drug Administration (FDA); 2016
91. Rowland M, Tozer TN. *Clinical pharmacokinetics/pharmacodynamics*. 4th ed. ed: Lippincott Williams and Wilkins Philadelphia; 2005.
92. McLean AJ, Le Couteur DG. Aging biology and geriatric clinical pharmacology. *Pharmacol Rev* 2004;56:163-84.
93. Benet LZ, Broccatelli F, Oprea TI. BDDCS applied to over 900 drugs. *AAPS J* 2011;13:519-47.
94. Le Couteur DG, McLean AJ. The aging liver. Drug clearance and an oxygen diffusion barrier hypothesis. *Clin Pharmacokinet* 1998;34:359-73.
95. Benedetti MS, Whomsley R, Canning M. Drug metabolism in the paediatric population and in the elderly. *Drug Discov Today* 2007;12:599-610.
96. Dean L. Clopidogrel Therapy and CYP2C19 Genotype. 2012 Mar 8 [Updated 2013 Mar 18]. Medical Genetics Summaries [Internet]. Bethesda (MD): National Center for Biotechnology Information (US). <http://www.ncbi.nlm.nih.gov/books/NBK84114>. Accessed June 1, 2017.; 2012.
97. Cusack BJ. Pharmacokinetics in older persons. *Am J Geriatr Pharmacother* 2004;2:274-302.
98. Kinirons MT, O'Mahony MS. Drug metabolism and ageing. *Br J Clin Pharmacol* 2004;57:540-4.
99. Liukas A, Kuusniemi K, Aantaa R, Virolainen P, Niemi M, Neuvonen PJ, et al. Pharmacokinetics of intravenous paracetamol in elderly patients. *Clin Pharmacokinet* 2011;50:121-9.
100. WHO. International Programme on Chemical Safety Harmonization Project. Characterization and application of physiologically based pharmacokinetic models in risk assessment. Harmonization Project Document No. 9. 2010

101. Sager JE, Yu J, Ragueneau-Majlessi I, Isoherranen N. Physiologically Based Pharmacokinetic (PBPK) Modeling and Simulation Approaches: A Systematic Review of Published Models, Applications, and Model Verification. *Drug Metab Dispos* 2015;43:1823-37.
102. Valentin J. Basic anatomical and physiological data for use in radiological protection: reference values: ICRP Publication 89. *Annals of the ICRP* 2002;32:1-277.
103. Dressman JB, Amidon GL, Reppas C, Shah VP. Dissolution testing as a prognostic tool for oral drug absorption: immediate release dosage forms. *Pharm Res* 1998;15:11-22.
104. Poulin P, Theil FP. A priori prediction of tissue:plasma partition coefficients of drugs to facilitate the use of physiologically-based pharmacokinetic models in drug discovery. *J Pharm Sci* 2000;89:16-35.
105. Poulin P, Schoenlein K, Theil FP. Prediction of adipose tissue: plasma partition coefficients for structurally unrelated drugs. *J Pharm Sci* 2001;90:436-47.
106. Rodgers T, Leahy D, Rowland M. Physiologically based pharmacokinetic modeling 1: predicting the tissue distribution of moderate-to-strong bases. *J Pharm Sci* 2005;94:1259-76.
107. Rodgers T, Rowland M. Physiologically based pharmacokinetic modelling 2: predicting the tissue distribution of acids, very weak bases, neutrals and zwitterions. *J Pharm Sci* 2006;95:1238-57.
108. Willmann S, Lippert J, Sevestre M, Solodenko J, Fois F, W. S. PK-Sim: a physiologically based pharmacokinetic 'whole-body' model. *Biosilico* 2003;1:121-4.
109. Willmann S, Lippert J, Schmitt W. From physicochemistry to absorption and distribution: predictive mechanistic modelling and computational tools. *Expert Opin Drug Metab Toxicol* 2005;1:159-68.
110. Loidl-Stahlhofen A, Hartmann T, Schottner M, Rohring C, Brodowsky H, Schmitt J, et al. Multilamellar liposomes and solid-supported lipid membranes (TRANSIL): screening of lipid-water partitioning toward a high-throughput scale. *Pharm Res* 2001;18:1782-8.
111. Saisho Y, Butler AE, Meier JJ, Monchamp T, Allen-Auerbach M, Rizza RA, et al. Pancreas volumes in humans from birth to age one hundred taking into account sex, obesity, and presence of type-2 diabetes. *Clin Anat* 2007;20:933-42.
112. Willmann S, Hohn K, Edginton A, Sevestre M, Solodenko J, Weiss W, et al. Development of a physiology-based whole-body population model for assessing the influence of individual variability on the pharmacokinetics of drugs. *J Pharmacokinet Pharmacodyn* 2007;34:401-31.
113. Edginton AN, Schmitt W, Willmann S. Development and evaluation of a generic physiologically based pharmacokinetic model for children. *Clin Pharmacokinet* 2006;45:1013-34.

114. Tiseo PJ, Thaler HT, Lapin J, Inturrisi CE, Portenoy RK, Foley KM. Morphine-6-glucuronide concentrations and opioid-related side effects: a survey in cancer patients. *Pain* 1995;61:47-54.
115. Waller ES, Massarella JW, Tomkiw MS, Smith RV, Doluisio JT. Pharmacokinetics of furosemide after three different single oral doses. *Biopharm Drug Dispos* 1985;6:109-17.
116. Ponto LL, Schoenwald RD. Furosemide (frusemide). A pharmacokinetic/pharmacodynamic review (Part I). *Clin Pharmacokinet* 1990;18:381-408.
117. Avdeef A, Barrett DA, Shaw PN, Knaggs RD, Davis SS. Octanol-, chloroform-, and propylene glycol dipelargonat-water partitioning of morphine-6-glucuronide and other related opiates. *J Med Chem* 1996;39:4377-81.
118. Cutler RE, Blair AD. Clinical pharmacokinetics of frusemide. *Clin Pharmacokinet* 1979;4:279-96.
119. Glare PA, Walsh TD. Clinical pharmacokinetics of morphine. *Ther Drug Monit* 1991;13:1-23.
120. Andreasen F, Christensen CK, Jacobsen FK, Jansen J, Mogensen CE, Pedersen OL. The individual variation in pharmacokinetics and pharmacodynamics of furosemide in young normal male subjects. *Eur J Clin Invest* 1982;12:247-55.
121. Rajagopalan P, Gastonguay MR. Population pharmacokinetics of ciprofloxacin in pediatric patients. *J Clin Pharmacol* 2003;43:698-710.
122. van Zanten AR, Polderman KH, van Geijlswijk IM, van der Meer GY, Schouten MA, Girbes AR. Ciprofloxacin pharmacokinetics in critically ill patients: a prospective cohort study. *J Crit Care* 2008;23:422-30.
123. Lipman J, Scribante J, Gous AG, Hon H, Tshukutsoane S. Pharmacokinetic profiles of high-dose intravenous ciprofloxacin in severe sepsis. The Baragwanath Ciprofloxacin Study Group. *Antimicrob Agents Chemother* 1998;42:2235-9.
124. Ruhnke M, Trautmann M, Borner K, Hopfenmuller W. Pharmacokinetics of ciprofloxacin in liver cirrhosis. *Chemotherapy* 1990;36:385-91.
125. Frost RW, Lettieri JT, Krol G, Shamblen EC, Lasseter KC. The effect of cirrhosis on the steady-state pharmacokinetics of oral ciprofloxacin. *Clin Pharmacol Ther* 1989;45:608-16.
126. Hackam DJ, Christou N, Khaliq Y, Duffy DR, Vaughan D, Marshall JC, et al. Bioavailability of oral ciprofloxacin in early postsurgical patients. *Arch Surg* 1998;133:1221-5.
127. Cohn SM, Cohn KA, Rafferty MJ, Smith AH, Degutis LC, Kowalsky SF, et al. Enteric absorption of ciprofloxacin during the immediate postoperative period. *J Antimicrob Chemother* 1995;36:717-21.

128. Gattis WA, Petros WP, Pickard WW, Drew RH, May DB, Hathorn JW. A prospective, open-label study of single-dose ciprofloxacin absorption after chemotherapy in patients with malignancy. *Pharmacotherapy* 1997;17:836-40.
129. Johnson EJ, MacGowan AP, Potter MN, Stockley RJ, White LO, Slade RR, et al. Reduced absorption of oral ciprofloxacin after chemotherapy for haematological malignancy. *J Antimicrob Chemother* 1990;25:837-42.
130. Shah A, Lettieri J, Nix D, Wilton J, Heller AH. Pharmacokinetics of high-dose intravenous ciprofloxacin in young and elderly and in male and female subjects. *Antimicrob Agents Chemother* 1995;39:1003-6.
131. Bayer A, Gajewska A, Stephens M, Stark JM, Pathy J. Pharmacokinetics of ciprofloxacin in the elderly. *Respiration* 1987;51:292-5.
132. Israel D, Gillum JG, Turik M, Harvey K, Ford J, Dalton H, et al. Pharmacokinetics and serum bactericidal titers of ciprofloxacin and ofloxacin following multiple oral doses in healthy volunteers. *Antimicrob Agents Chemother* 1993;37:2193-9.
133. Aggarwal P, Dutta S, Garg SK, Narang A. Multiple dose pharmacokinetics of ciprofloxacin in preterm babies. *Indian Pediatr* 2004;41:1001-7.
134. Peltola H, Ukkonen P, Saxen H, Stass H. Single-dose and steady-state pharmacokinetics of a new oral suspension of ciprofloxacin in children. *Pediatrics* 1998;101:658-62.
135. Salam MA, Dhar U, Khan WA, Bennish ML. Randomised comparison of ciprofloxacin suspension and pivmecillinam for childhood shigellosis. *Lancet* 1998;352:522-7.
136. Peltola H, Vaarala M, Renkonen OV, Neuvonen PJ. Pharmacokinetics of single-dose oral ciprofloxacin in infants and small children. *Antimicrob Agents Chemother* 1992;36:1086-90.
137. Hirata CA, Guay DR, Awni WM, Stein DJ, Peterson PK. Steady-state pharmacokinetics of intravenous and oral ciprofloxacin in elderly patients. *Antimicrob Agents Chemother* 1989;33:1927-31.
138. Kees F, Naber KG, Meyer GP, Grobecker H. Pharmacokinetics of ciprofloxacin in elderly patients. *Arzneimittelforschung* 1989;39:523-7.
139. Naber KG, Sorgel F, Kees F, Jaehde U, Schumacher H. Pharmacokinetics of ciprofloxacin in young (healthy volunteers) and elderly patients, and concentrations in prostatic fluid, seminal fluid, and prostatic adenoma tissue following intravenous administration. *Am J Med* 1989;87:57S-9S.
140. Pea F, Milaneschi R, Baraldo M, Lugatti E, Talmassons G, Furlanut M. Ciprofloxacin disposition in elderly patients with LRTI being treated with sequential therapy (200 mg intravenously twice daily followed by 500 mg per os twice daily): comparative pharmacokinetics and the role of therapeutic drug monitoring. *Ther Drug Monit* 2000;22:386-91.

141. Cios A, Wyska E, Szymura-Oleksiak J, Grodzicki T. Population pharmacokinetic analysis of ciprofloxacin in the elderly patients with lower respiratory tract infections. *Exp Gerontol* 2014;57:107-13.
142. Ljungberg B, Nilsson-Ehle I. Pharmacokinetics of ciprofloxacin in the elderly: increased oral bioavailability and reduced renal clearance. *Eur J Clin Microbiol Infect Dis* 1989;8:515-20.
143. LeBel M, Barbeau G, Bergeron MG, Roy D, Vallee F. Pharmacokinetics of ciprofloxacin in elderly subjects. *Pharmacotherapy* 1986;6:87-91.
144. Chandler MH, Toler SM, Rapp RP, Muder RR, Korvick JA. Multiple-dose pharmacokinetics of concurrent oral ciprofloxacin and rifampin therapy in elderly patients. *Antimicrob Agents Chemother* 1990;34:442-7.
145. Dan M, Golomb J, Gorea A, Braf Z, Berger SA. Concentration of ciprofloxacin in human prostatic tissue after oral administration. *Antimicrob Agents Chemother* 1986;30:88-9.
146. Guay DR, Awni WM, Peterson PK, Obaid S, Stein D, Breitenbucher R, et al. Single and multiple dose pharmacokinetics of oral ciprofloxacin in elderly patients. *Int J Clin Pharmacol Ther Toxicol* 1988;26:279-84.
147. Dan M, Verbin N, Gorea A, Nagar H, Berger SA. Concentrations of ciprofloxacin in human liver, gallbladder, and bile after oral administration. *Eur J Clin Pharmacol* 1987;32:217-8.
148. Rohwedder RW, Bergan T, Thorsteinsson SB, Scholl H. Transintestinal elimination of ciprofloxacin. *Diagn Microbiol Infect Dis* 1990;13:127-33.
149. Alvarez AI, Perez M, Prieto JG, Molina AJ, Real R, Merino G. Fluoroquinolone efflux mediated by ABC transporters. *J Pharm Sci* 2008;97:3483-93.
150. Vanwert AL, Srimaroeng C, Sweet DH. Organic anion transporter 3 (oat3/slc22a8) interacts with carboxyfluoroquinolones, and deletion increases systemic exposure to ciprofloxacin. *Mol Pharmacol* 2008;74:122-31.
151. Granfors MT, Backman JT, Neuvonen M, Neuvonen PJ. Ciprofloxacin greatly increases concentrations and hypotensive effect of tizanidine by inhibiting its cytochrome P450 1A2-mediated presystemic metabolism. *Clin Pharmacol Ther* 2004;76:598-606.
152. Sorgel F, Naber KG, Jaehde U, Reiter A, Seelmann R, Sigl G. Gastrointestinal secretion of ciprofloxacin. Evaluation of the charcoal model for investigations in healthy volunteers. *Am J Med* 1989;87:62S-5S.
153. Parry MF, Smego DA, Digiovanni MA. Hepatobiliary kinetics and excretion of ciprofloxacin. *Antimicrob Agents Chemother* 1988;32:982-5.
154. Thelen K, Coboeken K, Willmann S, Burghaus R, Dressman JB, Lippert J. Evolution of a detailed physiological model to simulate the gastrointestinal transit and absorption process in humans, part 1: oral solutions. *J Pharm Sci* 2011;100:5324-45.
155. Edginton AN, Schmitt W, Voith B, Willmann S. A mechanistic approach for the scaling of clearance in children. *Clin Pharmacokinet* 2006;45:683-704.

156. Willmann S, Becker C, Burghaus R, Coboeken K, Edginton A, Lippert J, et al. Development of a paediatric population-based model of the pharmacokinetics of rivaroxaban. *Clin Pharmacokinet* 2014;53:89-102.
157. Perissinotto E, Pisent C, Sergi G, Grigoletto F. Anthropometric measurements in the elderly: age and gender differences. *Br J Nutr* 2002;87:177-86.
158. Wahren J. [Average body weight and correlation weight in relation to age and sex]. *Z Morphol Anthropol* 1981;72:65-76.
159. Rea IM, Gillen S, Clarke E. Anthropometric measurements from a cross-sectional survey of community dwelling subjects aged over 90 years of age. *Eur J Clin Nutr* 1997;51:102-6.
160. Ravaglia G, Morini P, Forti P, Maioli F, Boschi F, Bernardi M, et al. Anthropometric characteristics of healthy Italian nonagenarians and centenarians. *Br J Nutr* 1997;77:9-17.
161. Eiben G, Dey DK, Rothenberg E, Steen B, Bjorkelund C, Bengtsson C, et al. Obesity in 70-year-old Swedes: secular changes over 30 years. *Int J Obes (Lond)* 2005;29:810-7.
162. Bartali B, Benvenuti E, Corsi AM, Bandinelli S, Russo CR, Di Iorio A, et al. Changes in anthropometric measures in men and women across the life-span: findings from the InCHIANTI study. *Soz Praventivmed* 2002;47:336-48.
163. Gillette-Guyonnet S, Nourhashemi F, Andrieu S, Cantet C, Albarede JL, Vellas B, et al. Body composition in French women 75+ years of age: the EPIDOS study. *Mech Ageing Dev* 2003;124:311-6.
164. Delarue J, Constans T, Malvy D, Pradignac A, Couet C, Lamisse F. Anthropometric values in an elderly French population. *Br J Nutr* 1994;71:295-302.
165. Dey DK, Bosaeus I, Lissner L, Steen B. Changes in body composition and its relation to muscle strength in 75-year-old men and women: a 5-year prospective follow-up study of the NORA cohort in Goteborg, Sweden. *Nutrition* 2009;25:613-9.
166. de Groot LC, Sette S, Zajkas G, Carbajal A, Amorim JA. Nutritional status: anthropometry. Euronut SENECA investigators. *Eur J Clin Nutr* 1991;45 Suppl 3:31-42.
167. Moody A. Adult anthropometric measures, overweight and obesity. In: Series Craig R MJ, editor. *Health Survey for England*. London: Health and Social Care Information Centre; 2013.1-39.
168. Janssen I, Heymsfield SB, Wang Z, Ross R. Skeletal muscle mass and distribution in 468 men and women aged 18–88 yr. *J Appl Physiol* 2000;89:81-8.
169. Baumgartner RN, Koehler KM, Gallagher D, Romero L, Heymsfield SB, Ross RR, et al. Epidemiology of sarcopenia among the elderly in New Mexico. *Am J Epidemiol* 1998;147:755-63.
170. Iannuzzi-Sucich M, Prestwood KM, Kenny AM. Prevalence of sarcopenia and predictors of skeletal muscle mass in healthy, older men and women. *J Gerontol A Biol Sci Med Sci* 2002;57:M772-7.

171. Gallagher D, Visser M, De Meersman RE, Sepúlveda D, Baumgartner RN, Pierson RN, et al. Appendicular skeletal muscle mass: effects of age, gender, and ethnicity. *J Appl Physiol* 1997;83:229-39.
172. Rolland Y, Lauwers-Cances V, Cournot M, Nourhashemi F, Reynish W, Riviere D, et al. Sarcopenia, calf circumference, and physical function of elderly women: a cross-sectional study. *J Am Geriatr Soc* 2003;51:1120-4.
173. Gouveia E, Blimkie CJ, Maia JA, Lopes C, Gouveia BR, Freitas DL. Multivariate analysis of lifestyle, constitutive and body composition factors influencing bone health in community-dwelling older adults from Madeira, Portugal. *Arch Gerontol Geriatr* 2014;59:83-90.
174. Kyle UG, Genton L, Slosman DO, Pichard C. Fat-free and fat mass percentiles in 5225 healthy subjects aged 15 to 98 years. *Nutrition* 2001;17:534-41.
175. Dittmar M. Reliability and variability of bioimpedance measures in normal adults: effects of age, gender, and body mass. *Am J Phys Anthropol* 2003;122:361-70.
176. Tichet J, Vol S, Goxe D, Salle A, Berrut G, Ritz P. Prevalence of sarcopenia in the French senior population. *J Nutr Health Aging* 2008;12:202-6.
177. Zoico E, Di Francesco V, Guralnik JM, Mazzali G, Bortolani A, Guariento S, et al. Physical disability and muscular strength in relation to obesity and different body composition indexes in a sample of healthy elderly women. *Int J Obes Relat Metab Disord* 2004;28:234-41.
178. Legrand D, Adriaensen W, Vaes B, Mathei C, Wallemacq P, Degryse J. The relationship between grip strength and muscle mass (MM), inflammatory biomarkers and physical performance in community-dwelling very old persons. *Arch Gerontol Geriatr* 2013;57:345-51.
179. Masanes F, Culla A, Navarro-Gonzalez M, Navarro-Lopez M, Sacanella E, Torres B, et al. Prevalence of sarcopenia in healthy community-dwelling elderly in an urban area of Barcelona (Spain). *J Nutr Health Aging* 2012;16:184-7.
180. Cruz-Jentoft AJ, Baeyens JP, Bauer JM, Boirie Y, Cederholm T, Landi F, et al. Sarcopenia: European consensus on definition and diagnosis: Report of the European Working Group on Sarcopenia in Older People. *Age Ageing* 2010;39:412-23.
181. Janssen I, Heymsfield SB, Ross R. Low relative skeletal muscle mass (sarcopenia) in older persons is associated with functional impairment and physical disability. *J Am Geriatr Soc* 2002;50:889-96.
182. Seidell JC, Oosterlee A, Deurenberg P, Hautvast JG, Ruijs JH. Abdominal fat depots measured with computed tomography: effects of degree of obesity, sex, and age. *Eur J Clin Nutr* 1988;42:805-15.
183. Schutz Y, Kyle UU, Pichard C. Fat-free mass index and fat mass index percentiles in Caucasians aged 18-98 y. *Int J Obes Relat Metab Disord* 2002;26:953-60.

184. Yliharsila H, Kajantie E, Osmond C, Forsen T, Barker DJ, Eriksson JG. Body mass index during childhood and adult body composition in men and women aged 56-70 y. *Am J Clin Nutr* 2008;87:1769-75.
185. Vache C, Rousset P, Gachon P, Gachon AM, Morio B, Boulier A, et al. Bioelectrical impedance analysis measurements of total body water and extracellular water in healthy elderly subjects. *Int J Obes Relat Metab Disord* 1998;22:537-43.
186. Deurenberg P, van der Kooij K, Evers P, Hulshof T. Assessment of body composition by bioelectrical impedance in a population aged greater than 60 y. *Am J Clin Nutr* 1990;51:3-6.
187. Gomez-Cabello A, Pedrero-Chamizo R, Olivares PR, Luzardo L, Juez-Bengoechea A, Mata E, et al. Prevalence of overweight and obesity in non-institutionalized people aged 65 or over from Spain: the elderly EXERNET multi-centre study. *Obes Rev* 2011;12:583-92.
188. Gillette-Guyonnet S, Nourhashemi F, Lauque S, Grandjean H, Vellas B. Body composition and osteoporosis in elderly women. *Gerontology* 2000;46:189-93.
189. Dey DK, Bosaeus I, Lissner L, Steen B. Body composition estimated by bioelectrical impedance in the Swedish elderly. Development of population-based prediction equation and reference values of fat-free mass and body fat for 70- and 75-y olds. *Eur J Clin Nutr* 2003;57:909-16.
190. Santana H, Zoico E, Turcato E, Tosoni P, Bissoli L, Olivieri M, et al. Relation between body composition, fat distribution, and lung function in elderly men. *Am J Clin Nutr* 2001;73:827-31.
191. Tanko LB, Movsesyan L, Mouritzen U, Christiansen C, Svendsen OL. Appendicular lean tissue mass and the prevalence of sarcopenia among healthy women. *Metabolism* 2002;51:69-74.
192. Bedogni G, Pietrobelli A, Heymsfield SB, Borghi A, Manzieri AM, Morini P, et al. Is body mass index a measure of adiposity in elderly women? *Obes Res* 2001;9:17-20.
193. Movsesyan L, Tanko LB, Larsen PJ, Christiansen C, Svendsen OL. Variations in percentage of body fat within different BMI groups in young, middle-aged and old women. *Clin Physiol Funct Imaging* 2003;23:130-3.
194. Sardinha LB, Teixeira PJ, Guedes DP, Going SB, Lohman TG. Subcutaneous central fat is associated with cardiovascular risk factors in men independently of total fatness and fitness. *Metabolism* 2000;49:1379-85.
195. Maden-Wilkinson TM, Degens H, Jones DA, McPhee JS. Comparison of MRI and DXA to measure muscle size and age-related atrophy in thigh muscles. *J Musculoskelet Neuronal Interact* 2013;13:320-8.
196. Bazzocchi A, Diano D, Ponti F, Andreone A, Sassi C, Albisinni U, et al. Health and ageing: a cross-sectional study of body composition. *Clin Nutr* 2013;32:569-78.
197. Horber FF, Gruber B, Thomi F, Jensen EX, Jaeger P. Effect of sex and age on bone mass, body composition and fuel metabolism in humans. *Nutrition* 1997;13:524-34.

198. Puggaard L, Larsen JB, Ebbesen E, Jeune B. Body composition in 85 year-old women: effects of increased physical activity. *Aging (Milano)* 1999;11:307-15.
199. Ravaglia G, Forti P, Maioli F, Boschi F, Cicognani A, Gasbarrini G. Measurement of body fat in healthy elderly men: a comparison of methods. *J Gerontol A Biol Sci Med Sci* 1999;54:M70-6.
200. Svendsen OL, Hassager C, Christiansen C. Age- and menopause-associated variations in body composition and fat distribution in healthy women as measured by dual-energy X-ray absorptiometry. *Metabolism* 1995;44:369-73.
201. Wang ZM, Deurenberg P, Guo SS, Pietrobelli A, Wang J, Pierson RN, Jr., et al. Six-compartment body composition model: inter-method comparisons of total body fat measurement. *Int J Obes Relat Metab Disord* 1998;22:329-37.
202. Tauchi H, Tsuboi K, Okutomi J. Age changes in the human kidney of the different races. *Gerontologia* 1971;17:87-97.
203. Meyer WW, Peter B, Solth K. [the Weight of Organs in the Older Age Groups (70-92 Years) and Their Relation to Age and Body Weight]. *Virchows Arch Pathol Anat Physiol Klin Med* 1963;337:17-32.
204. Puggaard L, Bjornsbo KS, Kock K, Luders K, Thobo-Carlsen B, Lammert O. Age-related decrease in energy expenditure at rest parallels reductions in mass of internal organs. *Am J Hum Biol* 2002;14:486-93.
205. Raab F. Post-mortale Organgewichte von Milz, Leber, Niere und Lunge in Relation zu Lebensalter, Körpergewicht und Körperlänge [PhD thesis]. Heidelberg: University of Heidelberg; 1984.
206. Griffiths GJ, Robinson KB, Cartwright GO, McLachlan MS. Loss of renal tissue in the elderly. *Br J Radiol* 1976;49:111-17.
207. Nyengaard JR, Bendtsen TF. Glomerular number and size in relation to age, kidney weight, and body surface in normal man. *Anat Rec* 1992;232:194-201.
208. Goyal VK. Changes with age in the human kidney. *Exp Gerontol* 1982;17:321-31.
209. Schmucker DL. Age-related changes in liver structure and function: Implications for disease ? *Exp Gerontol* 2005;40:650-9.
210. Grasedyck K, Jahnke M, Friedrich O, Schulz D, Lindner J. Aging of liver: morphological and biochemical changes. *Mech Ageing Dev* 1980;14:435-42.
211. Chouker A, Martignoni A, Dugas M, Eisenmenger W, Schauer R, Kaufmann I, et al. Estimation of liver size for liver transplantation: the impact of age and gender. *Liver Transpl* 2004;10:678-85.
212. Thompson EN, Williams R. Effect of age on liver function with particular reference to bromsulphalein excretion. *Gut* 1965;6:266-9.

213. Swift CG, Homeida M, Halliwell M, Roberts CJ. Antipyrine disposition and liver size in the elderly. *Eur J Clin Pharmacol* 1978;14:149-52.
214. Wynne HA, Cope LH, Mutch E, Rawlins MD, Woodhouse KW, James OF. The effect of age upon liver volume and apparent liver blood flow in healthy man. *Hepatology* 1989;9:297-301.
215. Marchesini G, Bua V, Brunori A, Bianchi G, Pisi P, Fabbri A, et al. Galactose elimination capacity and liver volume in aging man. *Hepatology* 1988;8:1079-83.
216. Spann W, Dustmann HO. Das menschliche Hirngewicht und seine Abhängigkeit von Lebensalter, Körperlänge, Todesursache und Beruf. *Dtsch Z Gesamte Gerichtl Med* 1965;56:299-317.
217. Howell TH. Brain weights in octogenarians. *J Am Geriatr Soc* 1981;29:450-2.
218. Howell TH. Brain weights in septuagenarians. *J Am Geriatr Soc* 1982;30:754-5.
219. Pakkenberg H, Voigt J. Brain weight of the Danes. *Cells Tissues Organs* 1964;56:297-307.
220. Dekaban AS. Changes in brain weights during the span of human life: relation of brain weights to body heights and body weights. *Ann Neurol* 1978;4:345-56.
221. Driscoll I, Davatzikos C, An Y, Wu X, Shen D, Kraut M, et al. Longitudinal pattern of regional brain volume change differentiates normal aging from MCI. *Neurology* 2009;72:1906-13.
222. Handmann E. Über das Hirngewicht des Menschen auf Grund von 1414 im Pathologischen Institut zu Leipzig vorgenommenen Hirnwägungen: Veit & Co.; 1906.
223. Roessle R, Roulet F. *Mass und Zahl in der Pathologie*: Springer; 1932.
224. Hartmann P, Ramseier A, Gudat F, Mihatsch MJ, Polasek W. Das Normgewicht des Gehirns beim Erwachsenen in Abhängigkeit von Alter, Geschlecht, Körpergrösse und Gewicht. *Pathologie* 1994;15:165-70.
225. Waldemar G, Hogg P, Paulson OB. Functional brain imaging with single-photon emission computed tomography in the diagnosis of Alzheimer's disease. *Int Psychogeriatr* 1997;9 Suppl 1:223-7; discussion 47-52.
226. Olivetti G, Melissari M, Capasso JM, Anversa P. Cardiomyopathy of the aging human heart. Myocyte loss and reactive cellular hypertrophy. *Circ Res* 1991;68:1560-8.
227. Olivetti G, Cigola E, Maestri R, Lagrasta C, Corradi D, Quaini F. Recent advances in cardiac hypertrophy. *Cardiovasc Res* 2000;45:68-75.
228. Lie JT, Hammond PI. Pathology of the senescent heart: anatomic observations on 237 autopsy studies of patients 90 to 105 years old. *Mayo Clin Proc* 1988;63:552-64.
229. Olivetti G, Giordano G, Corradi D, Melissari M, Lagrasta C, Gambert SR, et al. Gender differences and aging: effects on the human heart. *J Am Coll Cardiol* 1995;26:1068-79.

230. Pomerance A, Davies MJ. Pathological features of hypertrophic obstructive cardiomyopathy (HOCM) in the elderly. *Br Heart J* 1975;37:305-12.
231. Linzbach AJ, Akuamo-Boateng E. Die Alternsveränderungen des menschlichen Herzens. *Klin Wochenschr* 1973;51:156-63.
232. Heath D, Edwards C, Harris P. Post-mortem size and structure of the human carotid body. *Thorax* 1970;25:129-40.
233. Howell TH. Heart weights among octogenarians. *J Am Geriatr Soc* 1981;29:572-5.
234. Kumar NT, Liestol K, Loberg EM, Reims HM, Maehlen J. Postmortem heart weight: relation to body size and effects of cardiovascular disease and cancer. *Cardiovasc Pathol* 2014;23:5-11.
235. Paulsen S, Vetner M, Hagerup LM. Relationship between length of the left main coronary artery and heart weight. *Acta Pathol Microbiol Scand A* 1975;83:369-72.
236. Gaitskell K, Perera R, Soilleux EJ. Derivation of new reference tables for human heart weights in light of increasing body mass index. *J Clin Pathol* 2011;64:358-62.
237. Prentice A, Parsons TJ, Cole TJ. Uncritical use of bone mineral density in absorptiometry may lead to size-related artifacts in the identification of bone mineral determinants. *Am J Clin Nutr* 1994;60:837-42.
238. Fewtrell MS. Bone densitometry in children assessed by dual x ray absorptiometry: uses and pitfalls. *Arch Dis Child* 2003;88:795-8.
239. Nelson DA, Barondess DA. Whole body bone, fat and lean mass in children: comparison of three ethnic groups. *Am J Phys Anthropol* 1997;103:157-62.
240. Barondess DA, Nelson DA, Schlaen SE. Whole body bone, fat, and lean mass in black and white men. *J Bone Miner Res* 1997;12:967-71.
241. Gnudi S, Sitta E, Fiumi N. Relationship between body composition and bone mineral density in women with and without osteoporosis: relative contribution of lean and fat mass. *J Bone Miner Metab* 2007;25:326-32.
242. Bosity-Westphal A, Mast M, Eichhorn C, Becker C, Kutzner D, Heller M, et al. Validation of air-displacement plethysmography for estimation of body fat mass in healthy elderly subjects. *Eur J Nutr* 2003;42:207-16.
243. Henche SA, Torres RR, Pellico LG. An evaluation of patterns of change in total and regional body fat mass in healthy Spanish subjects using dual-energy X-ray absorptiometry (DXA). *Eur J Clin Nutr* 2008;62:1440-8.
244. Gull B, Karlsson B, Milsom I, Granberg S. Factors associated with endometrial thickness and uterine size in a random sample of postmenopausal women. *Am J Obstet Gynecol* 2001;185:386-91.

245. Sosnik H. Studies on the participation of tunica albuginea and rete testis (TA and RT) in the quantitative structure of human testis. *Gegenbaurs Morphol Jahrb* 1985;131:347-56.
246. Lanz Tv, Neuhäuser G. Metrische Untersuchungen an den Tubuli contorti des menschlichen Hodens. *Z Anat Entwicklungsgesch* 1963;123:462-89.
247. Stearns EL, MacDonnell JA, Kaufman BJ, Padua R, Lucman TS, Winter JS, et al. Declining testicular function with age. Hormonal and clinical correlates. *Am J Med* 1974;57:761-6.
248. Mahmoud AM, Goemaere S, El-Garem Y, Van Pottelbergh I, Comhaire FH, Kaufman JM. Testicular volume in relation to hormonal indices of gonadal function in community-dwelling elderly men. *J Clin Endocrinol Metab* 2003;88:179-84.
249. Westermark P, Wilander E. The influence of amyloid deposits on the islet volume in maturity onset diabetes mellitus. *Diabetologia* 1978;15:417-21.
250. Roessle R. [Beitrag zur Kenntnis der gesunden und der kranken Bauchspeicheldrüse] german. *Beitr path Anat* 1921;69:163-84.
251. Wittingen J, Frey CF. Islet concentration in the head, body, tail and uncinat process of the pancreas. *Ann Surg* 1974;179:412-4.
252. Sandby-Moller J, Poulsen T, Wulf HC. Epidermal thickness at different body sites: relationship to age, gender, pigmentation, blood content, skin type and smoking habits. *Acta Derm Venereol* 2003;83:410-3.
253. Leveque JL, Corcuff P, de Rigal J, Agache P. In vivo studies of the evolution of physical properties of the human skin with age. *Int J Dermatol* 1984;23:322-9.
254. Escoffier C, de Rigal J, Rochefort A, Vasselet R, Leveque JL, Agache PG. Age-related mechanical properties of human skin: an in vivo study. *J Invest Dermatol* 1989;93:353-7.
255. Shuster S, Black MM, McVitie E. The influence of age and sex on skin thickness, skin collagen and density. *Br J Dermatol* 1975;93:639-43.
256. Tan CY, Statham B, Marks R, Payne PA. Skin thickness measurement by pulsed ultrasound: its reproducibility, validation and variability. *Br J Dermatol* 1982;106:657-67.
257. Lock-Andersen J, Therkildsen P, de Fine Olivarius F, Gniadecka M, Dahlstrom K, Poulsen T, et al. Epidermal thickness, skin pigmentation and constitutive photosensitivity. *Photodermatol Photoimmunol Photomed* 1997;13:153-8.
258. Whitton JT, Everall JD. The thickness of the epidermis. *Br J Dermatol* 1973;89:467-76.
259. Tosti A, Fazzini M, Villardita S. Quantitative changes in epidermis of aged humans. *G Ital Chir Dermatol Oncol* 1987;2:180-4.
260. Gniadecka M, Nielsen OF, Wessel S, Heidenheim M, Christensen DH, Wulf HC. Water and protein structure in photoaged and chronically aged skin. *J Invest Dermatol* 1998;111:1129-33.

261. Braverman IM, Fonferko E. Studies in cutaneous aging: I. The elastic fiber network. *J Invest Dermatol* 1982;78:434-43.
262. Krumbhaar E, Lippincott S. The postmortem weight of the "normal" human spleen at different ages. *Am J Med Sci* 1939;197:344-57.
263. Prassopoulos P, Daskalogiannaki M, Raissaki M, Hatjidakis A, Gourtsoyiannis N. Determination of normal splenic volume on computed tomography in relation to age, gender and body habitus. *Eur Radiol* 1997;7:246-8.
264. Sprogøe-Jakobsen S, Sprogøe-Jakobsen U. The weight of the normal spleen. *Forensic Sci Int* 1997;88:215-23.
265. Williams LR. Reference Values for total blood volume and cardiac output in humans. In: Series. Tennessee: Dosimetry Research Group; 1994.49.
266. Kuikka JT, Lansimies E. Effect of age on cardiac index, stroke index and left ventricular ejection fraction at rest and during exercise as studied by radiocardiography. *Acta Physiol Scand* 1982;114:339-43.
267. Granath A, Strandell T. Relationships between Cardiac Output, Stroke Volume and Intracardiac Pressures at Rest and during Exercise in Supine Position and Some Anthropometric Data in Healthy Old Men. *Acta Med Scand* 1964;176:447-66.
268. Mezzani A, Grassi B, Giordano A, Corra U, Colombo S, Giannuzzi P. Age-related prolongation of phase I of VO₂ on-kinetics in healthy humans. *Am J Physiol Regul Integr Comp Physiol* 2010;299:R968-76.
269. Podlesch I, Ulmer WT. Über die Abhängigkeit von Herzminutenvolumen, Herzindex, Schlagvolumen, Schlagvolumenindex und Sauerstoffverbrauch vom Lebensalter. *Arch Kreislaufforsch* 1965;48:232-48.
270. Germing A, Gotzmann M, Rausse R, Brodherr T, Holt S, Lindstaedt M, et al. Normal values for longitudinal function of the right ventricle in healthy women >70 years of age. *Eur J Echocardiogr* 2010;11:725-8.
271. Chahal NS, Lim TK, Jain P, Chambers JC, Kooner JS, Senior R. Population-based reference values for 3D echocardiographic LV volumes and ejection fraction. *JACC Cardiovasc Imaging* 2012;5:1191-7.
272. Cain PA, Ahl R, Hedstrom E, Ugander M, Allansdotter-Johnsson A, Friberg P, et al. Age and gender specific normal values of left ventricular mass, volume and function for gradient echo magnetic resonance imaging: a cross sectional study. *BMC Med Imaging* 2009;9:2.
273. Cheitlin MD. Cardiovascular physiology-changes with aging. *Am J Geriatr Cardiol* 2003;12:9-13.
274. Umetani K, Singer DH, McCraty R, Atkinson M. Twenty-four hour time domain heart rate variability and heart rate: relations to age and gender over nine decades. *J Am Coll Cardiol* 1998;31:593-601.

275. Ryan SM, Goldberger AL, Pincus SM, Mietus J, Lipsitz LA. Gender- and age-related differences in heart rate dynamics: are women more complex than men? *J Am Coll Cardiol* 1994;24:1700-7.
276. Hoang K, Tan JC, Derby G, Blouch KL, Masek M, Ma I, et al. Determinants of glomerular hypofiltration in aging humans. *Kidney Int* 2003;64:1417-24.
277. Bauer JH, Brooks CS, Burch RN. Renal function and hemodynamic studies in low- and normal-renin essential hypertension. *Arch Intern Med* 1982;142:1317-23.
278. Fuiano G, Sund S, Mazza G, Rosa M, Caglioti A, Gallo G, et al. Renal hemodynamic response to maximal vasodilating stimulus in healthy older subjects. *Kidney Int* 2001;59:1052-8.
279. Ghose K, Burch A. Measurement of renal functions by double isotope techniques in elderly patients during tenoxicam therapy. *Arch Gerontol Geriatr* 1989;9:115-22.
280. Zoli M, Magalotti D, Bianchi G, Gueli C, Orlandini C, Grimaldi M, et al. Total and functional hepatic blood flow decrease in parallel with ageing. *Age Ageing* 1999;28:29-33.
281. Gentilcore D, Hausken T, Meyer JH, Chapman IM, Horowitz M, Jones KL. Effects of intraduodenal glucose, fat, and protein on blood pressure, heart rate, and splanchnic blood flow in healthy older subjects. *Am J Clin Nutr* 2008;87:156-61.
282. Gentilcore D, Nair NS, Vanis L, Rayner CK, Meyer JH, Hausken T, et al. Comparative effects of oral and intraduodenal glucose on blood pressure, heart rate, and splanchnic blood flow in healthy older subjects. *Am J Physiol Regul Integr Comp Physiol* 2009;297:R716-22.
283. Gentilcore D, Vanis L, Wishart JM, Rayner CK, Horowitz M, Jones KL. The alpha (alpha)-glucosidase inhibitor, acarbose, attenuates the blood pressure and splanchnic blood flow responses to intraduodenal sucrose in older adults. *J Gerontol A Biol Sci Med Sci* 2011;66:917-24.
284. Dunbar SL, Kenney WL. Effects of hormone replacement therapy on hemodynamic responses of postmenopausal women to passive heating. *J Appl Physiol* 2000;89:97-103.
285. Ho CW, Beard JL, Farrell PA, Minson CT, Kenney WL. Age, fitness, and regional blood flow during exercise in the heat. *J Appl Physiol* 1997;82:1126-35.
286. Minson CT, Wladkowski SL, Cardell AF, Pawelczyk JA, Kenney WL. Age alters the cardiovascular response to direct passive heating. *J Appl Physiol* 1998;84:1323-32.
287. Vanis L, Gentilcore D, Lange K, Gilja OH, Rigda RS, Trahair LG, et al. Effects of variations in intragastric volume on blood pressure and splanchnic blood flow during intraduodenal glucose infusion in healthy older subjects. *Am J Physiol Regul Integr Comp Physiol* 2012;302:R391-9.
288. Lesser GT, Deutsch S. Measurement of adipose tissue blood flow and perfusion in man by uptake of ⁸⁵Kr. *J Appl Physiol* 1967;23:621-30.

289. Andersson J, Karpe F, Sjostrom LG, Riklund K, Soderberg S, Olsson T. Association of adipose tissue blood flow with fat depot sizes and adipokines in women. *Int J Obes (Lond)* 2012;36:783-9.
290. Chen JJ, Rosas HD, Salat DH. Age-associated reductions in cerebral blood flow are independent from regional atrophy. *Neuroimage* 2011;55:468-78.
291. Lu H, Xu F, Rodrigue KM, Kennedy KM, Cheng Y, Flicker B, et al. Alterations in cerebral metabolic rate and blood supply across the adult lifespan. *Cereb Cortex* 2011;21:1426-34.
292. Hagstadius S, Risberg J. Regional cerebral blood flow characteristics and variations with age in resting normal subjects. *Brain Cogn* 1989;10:28-43.
293. Shin W, Horowitz S, Ragin A, Chen Y, Walker M, Carroll TJ. Quantitative cerebral perfusion using dynamic susceptibility contrast MRI: evaluation of reproducibility and age- and gender-dependence with fully automatic image postprocessing algorithm. *Magn Reson Med* 2007;58:1232-41.
294. Devous MD, Sr., Stokely EM, Chehabi HH, Bonte FJ. Normal distribution of regional cerebral blood flow measured by dynamic single-photon emission tomography. *J Cereb Blood Flow Metab* 1986;6:95-104.
295. Proctor DN, Newcomer SC, Koch DW, Le KU, MacLean DA, Leuenberger UA. Leg blood flow during submaximal cycle ergometry is not reduced in healthy older normally active men. *J Appl Physiol* 2003;94:1859-69.
296. Proctor DN, Koch DW, Newcomer SC, Le KU, Leuenberger UA. Impaired leg vasodilation during dynamic exercise in healthy older women. *J Appl Physiol* 2003;95:1963-70.
297. Amery A, Bossaert H, Verstraete M. Muscle blood flow in normal and hypertensive subjects. Influence of age, exercise, and body position. *Am Heart J* 1969;78:211-6.
298. Lassen NA, Lindbjerg J, Munck O. Measurement of Blood-Flow through Skeletal Muscle by Intramuscular Injection of Xenon-133. *Lancet* 1964;1:686-9.
299. Jaarsma C, Leiner T, Bekkers SC, Crijns HJ, Wildberger JE, Nagel E, et al. Diagnostic performance of noninvasive myocardial perfusion imaging using single-photon emission computed tomography, cardiac magnetic resonance, and positron emission tomography imaging for the detection of obstructive coronary artery disease: a meta-analysis. *J Am Coll Cardiol* 2012;59:1719-28.
300. Baliga RR, Rosen SD, Camici PG, Kooner JS. Regional myocardial blood flow redistribution as a cause of postprandial angina pectoris. *Circulation* 1998;97:1144-9.
301. Uren NG, Camici PG, Melin JA, Bol A, de Bruyne B, Radvan J, et al. Effect of aging on myocardial perfusion reserve. *J Nucl Med* 1995;36:2032-6.
302. Chareonthitawee P, Kaufmann PA, Rimoldi O, Camici PG. Heterogeneity of resting and hyperemic myocardial blood flow in healthy humans. *Cardiovasc Res* 2001;50:151-61.

303. Byrne C, Kuhl JT, Zacho M, Nordestgaard BG, Fuchs A, Frestad D, et al. Sex- and age-related differences of myocardial perfusion at rest assessed with multidetector computed tomography. *J Cardiovasc Comput Tomogr* 2013;7:94-101.
304. Antoni G, Lubberink M, Estrada S, Axelsson J, Carlson K, Lindsjo L, et al. In vivo visualization of amyloid deposits in the heart with ¹¹C-PIB and PET. *J Nucl Med* 2013;54:213-20.
305. Weinberg SL, Cagirgan CM, Grove GR, Smith G. Measurement of Relative Coronary Blood Flow by Precordial Monitoring. *Am J Cardiol* 1964;13:801-7.
306. Rosen BD, Fernandes VR, Nasir K, Helle-Valle T, Jerosch-Herold M, Bluemke DA, et al. Age, increased left ventricular mass, and lower regional myocardial perfusion are related to greater extent of myocardial dyssynchrony in asymptomatic individuals: the multi-ethnic study of atherosclerosis. *Circulation* 2009;120:859-66.
307. Czernin J, Muller P, Chan S, Brunken RC, Porenta G, Krivokapich J, et al. Influence of age and hemodynamics on myocardial blood flow and flow reserve. *Circulation* 1993;88:62-9.
308. Braverman IM, Fonferko E. Studies in cutaneous aging: II. The microvasculature. *J Invest Dermatol* 1982;78:444-8.
309. Smith CJ, Alexander LM, Kenney WL. Nonuniform, age-related decrements in regional sweating and skin blood flow. *Am J Physiol Regul Integr Comp Physiol* 2013;305:R877-85.
310. Kelly RI, Pearse R, Bull RH, Leveque JL, de Rigal J, Mortimer PS. The effects of aging on the cutaneous microvasculature. *J Am Acad Dermatol* 1995;33:749-56.
311. Rooke GA, Savage MV, Brengelmann GL. Maximal skin blood flow is decreased in elderly men. *J Appl Physiol (1985)* 1994;77:11-4.
312. Tikhonova IV, Tankanag AV, Chemeris NK. Age-related changes of skin blood flow during postocclusive reactive hyperemia in human. *Skin Res Technol* 2013;19:e174-81.
313. McNally K, Cotton R, Hogg A, Loizou G. PopGen: A virtual human population generator. *Toxicology* 2014;315:70-85.
314. Chumlea WC, Guo SS, Zeller CM, Reo NV, Baumgartner RN, Garry PJ, et al. Total body water reference values and prediction equations for adults. *Kidney Int* 2001;59:2250-8.
315. Bruce A, Andersson M, Arvidsson B, Isaksson B. Body composition. Prediction of normal body potassium, body water and body fat in adults on the basis of body height, body weight and age. *Scand J Clin Lab Invest* 1980;40:461-73.
316. Lesser GT, Markofsky J. Body water compartments with human aging using fat-free mass as the reference standard. *Am J Physiol* 1979;236:R215-20.
317. Sergi G, Lupoli L, Volpato S, Bertani R, Coin A, Perissinotto E, et al. Body fluid distribution in elderly subjects with congestive heart failure. *Ann Clin Lab Sci* 2004;34:416-22.

318. Steen B, Bruce A, Isaksson B, Lewin T, Svanborg A. Body composition in 70-year-old males and females in Gothenburg, Sweden. A population study. *Acta Med Scand Suppl* 1977;611:87-112.
319. Cals MJ, Bories PN, Devanlay M, Desveaux N, Luciani L, Succari M, et al. Extensive laboratory assessment of nutritional status in fit, health-conscious, elderly people living in the Paris area. Research Group on Aging. *J Am Coll Nutr* 1994;13:646-57.
320. Dirren H, Decarli B, Lesourd B, Schlienger JL, Deslypere JP, Kiepuski A. Nutritional status: haematology and albumin. Euronut SENECA investigators. *Eur J Clin Nutr* 1991;45 Suppl 3:43-52.
321. Veering BT, Burm AG, Souverijn JH, Serree JM, Spierdijk J. The effect of age on serum concentrations of albumin and alpha 1-acid glycoprotein. *Br J Clin Pharmacol* 1990;29:201-6.
322. Gardner MD, Scott R. Age- and sex-related reference ranges for eight plasma constituents derived from randomly selected adults in a Scottish new town. *J Clin Pathol* 1980;33:380-5.
323. Maes M, DeVos N, Wauters A, Demedts P, Maurits VW, Neels H, et al. Inflammatory markers in younger vs elderly normal volunteers and in patients with Alzheimer's disease. *J Psychiatr Res* 1999;33:397-405.
324. Faulkner WR, Meites S, editors. *Geriatric clinical chemistry: Reference values*. Washington (DC): American Association for Clinical Chemistry; 1994.
325. Holt DW, Hayler AM, Healey GF. Effect of age and plasma concentrations of albumin and alpha 1-acid glycoprotein on protein binding of disopyramide. *Br J Clin Pharmacol* 1983;16:344-5.
326. Mattila KS, Kuusela V, Pelliniemi TT, Rajamaki A, Kaihola HL, Juva K. Haematological laboratory findings in the elderly: influence of age and sex. *Scand J Clin Lab Invest* 1986;46:411-5.
327. Tietz NW, Shuey DF, Wekstein DR. Laboratory values in fit aging individuals--sexagenarians through centenarians. *Clin Chem* 1992;38:1167-85.
328. Fulop T, Jr., Worum I, Csongor J, Foris G, Leovey A. Body composition in elderly people. I. Determination of body composition by multiisotope method and the elimination kinetics of these isotopes in healthy elderly subjects. *Gerontology* 1985;31:6-14.
329. Praga M, Morales E. Obesity-related renal damage: changing diet to avoid progression. *Kidney Int* 2010;78:633-5.
330. Fried LF, Orchard TJ, Kasiske BL. Effect of lipid reduction on the progression of renal disease: a meta-analysis. *Kidney Int* 2001;59:260-9.
331. Luft FC, Fineberg NS, Miller JZ, Rankin LI, Grim CE, Weinberger MH. The effects of age, race and heredity on glomerular filtration rate following volume expansion and contraction in normal man. *Am J Med Sci* 1980;279:15-24.

332. Lindeman RD, Tobin JD, Shock NW. Association between blood pressure and the rate of decline in renal function with age. *Kidney Int* 1984;26:861-8.
333. Knight EL, Verhave JC, Spiegelman D, Hillege HL, de Zeeuw D, Curhan GC, et al. Factors influencing serum cystatin C levels other than renal function and the impact on renal function measurement. *Kidney Int* 2004;65:1416-21.
334. Matsuo S, Imai E, Horio M, Yasuda Y, Tomita K, Nitta K, et al. Revised equations for estimated GFR from serum creatinine in Japan. *Am J Kidney Dis* 2009;53:982-92.
335. Rule AD, Gussak HM, Pond GR, Bergstralh EJ, Stegall MD, Cosio FG, et al. Measured and estimated GFR in healthy potential kidney donors. *Am J Kidney Dis* 2004;43:112-9.
336. Peters AM, Perry L, Hooker CA, Howard B, Neilly MD, Seshadri N, et al. Extracellular fluid volume and glomerular filtration rate in 1878 healthy potential renal transplant donors: effects of age, gender, obesity and scaling. *Nephrol Dial Transplant* 2012;27:1429-37.
337. Walser M, Drew HH, Guldan JL. Prediction of glomerular filtration rate from serum creatinine concentration in advanced chronic renal failure. *Kidney Int* 1993;44:1145-8.
338. Grewal GS, Blake GM. Reference data for ⁵¹Cr-EDTA measurements of the glomerular filtration rate derived from live kidney donors. *Nucl Med Commun* 2005;26:61-5.
339. Back SE, Ljungberg B, Nilsson-Ehle I, Borga O, Nilsson-Ehle P. Age dependence of renal function: clearance of iohexol and p-amino hippurate in healthy males. *Scand J Clin Lab Invest* 1989;49:641-6.
340. Effersoe H, Rosenkilde P, Groth S, Jensen LI, Golman K. Measurement of renal function with iohexol. A comparison of iohexol, ^{99m}Tc-DTPA, and ⁵¹Cr-EDTA clearance. *Invest Radiol* 1990;25:778-82.
341. Barnfield M, Burniston M. Reference data for ^{99m}Tc-DTPA measurements of the GFR derived from live kidney donors. Paper presented at: 38th annual meeting of the British Nuclear Medicine Society; 2010 April 26-28; Harrogate, United Kingdom
342. Rhodin MM, Anderson BJ, Peters AM, Coulthard MG, Wilkins B, Cole M, et al. Human renal function maturation: a quantitative description using weight and postmenstrual age. *Pediatr Nephrol* 2009;24:67-76.
343. Claassen K, Thelen K, Coboeken K, Gaub T, Lippert J, Allegaert K, et al. Development of a Physiologically-Based Pharmacokinetic Model for Preterm Neonates: Evaluation with In Vivo Data. *Curr Pharm Des* 2015;21:5688-98.
344. Aitkenhead AR, Vater M, Achola K, Cooper CM, Smith G. Pharmacokinetics of single-dose i.v. morphine in normal volunteers and patients with end-stage renal failure. *Br J Anaesth* 1984;56:813-9.
345. Baillie SP, Bateman DN, Coates PE, Woodhouse KW. Age and the pharmacokinetics of morphine. *Age Ageing* 1989;18:258-62.

346. Hoskin PJ, Hanks GW, Aherne GW, Chapman D, Littleton P, Filshie J. The bioavailability and pharmacokinetics of morphine after intravenous, oral and buccal administration in healthy volunteers. *Br J Clin Pharmacol* 1989;27:499-505.
347. Osborne R, Joel S, Trew D, Slevin M. Morphine and metabolite behavior after different routes of morphine administration: demonstration of the importance of the active metabolite morphine-6-glucuronide. *Clin Pharmacol Ther* 1990;47:12-9.
348. Stuart-Harris R, Joel SP, McDonald P, Currow D, Slevin ML. The pharmacokinetics of morphine and morphine glucuronide metabolites after subcutaneous bolus injection and subcutaneous infusion of morphine. *Br J Clin Pharmacol* 2000;49:207-14.
349. Villesen HH, Banning AM, Petersen RH, Weinelt S, Poulsen JB, Hansen SH, et al. Pharmacokinetics of morphine and oxycodone following intravenous administration in elderly patients. *Ther Clin Risk Manag* 2007;3:961-7.
350. Westerling D, Hoglund P, Lundin S, Svedman P. Transdermal administration of morphine to healthy subjects. *Br J Clin Pharmacol* 1994;37:571-6.
351. Westerling D, Persson C, Hoglund P. Plasma concentrations of morphine, morphine-3-glucuronide, and morphine-6-glucuronide after intravenous and oral administration to healthy volunteers: relationship to nonanalgesic actions. *Ther Drug Monit* 1995;17:287-301.
352. Skarke C, Schmidt H, Geisslinger G, Darimont J, Lotsch J. Pharmacokinetics of morphine are not altered in subjects with Gilbert's syndrome. *Br J Clin Pharmacol* 2003;56:228-31.
353. Patwardhan RV, Johnson RF, Hoyumpa A, Jr., Sheehan JJ, Desmond PV, Wilkinson GR, et al. Normal metabolism of morphine in cirrhosis. *Gastroenterology* 1981;81:1006-11.
354. Andreasen F, Hansen U, Husted SE, Jansen JA. The pharmacokinetics of frusemide are influenced by age. *Br J Clin Pharmacol* 1983;16:391-7.
355. Keller E, Hoppe-Seyler G, Mumm R, Schollmeyer P. Influence of hepatic cirrhosis and end-stage renal disease on pharmacokinetics and pharmacodynamics of furosemide. *Eur J Clin Pharmacol* 1981;20:27-33.
356. Kerremans AL, Tan Y, van Baars H, van Ginneken CA, Gribnau FW. Furosemide kinetics and dynamics in aged patients. *Clin Pharmacol Ther* 1983;34:181-9.
357. Muhlberg W, Platt D, Neubig E. Pharmacokinetics and pharmacodynamics of furosemide in geriatric patients. *Arch Gerontol Geriatr* 1986;5:249-63.
358. Barbosa J, Barrón D, Jiménez-Lozano E, Sanz-Nebot V. Comparison between capillary electrophoresis, liquid chromatography, potentiometric and spectrophotometric techniques for evaluation of pK_a values of zwitterionic drugs in acetonitrile–water mixtures. *Analytica Chimica Acta* 2001;437:309-21.
359. Borner K, Hoffken G, Lode H, Koeppe P, Prinzing C, Glatzel P, et al. Pharmacokinetics of ciprofloxacin in healthy volunteers after oral and intravenous administration. *Eur J Clin Microbiol* 1986;5:179-86.

360. Varanda F, Pratas de Melo MJ, Caco AI, Dohrn R, Makrydaki FA, Voutsas E, et al. Solubility of antibiotics in different solvents. 1. Hydrochloride forms of tetracycline, moxifloxacin, and ciprofloxacin. *Ind Eng Chem Res* 2006;45:6368-74.
361. Gallicano K, Sahai J. Lack of gender effect on ciprofloxacin pharmacokinetics in humans. *Br J Clin Pharmacol* 1996;42:632-4.
362. Leibovitz E, Janco J, Piglansky L, Press J, Yagupsky P, Reinhart H, et al. Oral ciprofloxacin vs. intramuscular ceftriaxone as empiric treatment of acute invasive diarrhea in children. *Pediatr Infect Dis J* 2000;19:1060-7.
363. Luisada AA, Bhat PK, Knighten V. Changes of cardiac output caused by aging: an impedance cardiographic study. *Angiology* 1980;31:75-81.
364. Boyd E. Normal variability in weight of the adult human liver and spleen. *Arch Pathol Lab Med* 1933;16:350-72.
365. Benet LZ. Pharmacokinetics/pharmacodynamics of furosemide in man: a review. *J Pharmacokinet Biopharm* 1979;7:1-27.
366. Macintyre PE, Jarvis DA. Age is the best predictor of postoperative morphine requirements. *Pain* 1996;64:357-64.
367. Martinez M, Mistry B, Lukacova V, Polli J, Hoag S, Dowling T, et al. Use of Modeling and Simulation Tools for Understanding the Impact of Formulation on the Absorption of a Low Solubility Compound: Ciprofloxacin. *AAPS J* 2016;18:886-97.
368. Staib AH, Beermann D, Harder S, Fuhr U, Liermann D. Absorption differences of ciprofloxacin along the human gastrointestinal tract determined using a remote-control drug delivery device (HF-capsule). *Am J Med* 1989;87:66S-9S.
369. Tartaglione TA, Raffalovich AC, Poynor WJ, Espinel-Ingroff A, Kerkering TM. Pharmacokinetics and tolerance of ciprofloxacin after sequential increasing oral doses. *Antimicrob Agents Chemother* 1986;29:62-6.
370. Maharaj AR, Edginton AN. Examining Small Intestinal Transit Time as a Function of Age: Is There Evidence to Support Age-Dependent Differences among Children? *Drug Metab Dispos* 2016;44:1080-9.
371. Payen S, Serreau R, Munck A, Aujard Y, Aigrain Y, Bressolle F, et al. Population pharmacokinetics of ciprofloxacin in pediatric and adolescent patients with acute infections. *Antimicrob Agents Chemother* 2003;47:3170-8.
372. Leroux S, Turner MA, Guellec CB, Hill H, van den Anker JN, Kearns GL, et al. Pharmacokinetic Studies in Neonates: The Utility of an Opportunistic Sampling Design. *Clin Pharmacokinet* 2015;54:1273-85.
373. Zhao W, Hill H, Le Guellec C, Neal T, Mahoney S, Paulus S, et al. Population pharmacokinetics of ciprofloxacin in neonates and young infants less than three months of age. *Antimicrob Agents Chemother* 2014;58:6572-80.

374. Sadiq MW, Nielsen EI, Khachman D, Conil JM, Georges B, Houin G, et al. A whole-body physiologically based pharmacokinetic (WB-PBPK) model of ciprofloxacin: a step towards predicting bacterial killing at sites of infection. *J Pharmacokinet Pharmacodyn* 2017;44:69-79.
375. Ball K, Jamier T, Parmentier Y, Denizot C, Mallier A, Chenel M. Prediction of renal transporter-mediated drug-drug interactions for a drug which is an OAT substrate and inhibitor using PBPK modelling. *Eur J Pharm Sci* 2017;106:122-32.
376. Navid A, Ng DM, Wong SE, Lightstone FC. Application of a Physiologically Based Pharmacokinetic Model to Study Theophylline Metabolism and Its Interactions With Ciprofloxacin and Caffeine. *CPT Pharmacometrics Syst Pharmacol* 2016;5:74-81.
377. Hansmann S, Miyaji Y, Dressman J. An in silico approach to determine challenges in the bioavailability of ciprofloxacin, a poorly soluble weak base with borderline solubility and permeability characteristics. *Eur J Pharm Biopharm* 2017;122:186-96.
378. EP. Regulation (EC) No 1901/2006 of the European Parliament and of the Council on medicinal products for paediatric use and amending Regulation (EEC) No 1768/92, Directive 2001/20/EC, Directive 2001/83/EC and Regulation (EC) No 726/2004. European Parliament (EP) and of the Council EEC; 2006
379. FDA. Pediatric Study Plans. U.S. Department of Health and Human Services Food and Drug Administration (FDA); 2013
380. Kang BP, Slosberg E, Snodgrass S, Lebedinsky C, Berry DA, Corless CL, et al. The Signature Program: Bringing the Protocol to the Patient. *Clin Pharmacol Ther* 2015;98:124-6.
381. Berry SM, Broglio KR, Groshen S, Berry DA. Bayesian hierarchical modeling of patient subpopulations: efficient designs of Phase II oncology clinical trials. *Clin Trials* 2013;10:720-34.
382. Wacha H, Wagner D, Schafer V, Knothe H. Concentration of ciprofloxacin in bone tissue after single parenteral administration to patients older than 70 years. *Infection* 1990;18:173-6.
383. Gonzalez MA, Moranchel AH, Duran S, Pichardo A, Magana JL, Painter B, et al. Multiple-dose ciprofloxacin dose ranging and kinetics. *Clin Pharmacol Ther* 1985;37:633-7.
384. Ljungberg B, Nilsson-Ehle I. Pharmacokinetics of intravenous ciprofloxacin at three different doses. *J Antimicrob Chemother* 1988;22:715-20.
385. Hoffken G, Lode H, Prinzing C, Borner K, Koeppe P. Pharmacokinetics of ciprofloxacin after oral and parenteral administration. *Antimicrob Agents Chemother* 1985;27:375-9.
386. Dudley MN, Ericson J, Zinner SH. Effect of dose on serum pharmacokinetics of intravenous ciprofloxacin with identification and characterization of extravascular compartments using noncompartmental and compartmental pharmacokinetic models. *Antimicrob Agents Chemother* 1987;31:1782-6.

387. Bergan T, Thorsteinsson SB, Kolstad IM, Johnsen S. Pharmacokinetics of ciprofloxacin after intravenous and increasing oral doses. *Eur J Clin Microbiol* 1986;5:187-92.
388. Bergan T, Thorsteinsson SB, Solberg R, Bjornskau L, Kolstad IM, Johnsen S. Pharmacokinetics of ciprofloxacin: intravenous and increasing oral doses. *Am J Med* 1987;82:97-102.
389. Wingender W, Graefe KH, Gau W, Forster D, Beermann D, Schacht P. Pharmacokinetics of ciprofloxacin after oral and intravenous administration in healthy volunteers. *Eur J Clin Microbiol* 1984;3:355-9.
390. Wise R, Lockley RM, Webberly M, Dent J. Pharmacokinetics of intravenously administered ciprofloxacin. *Antimicrob Agents Chemother* 1984;26:208-10.
391. Drusano GL, Plaisance KI, Forrest A, Standiford HC. Dose ranging study and constant infusion evaluation of ciprofloxacin. *Antimicrob Agents Chemother* 1986;30:440-3.
392. Gonzalez MA, Moranchel AH, Duran S, Pichardo A, Magana JL, Painter B, et al. Multiple-dose pharmacokinetics of ciprofloxacin administered intravenously to normal volunteers. *Antimicrob Agents Chemother* 1985;28:235-9.
393. Nix DE, Spivey JM, Norman A, Schentag JJ. Dose-ranging pharmacokinetic study of ciprofloxacin after 200-, 300-, and 400-mg intravenous doses. *Ann Pharmacother* 1992;26:8-10.
394. Garraffo R, Drugeon HB. Comparative assessment of the pharmacokinetics and pharmacodynamics of ciprofloxacin after single i.v. doses of 200 and 400mg. *Drugs* 1995;49 Suppl 2:317-20.
395. Plaisance KI, Drusano GL, Forrest A, Bustamante CI, Standiford HC. Effect of dose size on bioavailability of ciprofloxacin. *Antimicrob Agents Chemother* 1987;31:956-8.
396. Drusano GL, Weir M, Forrest A, Plaisance K, Emm T, Standiford HC. Pharmacokinetics of intravenously administered ciprofloxacin in patients with various degrees of renal function. *Antimicrob Agents Chemother* 1987;31:860-4.
397. Jaehde U, Sorgel F, Reiter A, Sigl G, Naber KG, Schunack W. Effect of probenecid on the distribution and elimination of ciprofloxacin in humans. *Clin Pharmacol Ther* 1995;58:532-41.
398. Davis RL, Koup JR, Williams-Warren J, Weber A, Heggen L, Stempel D, et al. Pharmacokinetics of ciprofloxacin in cystic fibrosis. *Antimicrob Agents Chemother* 1987;31:915-9.
399. Drusano GL, Standiford HC, Plaisance K, Forrest A, Leslie J, Caldwell J. Absolute oral bioavailability of ciprofloxacin. *Antimicrob Agents Chemother* 1986;30:444-6.
400. Lettieri JT, Rogge MC, Kaiser L, Echols RM, Heller AH. Pharmacokinetic profiles of ciprofloxacin after single intravenous and oral doses. *Antimicrob Agents Chemother* 1992;36:993-6.

401. Catchpole C, Andrews JM, Woodcock J, Wise R. The comparative pharmacokinetics and tissue penetration of single-dose ciprofloxacin 400 mg i.v. and 750 mg po. *J Antimicrob Chemother* 1994;33:103-10.
402. Shah A, Lettieri J, Kaiser L, Echols R, Heller AH. Comparative pharmacokinetics and safety of ciprofloxacin 400 mg i.v. thrice daily versus 750 mg po twice daily. *J Antimicrob Chemother* 1994;33:795-801.
403. Shah A, Liu MC, Vaughan D, Heller AH. Oral bioequivalence of three ciprofloxacin formulations following single-dose administration: 500 mg tablet compared with 500 mg/10 mL or 500 mg/5 mL suspension and the effect of food on the absorption of ciprofloxacin oral suspension. *J Antimicrob Chemother* 1999;43 Suppl A:49-54.
404. Davis RL, Koup JR, Williams-Warren J, Weber A, Smith AL. Pharmacokinetics of three oral formulations of ciprofloxacin. *Antimicrob Agents Chemother* 1985;28:74-7.
405. Hoffler D, Dalhoff A, Gau W, Beermann D, Michl A. Dose- and sex-independent disposition of ciprofloxacin. *Eur J Clin Microbiol* 1984;3:363-6.
406. Gonzalez MA, Uribe F, Moisen SD, Fuster AP, Selen A, Welling PG, et al. Multiple-dose pharmacokinetics and safety of ciprofloxacin in normal volunteers. *Antimicrob Agents Chemother* 1984;26:741-4.
407. Ledergerber B, Bettex JD, Joos B, Flepp M, Luthy R. Effect of standard breakfast on drug absorption and multiple-dose pharmacokinetics of ciprofloxacin. *Antimicrob Agents Chemother* 1985;27:350-2.
408. Aronoff GE, Kenner CH, Sloan RS, Pottratz ST. Multiple-dose ciprofloxacin kinetics in normal subjects. *Clin Pharmacol Ther* 1984;36:384-8.
409. LeBel M, Bergeron MG, Vallee F, Fiset C, Chasse G, Bigonnesse P, et al. Pharmacokinetics and pharmacodynamics of ciprofloxacin in cystic fibrosis patients. *Antimicrob Agents Chemother* 1986;30:260-6.
410. Brumfitt W, Franklin I, Grady D, Hamilton-Miller JM, Iliffe A. Changes in the pharmacokinetics of ciprofloxacin and fecal flora during administration of a 7-day course to human volunteers. *Antimicrob Agents Chemother* 1984;26:757-61.
411. Loi CM, Parker BM, Cusack BJ, Vestal RE. Aging and drug interactions. III. Individual and combined effects of cimetidine and cimetidine and ciprofloxacin on theophylline metabolism in healthy male and female nonsmokers. *J Pharmacol Exp Ther* 1997;280:627-37.
412. Bergan T, Delin C, Johansen S, Kolstad IM, Nord CE, Thorsteinsson SB. Pharmacokinetics of ciprofloxacin and effect of repeated dosage on salivary and fecal microflora. *Antimicrob Agents Chemother* 1986;29:298-302.
413. Wagenlehner FM, Wydra S, Onda H, Kinzig-Schippers M, Sorgel F, Naber KG. Concentrations in plasma, urinary excretion, and bactericidal activity of linezolid (600 milligrams) versus those of ciprofloxacin (500 milligrams) in healthy volunteers receiving a single oral dose. *Antimicrob Agents Chemother* 2003;47:3789-94.

414. Kara M, Hasinoff BB, McKay DW, Campbell NR. Clinical and chemical interactions between iron preparations and ciprofloxacin. *Br J Clin Pharmacol* 1991;31:257-61.
415. Crump B, Wise R, Dent J. Pharmacokinetics and tissue penetration of ciprofloxacin. *Antimicrob Agents Chemother* 1983;24:784-6.
416. Boy D, Well M, Kinzig-Schippers M, Sorgel F, Ankel-Fuchs D, Naber KG. Urinary bactericidal activity, urinary excretion and plasma concentrations of gatifloxacin (400 mg) versus ciprofloxacin (500 mg) in healthy volunteers after a single oral dose. *Int J Antimicrob Agents* 2004;23 Suppl 1:S6-16.
417. Gotfried MH, Danziger LH, Rodvold KA. Steady-state plasma and intrapulmonary concentrations of levofloxacin and ciprofloxacin in healthy adult subjects. *Chest* 2001;119:1114-22.
418. Esposito S, Miniero M, Barba D, Sagnelli E. Pharmacokinetics of ciprofloxacin in impaired liver function. *Int J Clin Pharmacol Res* 1989;9:37-41.
419. Gasser TC, Ebert SC, Graversen PH, Madsen PO. Ciprofloxacin pharmacokinetics in patients with normal and impaired renal function. *Antimicrob Agents Chemother* 1987;31:709-12.
420. Boerema JB, Dalhoff A, Debruyne FM. Ciprofloxacin distribution in prostatic tissue and fluid following oral administration. *Chemotherapy* 1985;31:13-8.
421. Frost RW, Carlson JD, Dietz AJ, Jr., Heyd A, Lettieri JT. Ciprofloxacin pharmacokinetics after a standard or high-fat/high-calcium breakfast. *J Clin Pharmacol* 1989;29:953-5.
422. Overholser BR, Kays MB, Forrest A, Sowinski KM. Sex-related differences in the pharmacokinetics of oral ciprofloxacin. *J Clin Pharmacol* 2004;44:1012-22.
423. Dan M, Zuabi T, Quassem C, Rotmensch HH. Distribution of ciprofloxacin in ascitic fluid following administration of a single oral dose of 750 milligrams. *Antimicrob Agents Chemother* 1992;36:677-8.
424. Weinstein MP, Deeter RG, Swanson KA, Gross JS. Crossover assessment of serum bactericidal activity and pharmacokinetics of ciprofloxacin alone and in combination in healthy elderly volunteers. *Antimicrob Agents Chemother* 1991;35:2352-8.
425. Yuk JH, Nightingale CN, Quintiliani R. Ciprofloxacin levels when receiving sucralfate. *JAMA* 1989;262:901.
426. Lubart E, Berkovitch M, Leibovitz A, Britzi M, Soback S, Bukasov Y, et al. Pharmacokinetics of ciprofloxacin in hospitalized geriatric patients: comparison between nasogastric tube and oral administration. *Ther Drug Monit* 2013;35:653-6.

Appendix

Table A-1 Patient characteristics and mean pharmacokinetic parameters in ciprofloxacin studies using intravenous dosing reported in the literature

Dosage		Infusion Time [min]	Population		n	Females [%]	AUC [mg·h/L]	CL [L/h]	Reference
[mg]	Regime		Age [years] (Range)	Weight [kg] (Range)					
20		30	80.85 (60-96)		20	60			[382]
25	BID	10	(19-45)	(49.9-71.8)	9	0	0.73±0.12	1.878±0.324 ^e	[383]
50		3	28 (21-34)	69.3 (61-79)	8	0	1.45±0.33	33.72±7.29	[384]
50		15	30 (22-34)	67 (52-80)	12	50	1.23±0.2	41.58±7.2	[359]
50		15	30 (22-34)	67.5 (51-80.5)	12	50	1.2±0.2	41.22±7.8 ^d	[385]
50	BID	10	(19-45)	(49.9-71.8)	9	0	1.59±0.15	1.908±0.18 ^e	[383]
75	BID	10	(19-45)	(49.9-71.8)	9	0	2.47±0.4	2.124±0.408 ^e	[383]
100		30	23	81.5	9	0	2.24±0.54	0.576±0.1254 ^e	[386]
100		3	26 (21-40)	68 (54-85)	12	50	2.54±0.51	40.71±7.01	[387, 388]
100		3	28 (21-34)	69.3 (61-79)	8	0	2.9±0.36	32.82±4.344	[384]
100		5	29	75	6	0		9.62±2.29 ^e	[389]
100		60	29.2 (23-42)	78.5 (65-85)	6	0	2.81±0.57	34.02±5.32	[390]
100		15	30 (22-34)	67 (52-80)	12	50	2.88±0.52	36±8.4	[359]
100		15	30 (22-34)	67.5 (51-80.5)	12	50	3±0.5	31.8±6.24 ^d	[385]
100		30	(21-29)		6	0		23±9.1 ^d	[391]
100		30	(21-29)		6	0		22.5±8.9 ^d	[391]
100		30	(21-29)		6	0	3.94±1.25	24.6±10.4 ^d	[391]
100	BID	30	(18-46)	(54.8-73)	9	0	3.4±0.49	30.1±3.4 ^d	[392]
150		30	23	81.5	9	0	3.36±0.74	0.5742±0.1212 ^e	[386]
150	BID	30	(18-46)	(54.8-73)	9	0	5.14±0.77	29.8±4 ^d	[392]
200		30	23	81.5	9	0	5.17±0.87	0.489±0.0726 ^e	[386]
200		30	24.3 (20-30)	78 (64-91)	12	0	5.2021±1.3916	41±11.3	[393]
200		30	25.4 (19-39)	66.6 (50-82)	10	50	5.52±1.95		[394]
200		30	27 (19-33)	79 (67-83)	12	0	5.37±0.72	37.92±4.5	[139]
200		10	27.1 (22-30)	77.3 (60.5-89.4)	8	0	5.97±0.91	26.8±5.71 ^d	[395]
200		10	27.125 (22-30)	77.3375 (60.5-89.4)	8	0		26.8±5.7 ^d	[396]
200		30	29.3 (21-38)	67.1	12	50	5.73±1.38	36.66±8.04	[397]
200		20	28 (23-34)	66 (58-73)	10	50	5.31±1.12	39.12±7.98	[359]

Dosage		Infusion Time [min]	Population				AUC [mg·h/L]	CL [L/h]	Reference
[mg]	Regime		Age [years] (Range)	Weight [kg] (Range)	n	Females [%]			
200	BID	60	72.6 (65.4-87.6)	65.6 (42-101)	17	35	5.5±1.8 ^b	0.588±0.258 ^e	[140]
200	BID	30	72.96 (44-96)	67.09 (40-111)	44	95.5	13.71±5.5 ^b		[141]
200		30	74 (57-84)	72 (52-80)	17	0	8.17±2.62	26.46±7.02	[138]
200		30	74 (57-84)	72 (50-80)	14	0	8.79±2.73	24.42±6.24	[139]
200	BID	60	77 (66-90)	66 (49.1-102.7)	9	78	13.3±4.8	0.2598±0.1194 ^e	[137]
200		30	(23-32)	75.9	12	0	6.38±1.05	32±4.77	[398]
200		30	(21-29)		6	0		23.7±5.1 ^d	[391]
200		30	(21-29)		6	0		23.3±5 ^d	[391]
200		30	(21-29)		6	0	7.22±1.77	25.2±5.8 ^d	[391]
200		10	(21-29)		12	0		28.5±4.7 ^d	[399]
200	BID	30	(18-46)	(54.8-73)	9	0	7.7±1.38	26.9±4.1 ^d	[392]
250		5	28 (21-34)	69.3 (61-79)	8	0	8.11±0.94	29.28±3.504	[384]
250		5	69 (63-76)	76.9	8	0	8.9±0.83	26.04±3.222 ^d	[142]
300		30	24.3 (20-30)	78 (64-91)	12	0	8.7143±1.8886	35.7±5.8	[393]
300		60	27.3 (21-35)	73	12	0	8.6±1.5	36.18±7.62	[400]
400	BID	30	24.3 (20-30)	78 (64-91)	12	0	11.0999±1.0934	36.5±3.8	[393]
400		60	24.7	77.3	12	0	11.2±0.672	35.6±2.136	[130]
400			25.4 (19-39)	66.6 (50-82)	10	50	11.22±3.5		[394]
400	TID	60	25.75	74.95	12	50	8.75±1.165	31.5±5.355	[130]
400		60	26.8	60.2	12	100	14.4±2.304	27.7±4.432	[130]
400		60	27.3	74.9 (63.3-84.5)	6	0	14.2±1.1		[401]
400		60	27.3 (21-35)	73	12	0	11.4±1.6	35.82±4.92	[400]
400		60	28.2	73.3	18	0	24.2±5.1 ^c	51.72±11.28 ^d	[402]
400	TID	60	28.2	73.3	18	0	32.9±8.83 ^c	38.94±9.96 ^d	[402]
400		60	67.7	90	12	0	13.7±0.822	29.2±1.752	[130]
400	BID	60	68.25	73.3	12	50	0±0	24.8±5.208	[130]
400		60	68.8	67.9	12	100	19±3.23	21.1±3.587	[130]

Grey shading indicated studies used for model building

Frequency of dose administration: BID: twice daily; TID: thrice daily

^a Dose on mg/kg basis;

^b AUC_{0-12h}

^c AUC_{0-24h}

^d Clearance normalized to body surface area [L/h/1.73m²]

^e Clearance normalized to body weight [L/h/kg]

Table A-2 Patient characteristics and mean pharmacokinetic parameters in ciprofloxacin studies using oral dosing reported in the literature

Dosage		Population				AUC [mg·h/L]	CL [L/h]	C _{max} [mg/L]	Study
[mg]	Regime	Age [years] (Range)	Weight [kg] (Range)	n	Females [%]				
Suspension									
10 ^a	BID	(2-4)		11	35			1.43	[135]
10 ^a	BID	(5-10)		12	35			1.44	[135]
10 ^a	BID	(11-15)		10	35			1.48	[135]
10 ^a	TID	0.675 (0.3-0.8)	7.675 (6.4-8.8)	4	50	10.8±1.28	16.4±1.44 ^e	2.83±1.49	[134]
10 ^a		0.675 (0.3-0.8)	7.675 (6.4-8.8)	4	50			1.99±1.3	[134]
10 ^a	TID	1.33 (1.1-1.6)	11 (10.7-11.4)	3	33	7.7±1.09	18.3±1.22 ^e	3.57±0.35	[134]
10 ^a		1.33 (1.1-1.6)	11 (10.7-11.4)	3	33			2.43±1.07	[134]
10 ^a	TID	3.733 (2.5-5.3)	15.86 (11.9-20)	5	33	9±1.33	17.3±1.73 ^e	2.73±1.61	[134]
10 ^a		3.733 (2.5-5.3)	15.86 (11.9-20)	5	33			2.67±1.12	[134]
10 ^a	TID	6.66 (6.3-7.1)	22.46 (20.7-23.8)	4	100	8.1±1.4	24.4±1.28 ^e	1.95±1.14	[134]
10 ^a		6.66 (6.3-7.1)	22.46 (20.7-23.8)	4	100			2.08±1.53	[134]
15.00 ^a		0.2 (0.096154-	5.5 (4.1-7.1)	7	43	16.1±7.4		3.3±1.3	[136]
15.00 ^a		2 (1-4.667)	11.8 (8.3-17.3)	7	43	3.93±1.83		1.59±0.73	[136]
500		25.7 (19-39)	71.3 (57.6-90.7)	36	0	12.0		2.4	[403]
500		29.6 (20-40)	76.7 (61.9-89.8)	32	0	7.3		1.5	[403]
500		29.6 (20-40)	76.7 (61.9-89.8)	32	0	8.0		1.6	[403]
500		(24-40)	78	18	0	13.5±3.01	38.8±9.05	3.23±1.13	[404]
Tablet									
50		30 (22-34)	67.5 (51-80.5)	12	50	1±0.3		0.28±0.08	[385]
100		19	67.5 (58.5-74)	6	50			0.52±0.14	[375]
100		26 (21-40)	68 (54-85)	12	50	2.1±0.97		0.73±0.28	[387, 388]
100		28		8	0	1.289±0.529		0.381±0.153	[405]
100		28		7	100	1.485±0.549		0.437±0.154	[405]
100		29.4 (21-35)	67 (52-80)	12	50	1.77±0.64		0.37±0.11	[359]
100		30 (22-34)	67.5 (51-80.5)	12	50	1.9±0.6		0.49±0.13	[385]
100		74	60.25 (30.5-84.2)	9	50				[375]
100		(30-40)	76.9 (70-85.7)	4	50				[375]
200		27.1 (22-30)	77.3 (60.5-89.4)	8	0	4.18±1.1	39.1±7.28 ^d	1.18±0.2	[395]
200		(21-29)		12	0		41.67±6.44	1.2055±0.229	[399]
250		24 (20-30)	72 (61-81)	10	0	5.55±0.34		1.2±0.1	[131]

Dosage [mg]	Regime	Age [years] (Range)	Population Weight [kg] (Range)	n	Females [%]	AUC [mg·h/L]	CL [L/h]	C _{max} [mg/L]	Study
250	BID	24.7 (19-45)	68.4 (55.2-91)	9	0	5.33±0.61		1.35±0.19	[406]
250		25.7 (22-37)	63 (47.5-79)	10	50			1.35±0.17	[407]
250	BID	25.7 (22-37)	63 (47.5-79)	10	50			1.41±0.32	[407]
250		26 (21-40)	68 (54-85)	12	50	5.28±2.41		1.59±0.57	[387, 388]
250		27.3	75	12	0		0.823±0.297 ^e		[408]
250	BID	27.3	75	12	0		0.629±0.164 ^e		[408]
250	BID	28		8	0	3.02±0.965		0.935±0.331	[405]
250	BID	28		8	100	4.195±1.07		1.182±0.236	[405]
250		28 (22-34)	69.4	8	0	4.7±0.7		1.24±0.32	[142]
250		29	75	6	0			0.94±0.28	[389]
250		29.4 (21-35)	67 (52-80)	10	50	4.23±1.11			[359]
250		67 (60-73)	65 (57-74)	10	40	7.43±0.77 ^c		1.7±0.1	[131]
250		69 (63-76)	76.9	8	0	6.4±1.08		1.47±0.4	[142]
250		(22-26)		8	0	3.7±1 ^c		0.76±0.22	[369]
500		22.3 (19-25)	62 (59.8-75)	12	50	10±2.78	38.238±10.14	2.26±0.75	[409]
500	TID	22.3 (19-25)	62 (59.8-75)	12	50	13.93±5.32	41.436±17.82	3.51±1.33	[409]
500	BID	24.7 (19-45)	68.4 (55.2-91)	9	0	13.94±2.86 ^b		2.89±0.54	[406]
500		24.8 (19-40)	73.3 (57.3-95.5)	12	0	11.8±3.6			[410]
500	BID	24.8 (19-40)	73.3 (57.3-95.5)	12	0	18.5±5.8			[410]
500		25	76.2	14	0	10.6±2.3 ^b		2.5±0.6	[132]
500	BID	25	76.2	14	0	14.7±2.7 ^b		3±0.6	[132]
500	BID	25 (22-40)	77.4	8	0	10.35±0.86 ^b			[411]
500	BID	25.7 (19-39)	71.3 (57.6-90.7)	36	0	11.8		2.2	[403]
500		26 (21-30)	68 (54-85)	12	50	9.6±4.2		2.8±1.3	[412]
500	BID	26 (21-30)	68 (54-85)	12	50	9.6±4.5		2.3±1.1	[412]
500		26 (21-40)	68 (54-85)	12	50	9.61±4.18		2.77±1.26	[387, 388]
500		27 (19-42)	68.3 (57.8-86.6)	12	50	10.2±1.9 ^c	60.06±13.212	2.46±0.481	[413]
500		27.3 (21-35)	73	12	0	10.7±2.6		2.7±0.8	[400]
500		28		8	0	7.383±1.6		2.158±0.646	[405]
500		28		7	100	7.084±2.86		1.959±0.503	[405]
500		28 (22-34)	69.4	8	0	10.3±2.6		2.35±0.52	[142]
500	BID	28 (22-34)	69.4	8	0	14.3±2.8		3.1±0.79	[142]
500	BID	28 (22-33)	70.4	8	100	12.97±0.75 ^b			[411]
500		28.3 (20-42)		8	12.5	16.2±4.6		3±1	[414]
500		29 (23-41)	78 (69-83)	6	0	9.9±2.43		2.3±0.7	[415]
500		28 (23-34)	67 (52-80)	10	50	6.78±1.32		1.51±0.36	[359]

Dosage [mg]	Regime	Age [years] (Range)	Population Weight [kg] (Range)	n	Females [%]	AUC [mg·h/L]	CL [L/h]	C _{max} [mg/L]	Study
500		30 (19-43)	74.8 (63-91)	12	50	10.6±2.3	48.84±13.86	2.12±0.5	[416]
500	BID	31 (21-48)	77.3	12	50				[417]
500		36		7	57	10.1		2.35±0.95	[418]
500		60		17	0	9.8±4	60.12±27.78	2.2±1.1	[419]
500		65.3	75.8	8	0				[420]
500	BID	67.3	77.1	8	0				[420]
500		69 (63-76)	76.9	8	0	13.8±1.75		2.83±0.61	[142]
500	BID	69 (63-76)	76.9	8	0	20.5±3.4		3.3±0.38	[142]
500	BID	71 (65-76)	84.5	8	0	13.68±0.74 ^b			[411]
500	BID	72 (65-78)	67.5	8	100	19.28±1.03 ^b			[411]
500	BID	72.6 (65.4-87.6)	65.6 (42-101)	17	35	11.4±4.3 ^b	0.636±0.222 ^e	2.6±1	[140]
500		75.4 (71-86)	65.1 (51-79)	12	0	20.88±8.68	23.64±4.35		[143]
500		(24-40)	78	18	0	10±2.18	50.2±11.8	2.83±0.68	[404]
500		(24-40)	78	18	0	12.7±2.89	42±10.2	2.91±0.74	[404]
500		(22-26)		11	0	7.6±2.6 ^c		1.6±0.79	[369]
750		23 (19-26)	78.7	12	0	12.71±2.58	28.94±16.43	2.23±0.5	[421]
750	BID	24.7 (19-45)	68.4 (55.2-91)	9	0	22.07±6.37 ^b		4.15±0.72	[406]
750		25	76.2	14	0	15.6±3.1 ^b		3.3±0.7	[132]
750	BID	25	76.2	14	0	21.1±6.1 ^b		4.4±1.1	[132]
750		26 (24-37)	54.6 (52.3-71.8)	7	100		28.3	5.2	[422]
750		27.1 (22-30)	77.3 (60.5-89.4)	8	0	15.3±3.77	42.2±8.05 ^d	2.97±0.64	[395]
750		27.3	74.9 (63.3-84.5)	6	0	19.2±1.1		3.9±1.7	[401]
750		27.3 (21-35)		12	0	16.8±4.8		3.8±1.5	[400]
750		28.2	73.3	18	0	23.8±7.22 ^c	70.5±31.14 ^d	3.01±0.88	[402]
750	BID	28.2	73.3	18	0	31.6±12.3 ^c	53.76±18.36 ^d	3.59±1.34	[402]
750		28 (23-34)	67 (52-80)	12	50	8.77±1.09		1.97±0.5	[359]
750		30 (22-34)	67.5 (51-80.5)	12	50	12.2±2.9		2.65±0.48	[385]
750		30 (24-43)	86.6 (67.9-106.8)	8	0		44.4	3.6	[422]
750		33	65	24	100	16.1±3.95	47.33±15.46	3.19±0.5	[361]
750		36	74	24	0	13.42±2.59	54.27±10.6	3.14±0.77	[361]
750		60		17	0	15.6±9.1	70.38±48.9	2.8±1.5	[419]
750		60.8 (58-77)	64.3 (50-93)	10	90				[147]
750		65.3 (42-85)	71.8 (62-88)	10	50				[423]
750		67.8	75.8	6	50	20.9±7.7	42.1±20	5.1±1.4	[424]
750		68.6		5	0				[425]
750		70 (61-82)	70 (58-80)	5	50				[145]

Dosage		Population				AUC [mg·h/L]	CL [L/h]	C _{max} [mg/L]	Study
[mg]	Regime	Age [years] (Range)	Weight [kg] (Range)	n	Females [%]				
750		73 (68-76)	62.1 (47.7-69.5)	6	0	35.1±6.3	0.35±0.06 ^e	5.9±0.7	[144]
750	BID	73 (68-76)	62.1 (47.7-69.5)	6	0	33.1±12.2	0.41±0.15 ^e	6.2±1.8	[144]
750	BID	73 (68-76)	62.1 (47.7-69.5)	6	0	34.7±9.8	0.38±0.11 ^e	6.2±1.6	[144]
750	BID	78 (66-90)	63.4 (49.1-66.6)	6	78	39.9±11.2		7.6±2.2	[137]
750		79.1 (64-92)	56.5 (43.6-95.7)	20	40	41.92±17.22 ^b	0.4014±0.2238 ^e	6.58±2.88	[146]
750	BID	79.1 (64-92)	56.5 (43.6-95.7)	20	40	47.7±19.61	0.3366±0.1518 ^e	8.83±2.79	[146]
750	BID	81.3		10	60			3.3±2.16	[426]
750		(23-32)	75.9	12	0	16.7±5.1	51.9±28.4	3.34±1.34	[398]
750		(22-26)		11	0	12.9±3 ^c		2.54±0.54	[369]
1000		26 (21-40)	68 (54-85)	12	50	22.84±9.41		5.57±1.21	[387, 388]
1000		28		7	0	11.611±2.998		3.619±0.844	[405]
1000		28		8	100	14.683±5.413		3.763±0.924	[405]
1000		(22-26)		11	0	16.6±2.4 ^c		3.38±0.56	[369]

Grey shading indicated studies used for model building

Frequency of dose administration: BID: twice daily; TID: thrice daily

^a Dose on mg/kg basis;

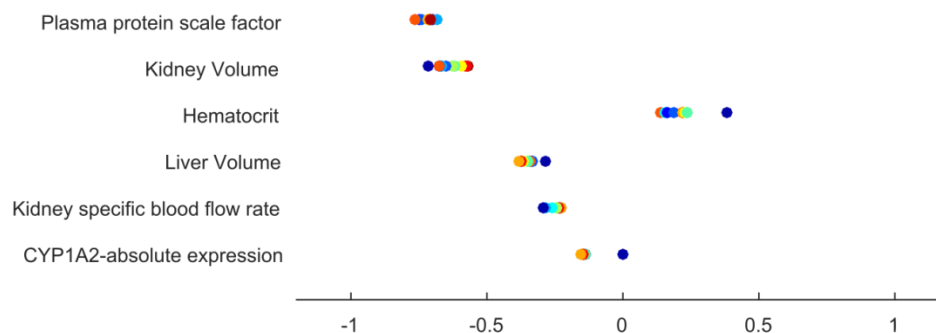
^b AUC_{0-12h}

^c AUC_{0-24h}

^d Clearance normalized to body surface area [L/h/1.73m²]

^e Clearance normalized to body weight [L/h/kg]

System parameters



Compound parameters

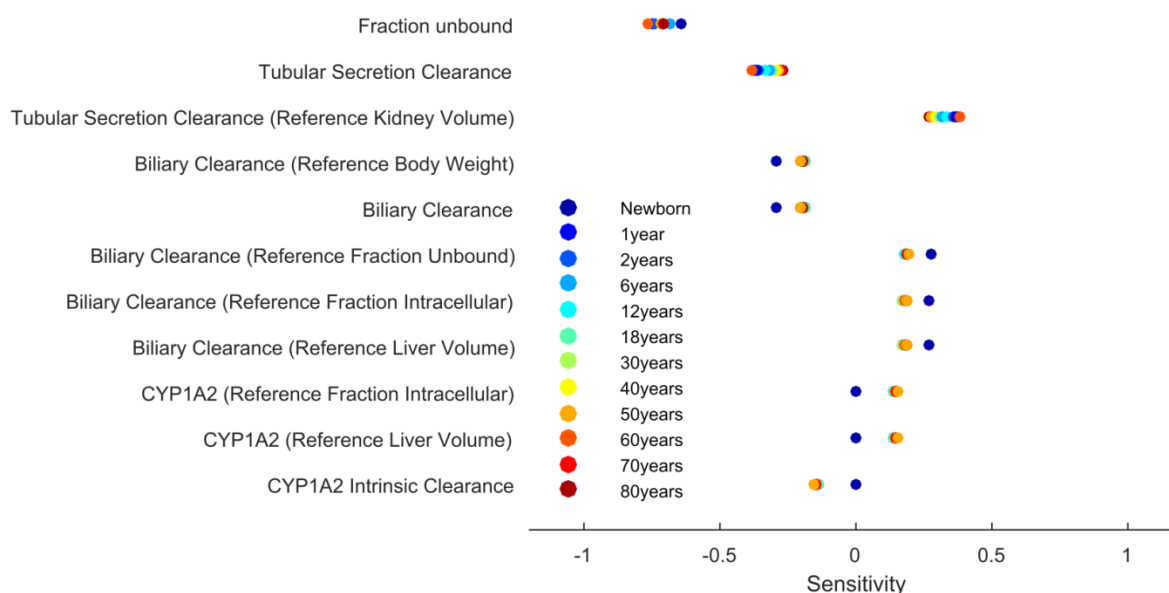
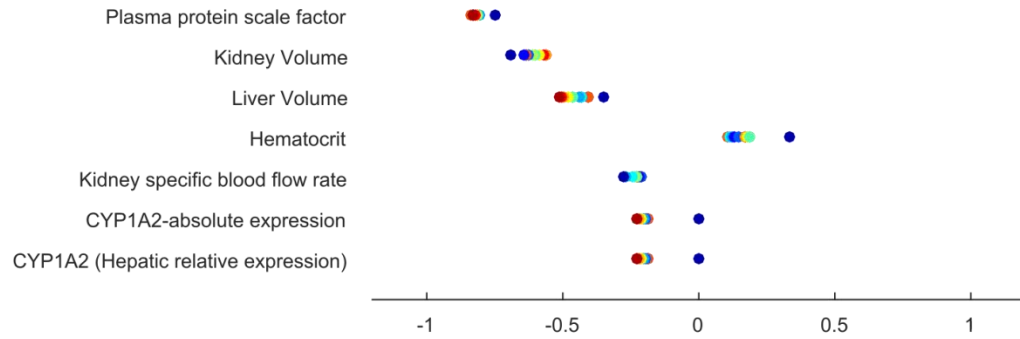


Figure A-1 Listing of the most sensitive parameters comprising 90 % of the entire variability in a descending order towards AUC_{inf} after intravenous administration. The X-axis describes sensitivity values and their positive or negative impact on AUC_{inf} . Model parameters are classified of either compound or system origin. The color code represents the different ages. Parameters assigned with the term *Reference* represent compound-specific reference values applied to convert plasma clearance to an intrinsic clearance normalized to the organ or tissue size where the process occurs.
* Dose is not depicted and contributes with a sensitivity of 1

System parameters



Compound parameters

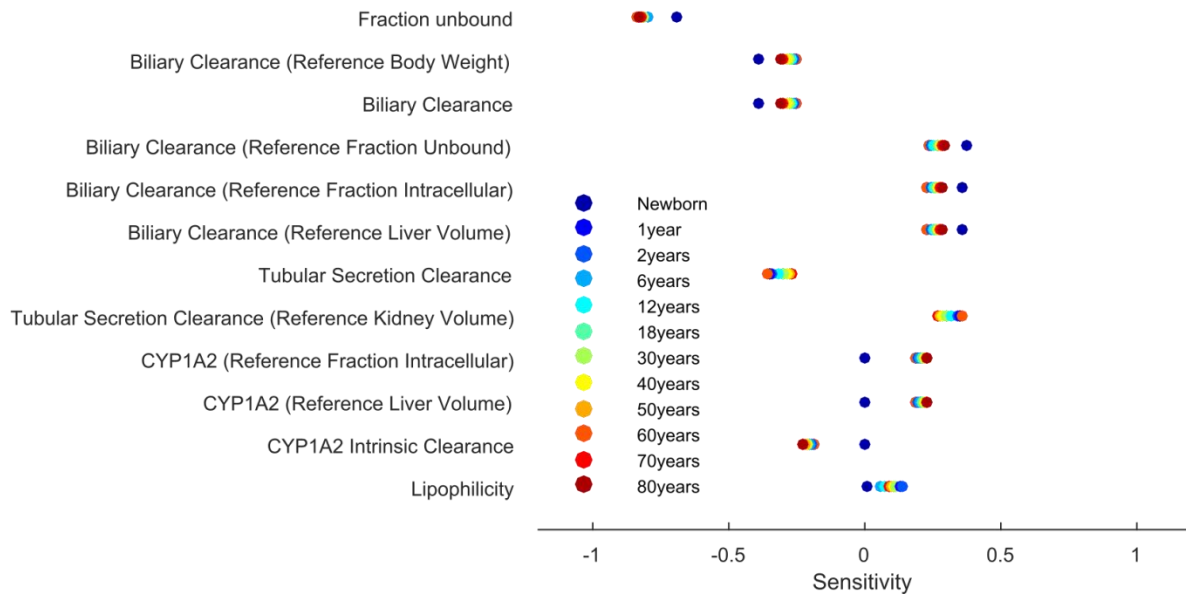


Figure A-2 Listing of the most sensitive parameters comprising 90 % of the entire variability in a descending order towards AUC_{inf} after oral administration. The X-axis describes sensitivity values and their positive or negative impact on AUC_{inf} . Model parameters are classified of either compound or system origin. The color code represents the different ages. Parameters assigned with the term *Reference* represent compound-specific reference values applied to convert plasma clearance to an intrinsic clearance normalized to the organ or tissue size where the process occurs.

* Dose is not depicted and contributes with a sensitivity of 1

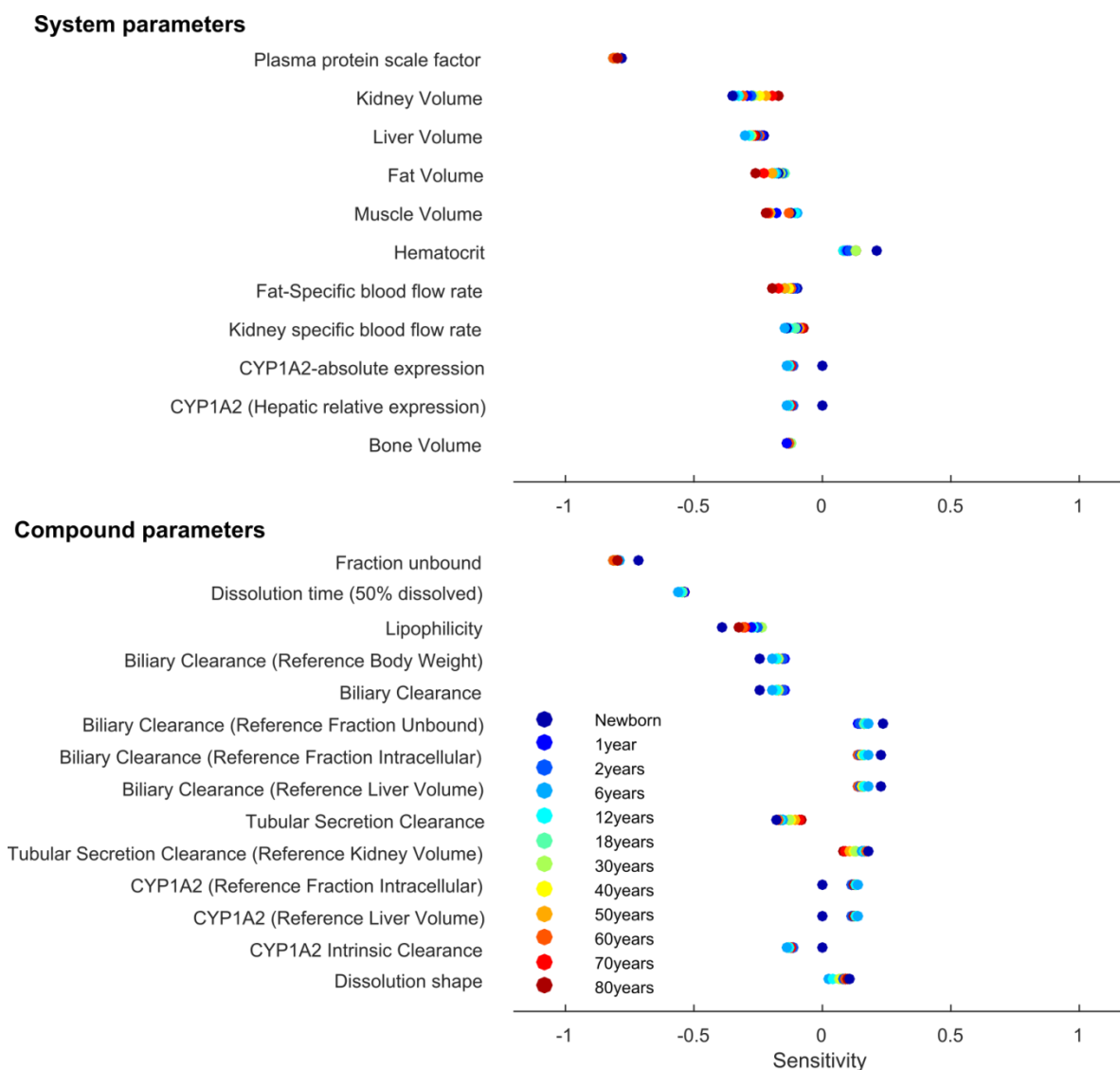


Figure A-3 Listing of the most sensitive parameters comprising 90 % of the entire variability in a descending order towards C_{max} after oral administration. The X-axis describes sensitivity values and their positive or negative impact on C_{max} . Model parameters are classified of either compound or system origin. The color code represents the different ages. Parameters assigned with the term *Reference* represent compound-specific reference values applied to convert plasma clearance to an intrinsic clearance normalized to the organ or tissue size where the process occurs.

* Dose is not depicted and contributes with a sensitivity of 1